

The Scientific Program of \bar{P} ANDA and PAX experiments

- The history of antiprotons;
- Overview of the FAIR facility and of the HESR;
- The \bar{P} ANDA experimental program;
- The \bar{P} ANDA detector;
- The PAX scientific program;
- The PAX experimental setup;
- Antiproton polarization possibilities.

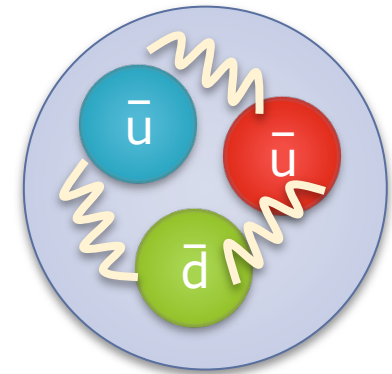
The history of antiprotons

Antiprotons were postulated in the thirties of past century, and discovered at Berkley in 1995.



Edward Lofgren (center), head of the Bevatron, (left to right) E. Segre, C. Wiegand, O. Chamberlain and T. Ypsilantis.

It has been the first particle discovered at an accelerator opening the modern era of "particle physics".



The Bevatron could collide two proton beams at an energy of 6.2 GeV, expected to be the optimum for producing antiprotons.

Antiprotons are powerful tools

High Energy:

$\bar{p}p$ -Colliders (CERN, Fermilab)
Discovery of Z^0 , W^\pm
Discovery of t-quark

Medium Energy:

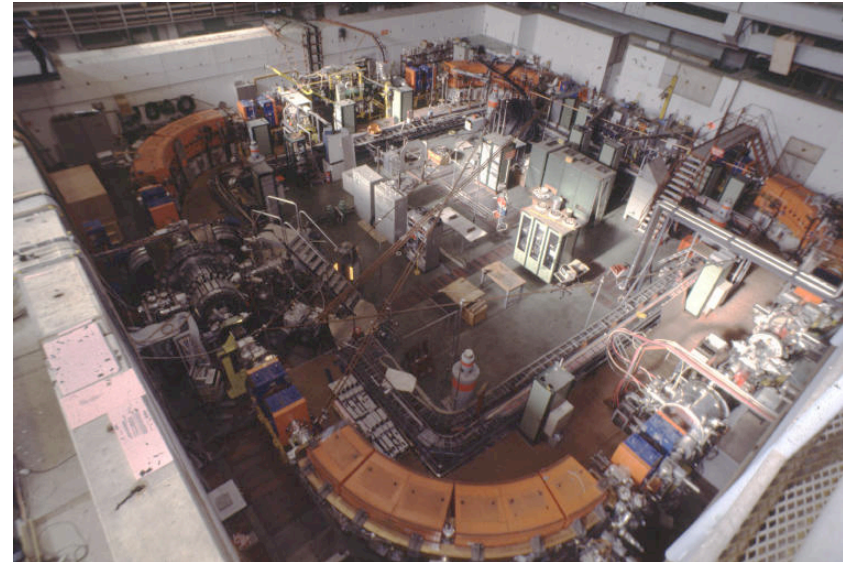
Conventional \bar{p} -beams (LBL, BNL, CERN, Fermilab, KEK, ...)
 \bar{p} -Storage Rings (LEAR (CERN); Antiproton Accumulator (Fermilab))
Meson Spectroscopy (u, d, s, c)
 \bar{p} -nucleus interaction
Hypernuclei
Antihydrogen first production
CP-violation

Low Energy (Stopped \bar{p} 's):

Conventional \bar{p} -beams
 \bar{p} -Storage Rings (LEAR, AD (CERN))
 \bar{p} -Atoms ($\bar{p}\text{He}$)
 \bar{p}/p -mass ratio
Antihydrogen

The LEAR machine

Beam intensity	$10^4 \div 10^6 \bar{p}/s$
Beam momentum	$100 \div 2000 \text{ MeV}/c$
$\Delta p/p$	10^{-3}
Machine vacuum	$10^{-11} \div 10^{-12} \text{ Torr}$
circumference	78.54 m



Four glueball candidates: $f_0(1500)$, $f_0(1370)$, $f_0(1710)$ 0^{++}

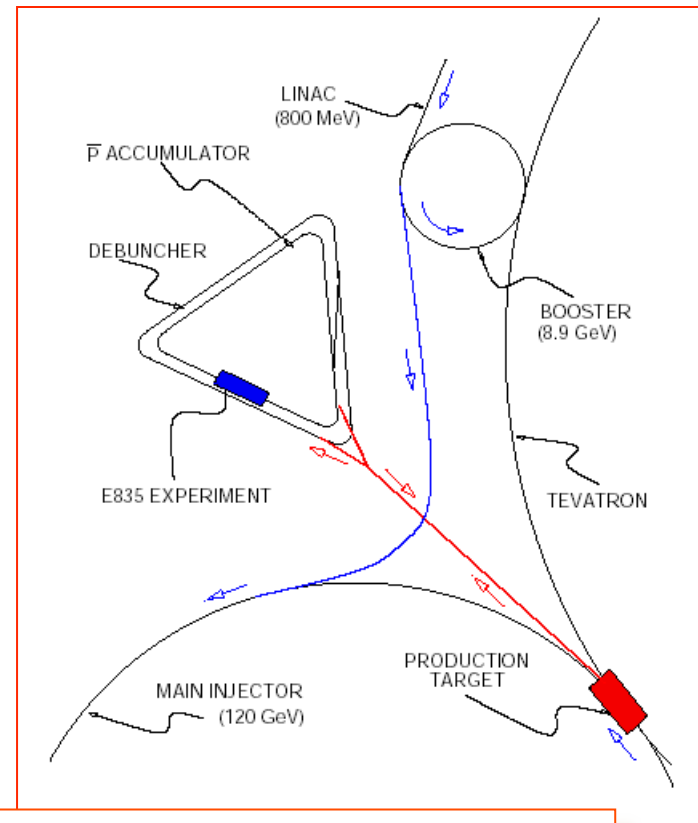
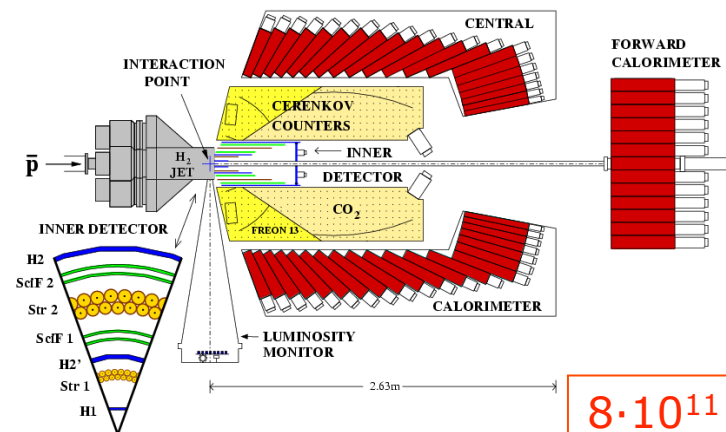
$\eta(1440)$ 0^{-+}

Two hybrids candidates: $\pi_1(1400)$, $\pi_1(1600)$ 1^{-+}

First production of antimatter

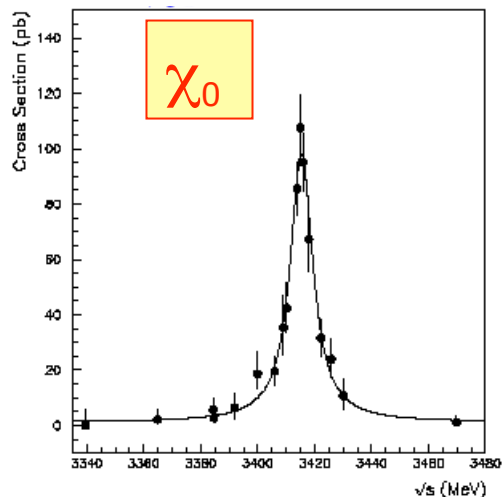
The Fermilab \bar{p}

Many results on charmonium came from E760-E835 experiments at Fermilab Antiproton Accumulator

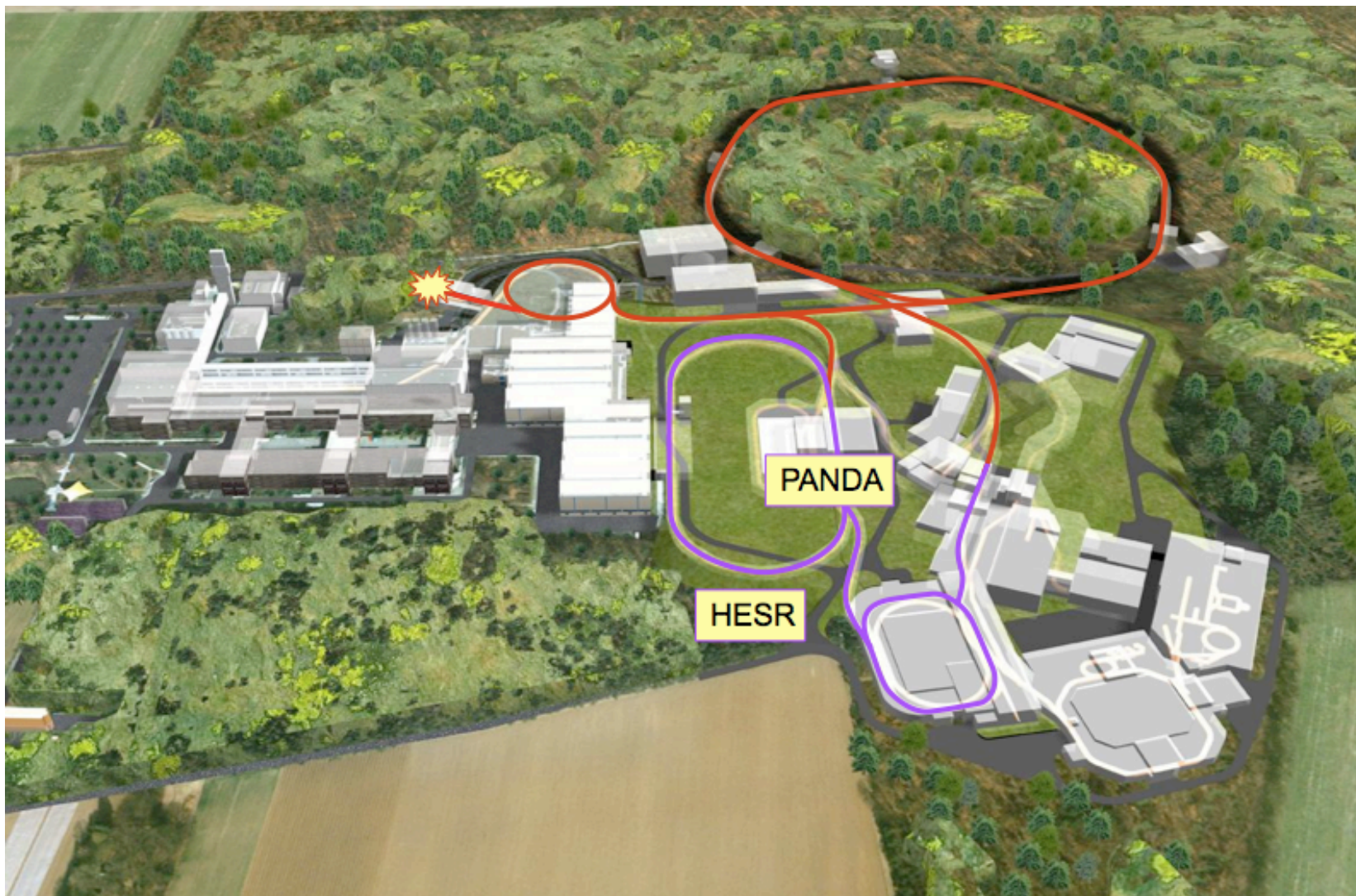


$8 \cdot 10^{11}$ \bar{p} per stack
 accumulation rate $4 \cdot 10^{10}$ \bar{p}/h
 \bar{p} accumulated at 8.9 GeV/c and decelerated decreasing dipole current "fine scan" using stochastic cooling

Initial beam intensity 10^{12} \bar{p}
 Gas jet target density $10^{12} \div 10^{14}$ atoms/cm³
 to keep luminosity constant $2 \cdot 10^{31}$ cm⁻²sec⁻¹
 Momentum spread $\Delta p/p$ $10^{-4} \rightarrow \sigma(\sqrt{s})$ 200 KeV

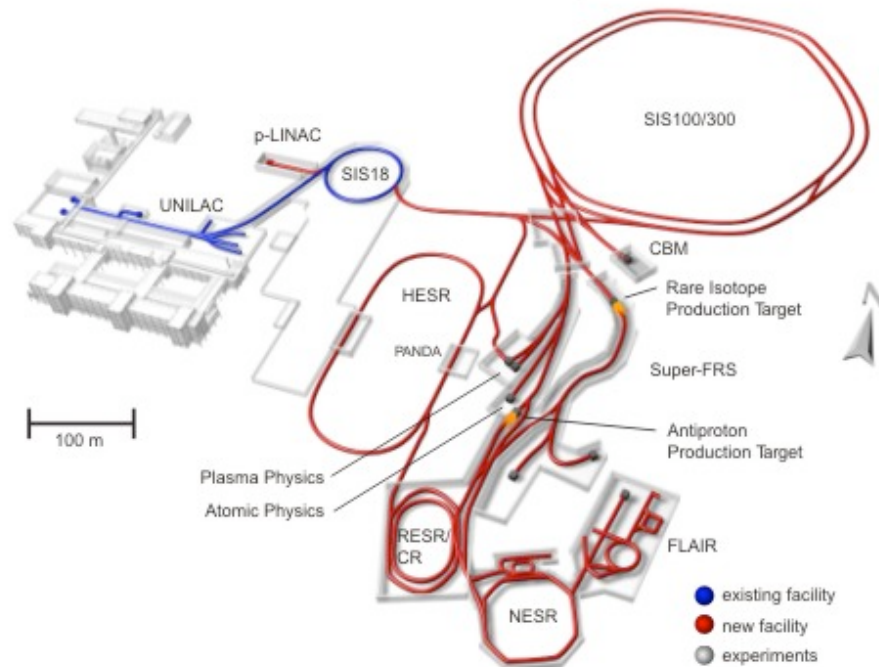


Artistic view of FAIR



The Facility

FAIR Facility for **A**ntiproton and **I**on **R**esearch



Antiproton production

- Proton Linac 50 MeV
- Accelerate p in SIS18 / 100
- Produce \bar{p} on Cu target
- Collect in CR, cool in RESR

Primary Beams

- $10^{12}/s$; 1.5-2 GeV/u; $^{238}\text{U}^{28+}$
- Factor 100-1000 over present intensity
- $2 \times 10^{13}/s$ 30 GeV protons up to 90 GeV
- $10^{10}/s$ $^{238}\text{U}^{73+}$ up to 35 GeV/u
- 50 MeV new proton Linac

Secondary Beams

- Broad range of radioactive beams up to 1.5 - 2 GeV/u
- Intensity up to factor 10 000 over present
- Antiprotons 1.5 - 15 GeV/c

Storage and Cooler Rings

- 10^{11} stored and cooled 0.8 - 14.5 GeV antiprotons

Parallel operation

- up to 4 different independent experiments

The High Energy Storage Ring

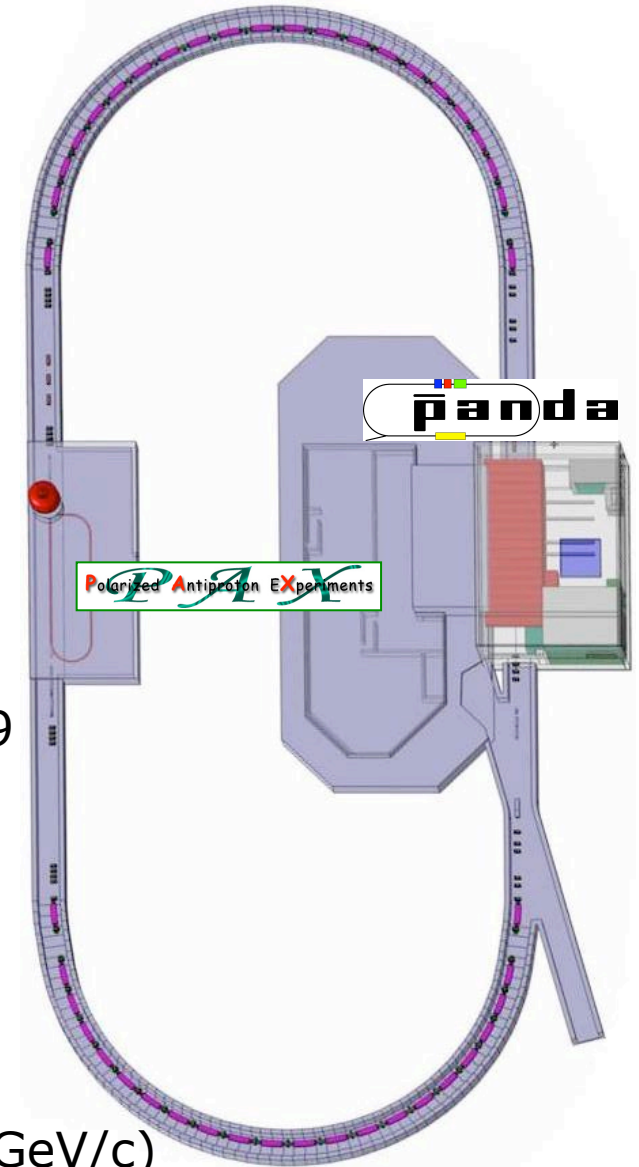
- Circumference 574 m
- $P_{\text{beam}} = 1,5 - 15 \text{ GeV/c}$
- $N_{\text{stored}} = 5 \times 10^{10} \bar{p}$
- Internal thick Target $4 \times 10^{15} \text{ cm}^{-2}$
- Beam lifetime $> 30 \text{ min}$

High resolution mode

- $\delta p/p \sim 4 \times 10^{-5}$ (electron cooling up to 8.9 GeV/c)
- Luminosity = $10^{31} \text{ cm}^{-2} \text{ s}^{-1}$

High luminosity mode

- Luminosity = $2 \times 10^{32} \text{ cm}^{-2} \text{ s}^{-1}$
- $\delta p/p \sim 10^{-4}$ (stochastic cooling from 3.8 GeV/c)

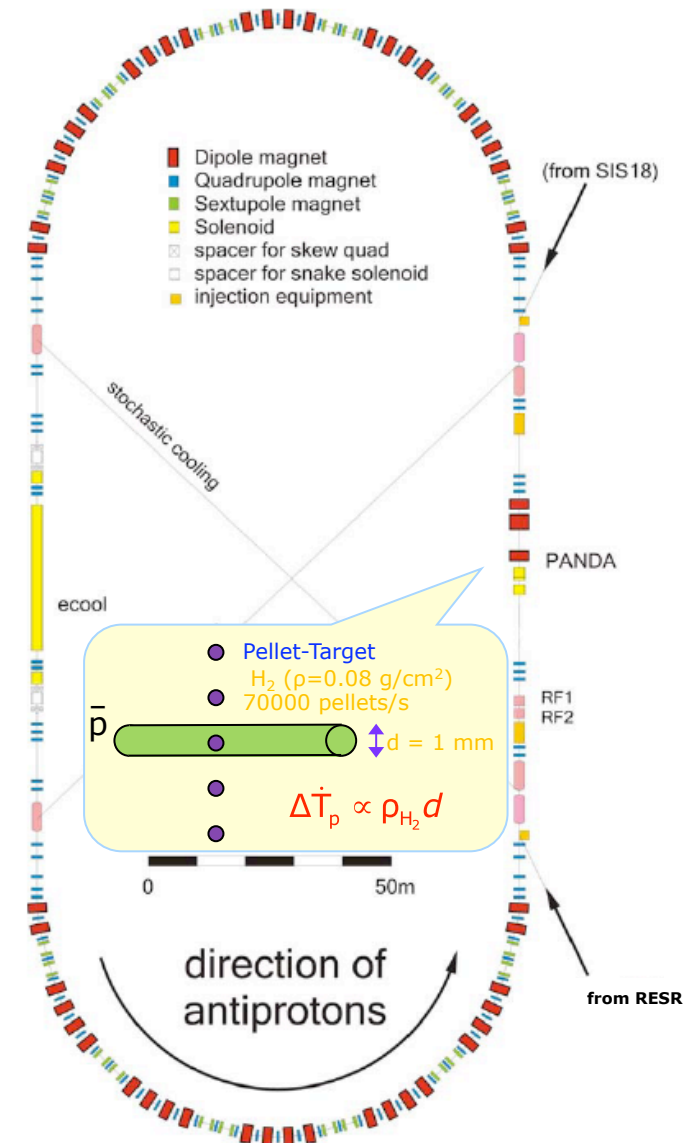


The HESR operation

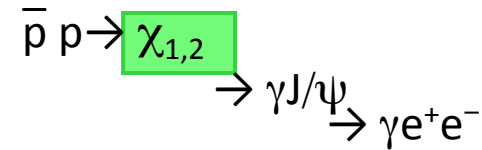
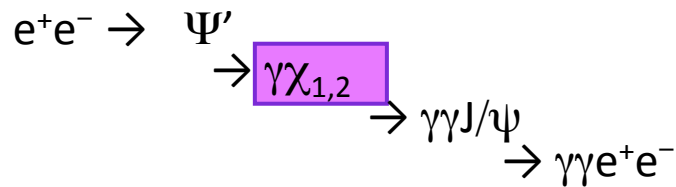
Effective target thickness (pellets): $4 \times 10^{15} \text{ cm}^{-2}$

Beam radius at target (r_{ma}): 0.3 mm

	High Resolution Mode	High Luminosity Mode
Momentum range	1.5 – 8.9 GeV/c	1.5 – 15 GeV/c
Number of antiprotons	10^{10}	10^{11}
Peak luminosity	$2 \times 10^{31} \text{ cm}^{-2} \text{ s}^{-1}$	$2 \times 10^{32} \text{ cm}^{-2} \text{ s}^{-1}$
Momentum resolution (r _{ma})	$\Delta p/p \leq 4 \times 10^{-5}$	$\Delta p/p \leq 1 \times 10^{-4}$
Beam cooler	Electron $\leq 8.9 \text{ GeV/c}$	Stochastic $\geq 3.8 \text{ GeV/c}$



Antiproton's power

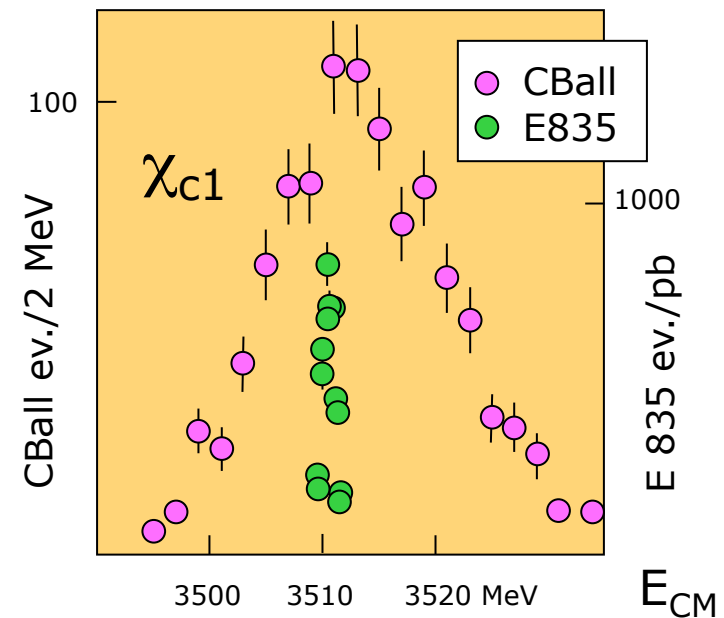


- e^+e^- interactions:

- Only 1^{--} states are formed
- Other states only by secondary decays (moderate mass resolution)

- $\bar{p}p$ reactions:

- All states directly formed (very good mass resolution)

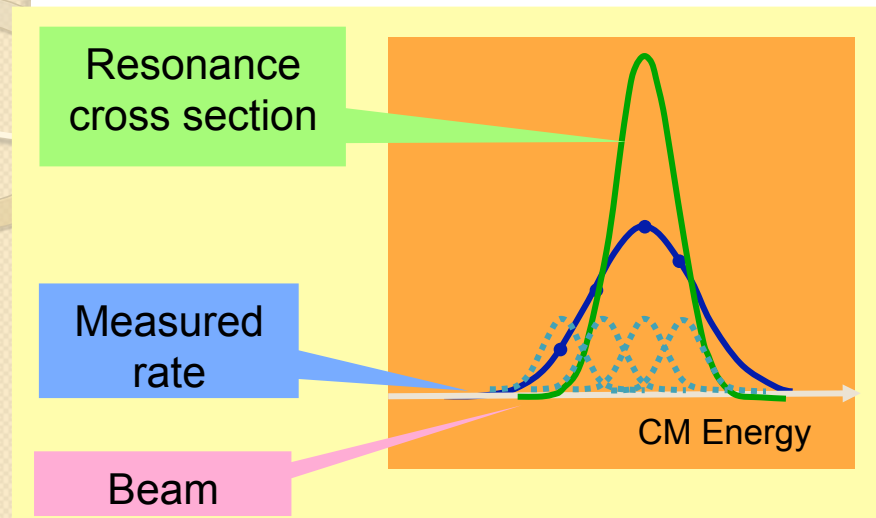


$$\text{Br}(\bar{p}p \rightarrow \eta_c) = 1.2 \cdot 10^{-3}$$

$$\text{Br}(e^+e^- \rightarrow \psi) \cdot \text{Br}(\psi \rightarrow \gamma\eta_c) = 2.5 \cdot 10^{-5}$$

Antiproton's power

\bar{p} -beams can be cooled → Excellent resonance resolution



- e^+e^- : typical mass res. ~ 10 MeV
- Fermilab: 240 keV
- HESR: ~ 30 keV

The production rate of a certain final state ν is a convolution of the **BW cross section** and the **beam energy distribution function $f(E, \Delta E)$** :

$$\nu = L_0 \left\{ \epsilon \int dE f(E, \Delta E) \sigma_{BW}(E) + \sigma_b \right\}$$

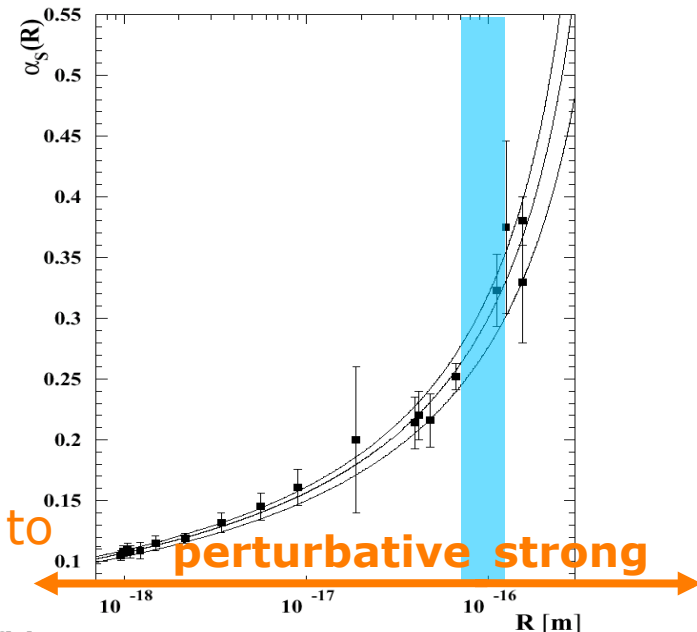
The resonance mass M_R , total width Γ_R and product of branching ratios into the initial and final state $B_{in} B_{out}$ can be extracted by measuring the formation rate for that resonance as a function of the cm energy E .

Antiproton Scientific Program

The opportunities offered by antiprotons aim to clarify some open problems related with QCD

- ▶ Why we do not observe free quarks?
Charmonium spectroscopy
→ quark confinement
- ▶ Why only color singlet are allowed?
Hadrons (qqq or $q\bar{q}$)
Gluonic excitations
Multi-quark systems
- ▶ Which is the mechanism giving mass to hadrons?
Partial restoration of chiral symmetry → $\bar{p}A$ interaction
Meson properties in the nuclear medium
- ▶ Which is the structure of the Nucleon?
Hard scattering processes & soft fragmentation → From partons to hadrons

Strong coupling constant vs R



QCD

The \bar{P} ANDA Physics Program

The \bar{P} ANDA (\bar{P} ANihilation at D Armstadt) scientific program covers a wide range of physics topics

- QCD Bound States: ordinary and extra-ordinary;
- Non-perturbative QCD Dynamics;
- Structure of the nucleon using electromagnetic processes;
- Hadrons in Nuclear Medium;
- Hypernuclear Physics;
- Electroweak Physics;



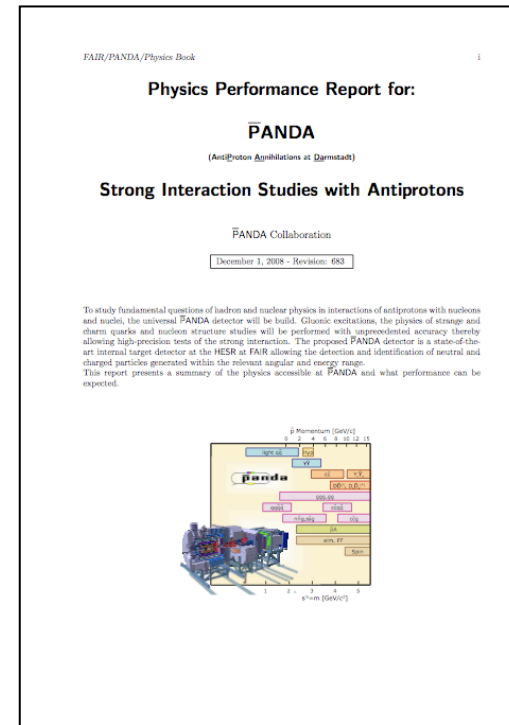
23 benchmark channels, related to these topics, have been identified

The $\bar{\text{P}}\text{ANDA}$ Physics Book

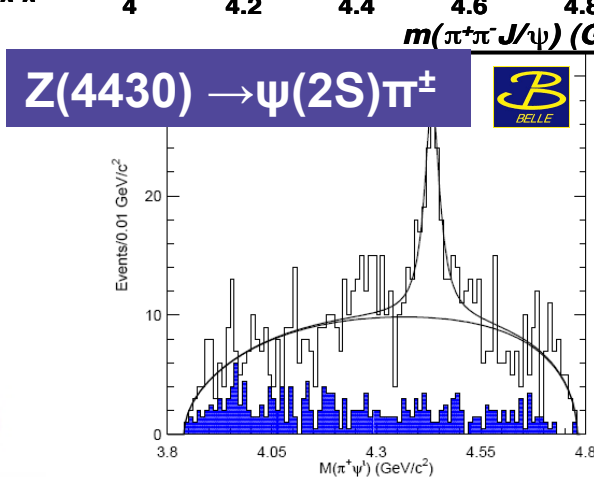
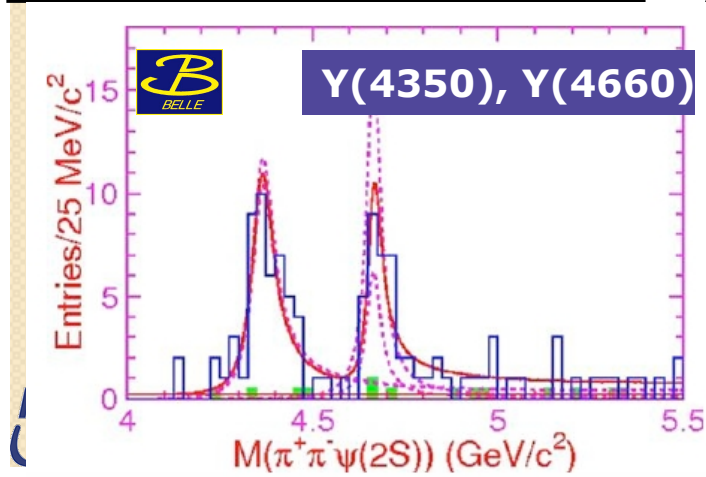
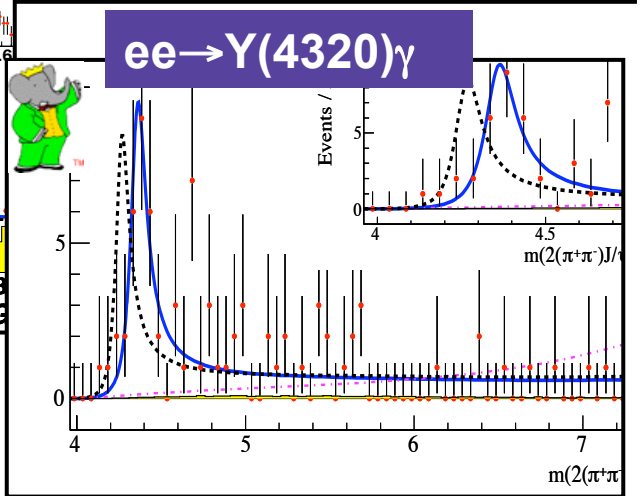
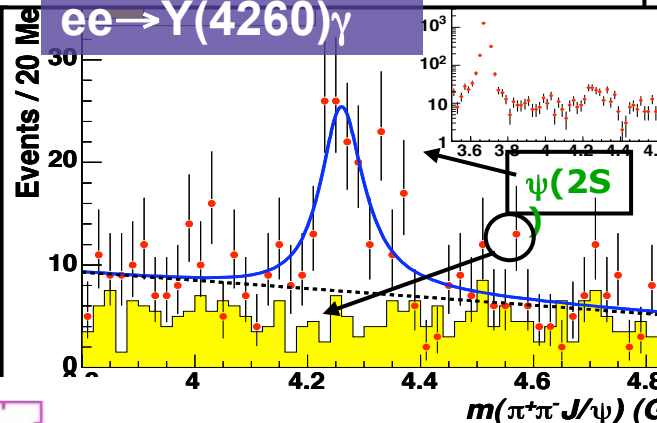
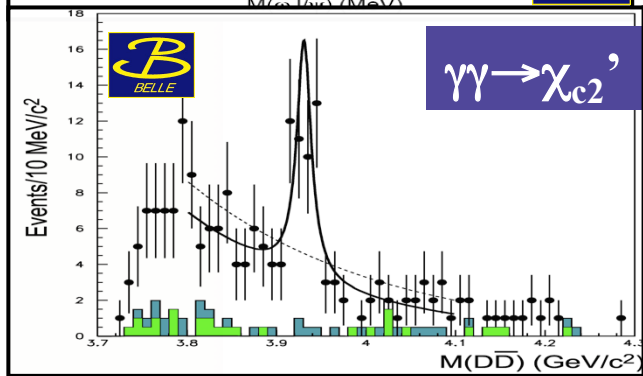
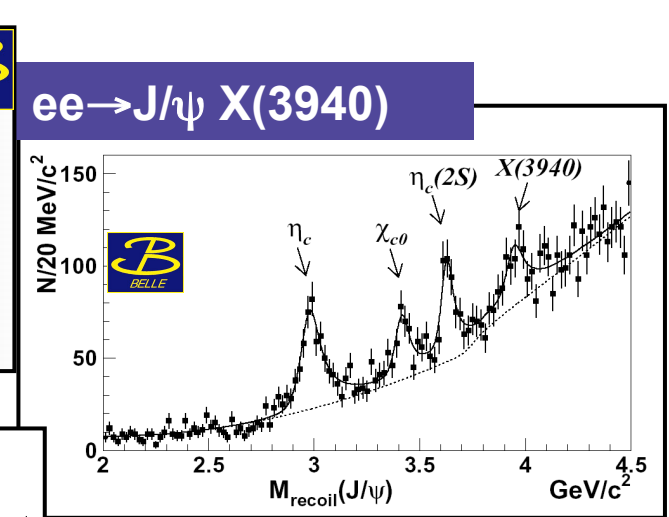
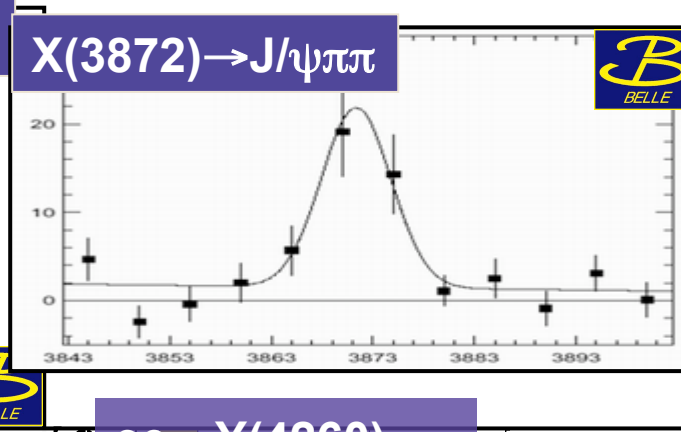
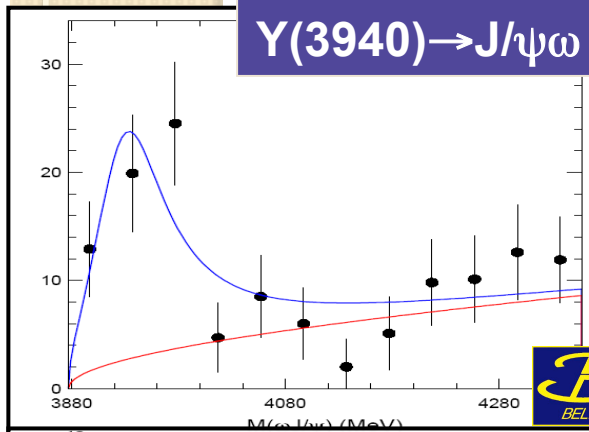
2008 has seen a big effort of the Collaboration preparing the $\bar{\text{P}}\text{ANDA}$ Physics Book.

More than 200 pages have been produced to describe **all the aspects of the scientific program.**

1.2 Billion of simulated events have been produced to **evaluate detector performance on many benchmark channels.**



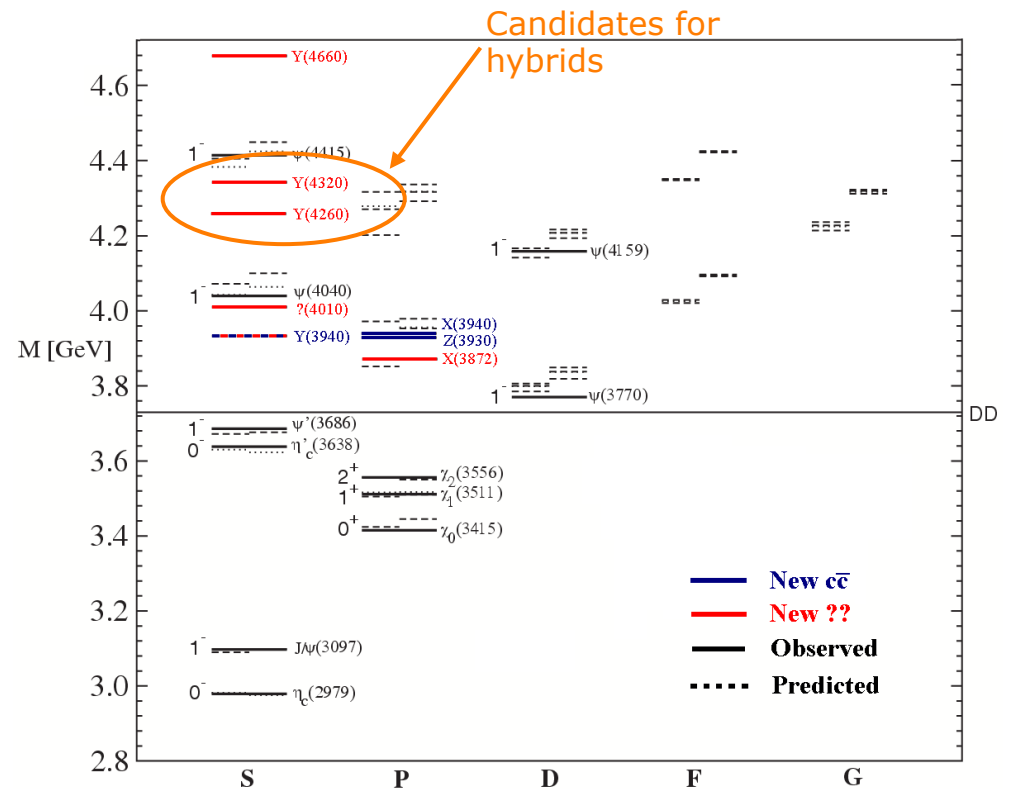
New states at B-factories



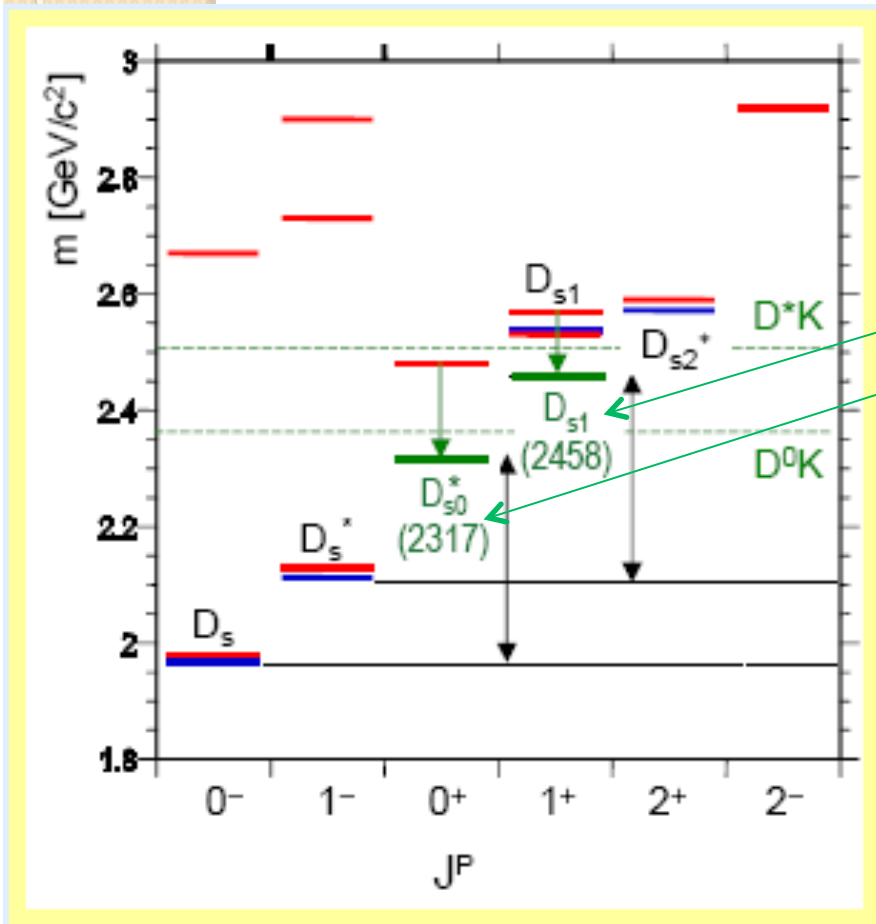
Charmonium and charmonium like states

Several states denoted as X , Y and Z have been recently detected, mainly at B-factories. Some of them do not fit the charmonium spectrum and an intense debate is going on about which could be exotics.

These states can be detected with the PANDA spectrometer with sufficient event rates and background suppression.



Open Charm states



- Potential model —
- Old measurements —
- New observations (BaBar, CLEO-c, Belle) —

- Open charm states are the QCD analogue of hydrogen atom for QED
- Narrow states $D_{s0}(2317)$ and $D_{s1}(2458)$ recently discovered at B-factories do not fit theoretical calculations.
- Quantum numbers for the newest states $D_{sJ}(2700)$ and $D_{sJ}(2880)$ are open
- At full luminosity \bar{p} annihilation at momenta larger than 6.4 GeV/c will produce large numbers of $D\bar{D}$ pairs.
- Despite small signal/background ratio (5×10^{-6}) background situation favorable because of limited phase space for additional hadrons in the same process.

Benchmark channels

Benchmark channels involving charmonium

Benchmark channels involving open charm

$$\begin{aligned} \bar{p}p &\rightarrow J/\Psi\omega \rightarrow e^+e^-\pi^+\pi^-\pi^0 \\ \bar{p}p &\rightarrow J/\Psi\pi^+\pi^- \rightarrow e^+e^-\pi^+\pi^- \\ \bar{p}p &\rightarrow J/\Psi\pi^0\pi^0 \rightarrow e^+e^-4\gamma \\ \bar{p}p &\rightarrow J/\Psi\eta \rightarrow e^+e^-2\gamma \\ \bar{p}p &\rightarrow J/\Psi\gamma \rightarrow e^+e^-\gamma \\ \bar{p}p &\rightarrow \chi_{c1}\gamma \rightarrow J/\Psi\gamma\gamma \rightarrow e^+e^-2\gamma \\ \bar{p}p &\rightarrow \psi(2S)\pi^+\pi^- \\ \bar{p}p &\rightarrow \tilde{\eta}_{c1}\eta \rightarrow \chi_{c0}\pi^0\pi^0\eta \\ \bar{p}p &\rightarrow h_c \rightarrow \eta_c\gamma \rightarrow \phi\phi\gamma \\ \bar{p}p &\rightarrow h_c \rightarrow \eta_c\gamma \rightarrow 3\gamma \end{aligned}$$

$$\begin{aligned} \bar{p}p &\rightarrow \psi(3770) \rightarrow D^+D^- \\ \bar{p}p &\rightarrow \psi(4040) \rightarrow D^{*+}D^{*-} \\ \bar{p}p &\rightarrow \tilde{\eta}_{c1}\eta \rightarrow D^0\bar{D}^{*0}\eta \end{aligned}$$

Y(3940)

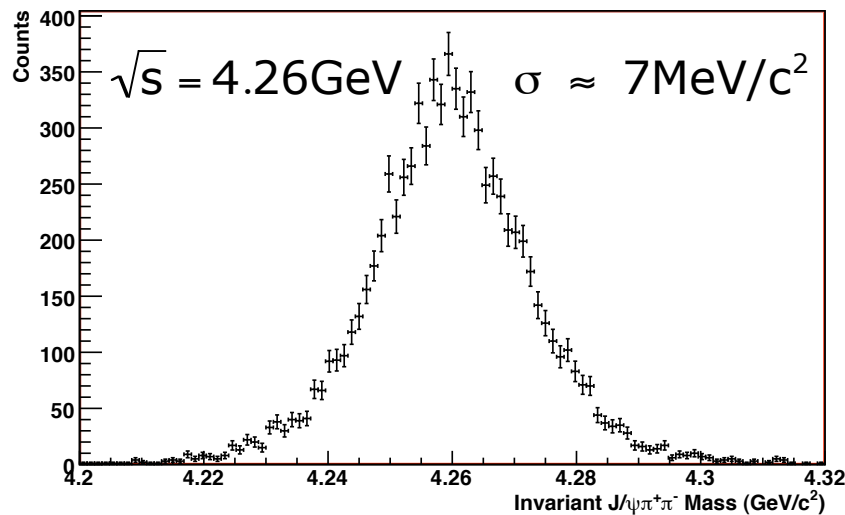
X(3872), Y(4260)

Y(4350), Y(4660)

Y(4260)

The reaction $\bar{p}p \rightarrow J/\Psi\pi^+\pi^- \rightarrow e^+e^-\pi^+\pi^-$ has been simulated at different c.m. energies.

Here the **results related with Y(4260)**, 1^{--} state observed by Babar in initial state radiation events are reported.



\sqrt{s} [GeV]	Eff [%]
3.526	28
3.686	31
3.872	32
4.260	33
4.600	31
5.000	30

signal channel: $\bar{p}p \rightarrow J/\Psi\pi^+\pi^- \rightarrow e^+e^-\pi^+\pi^-$

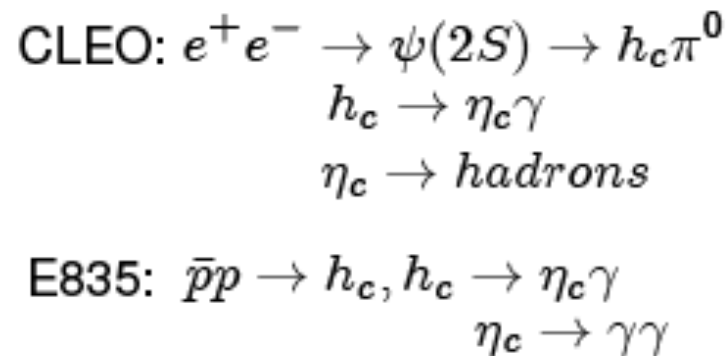
main background: $\bar{p}p \rightarrow \pi^+\pi^-\pi^+\pi^-$ $\sigma = 50 \mu\text{b}$ at $\sqrt{s} = 4.26 \text{ GeV}$

final S/B ratio 2

Analysis done by
E. Fioravanti

h_c

The determination of this state is extremely important since it is related to the **spin contribution of the confinement potential**.
two recent measurements report: $M=3525$ MeV, Γ unknown



Channel	σ (nb)
$\bar{p}p \rightarrow \pi^0 \pi^0$	31.4
$\bar{p}p \rightarrow \pi^0 \gamma$	1.4
$\bar{p}p \rightarrow \pi^0 \eta$	33.6
$\bar{p}p \rightarrow \eta \eta$	34.0
$\bar{p}p \rightarrow \pi^0 \eta'$	50.0

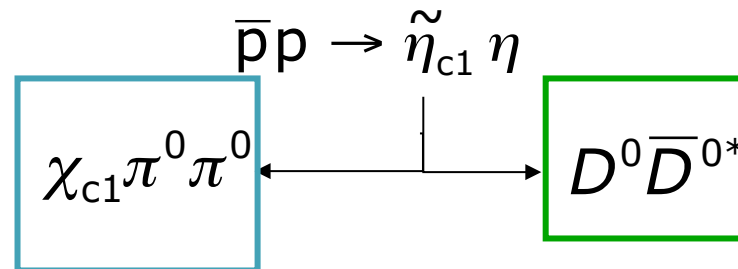
main background contribution to the channel $h_c \rightarrow \eta_c \gamma \rightarrow \gamma\gamma$

Channel	S/B ratio
$\bar{p}p \rightarrow \pi^0 \pi^0$	> 94
$\bar{p}p \rightarrow \pi^0 \gamma$	> 164
$\bar{p}p \rightarrow \pi^0 \eta$	> 88
$\bar{p}p \rightarrow \eta \eta$	> 87
$\bar{p}p \rightarrow \pi^0 \eta'$	> 250

S/B ratio in the hypothesis of signal $\sigma=33$ nb

Exotic states

PANDA strategy to look for an hypothetical hybrid $\tilde{\eta}$ ($J^{PC}=1^{-+}$, mass $\sim 4.3 \text{ GeV}/c^2$, width 20 MeV) is that of searching it in the channels:



Signal &
Background reactions

B

$\bar{p}p \rightarrow$		B
$\tilde{\eta}_{c1} \eta$	33 pb	$0.82\% \times \mathcal{B}(\tilde{\eta}_{c1} \rightarrow \chi_{c1} \pi^0 \pi^0)$
$\chi_{c0} \pi^0 \pi^0 \eta$		0.03 %
$\chi_{c1} \pi^0 \eta \eta$		0.32 %
$\chi_{c1} \pi^0 \pi^0 \pi^0 \eta$		0.81 %
$J/\psi \pi^0 \pi^0 \pi^0 \eta$		2.26 %

Signal &
Background reactions

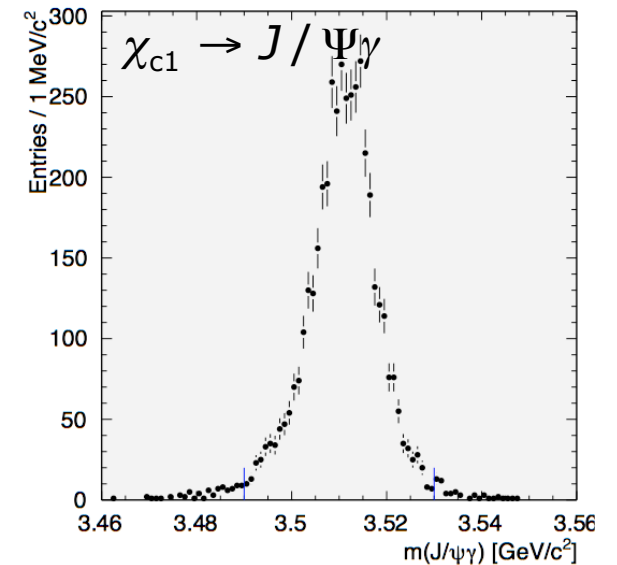
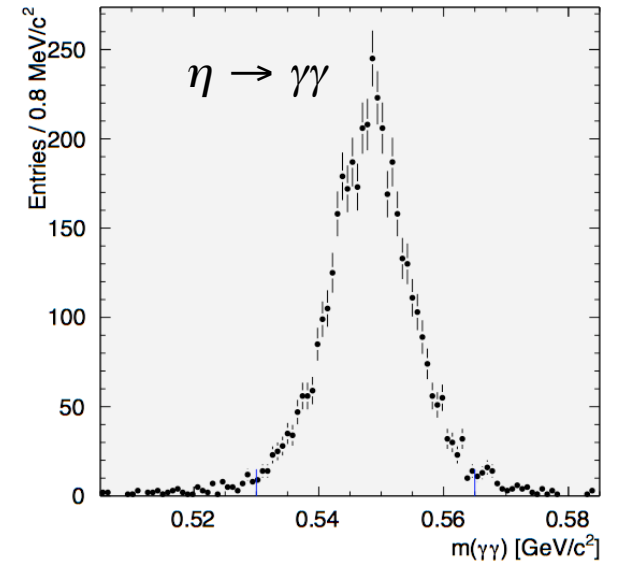
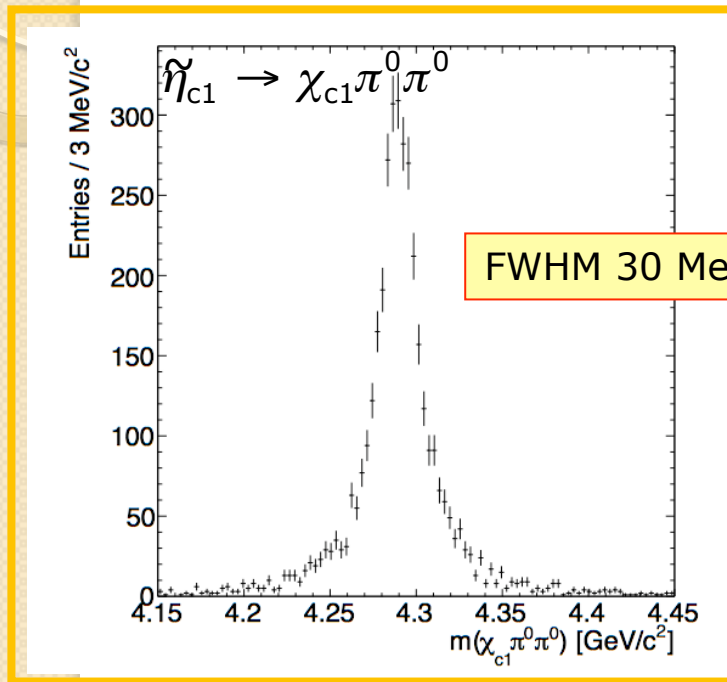
B

$\bar{p}p \rightarrow$	B
$\tilde{\eta}_{c1} \eta$	$0.47\% \times \mathcal{B}(\tilde{\eta}_{c1} \rightarrow D^0 \bar{D}^{*0})$
$D^0 \bar{D}^{*0} \eta$	$3.2\% \times \mathcal{B}(D^0 \rightarrow K^- \pi^+ \pi^0 \pi^0) = 0.16\%*$
$D^0 \bar{D}^{*0} \pi^0$	1.17%

Charmonium hybrid

$$\bar{p}p \rightarrow \tilde{\eta}_{c1} \eta$$

$$\chi_{c1} \pi^0 \pi^0$$



We generated $2 \cdot 10^5$ events at 15 GeV/c with:

$$\chi_{c1} \rightarrow J/\Psi \gamma$$

$$\searrow$$

$$e^+ e^-$$

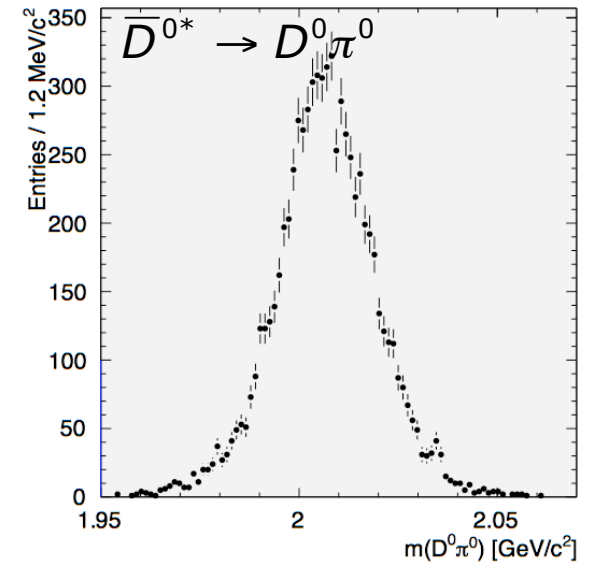
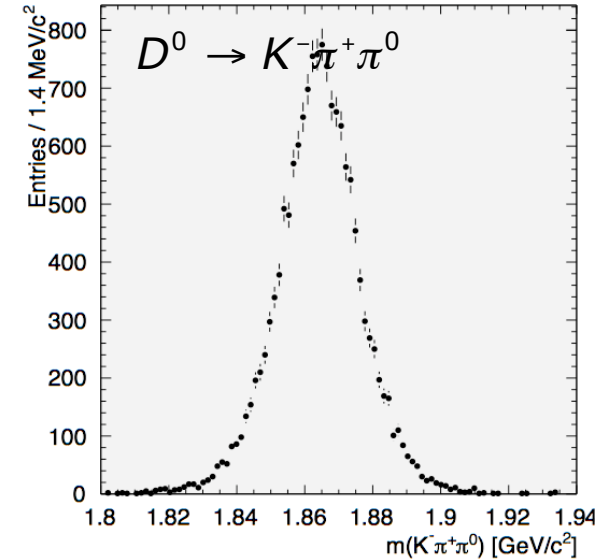
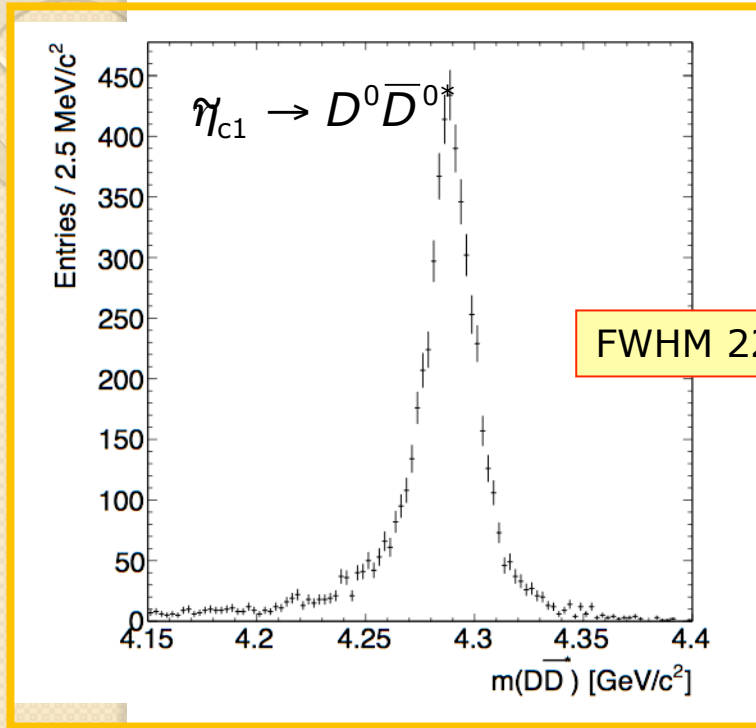
9C fit: beam, η , χ_{c1} , J/Ψ and π^0 mass constraints.
 Final reconstruction efficiency 6,83%,
 background suppression 10^3

Analysis done by
 M. Pelizäus

Charmonium hybrid

$$\bar{p}p \rightarrow \tilde{\eta}_{c1} \eta$$

$$\rightarrow D^0 \bar{D}^{0*}$$



We generated $1 \cdot 10^6$ events at 15 GeV/c with

$$\bar{D}^{0*} \rightarrow D^0 \pi^0 \quad D^0 \rightarrow K^- \pi^+ \pi^0 \quad \eta \rightarrow \gamma\gamma$$

11C fit: beam, D^0 , D^{0*} , η and π^0 mass constraints.

Final reconstruction efficiency 5,17%,
background suppression 10^5

Analysis done by
M. Pelizäus

$\bar{p}p \rightarrow D\bar{D}$ reconstruction

The main focus of this benchmark study is to check the ability to separate the charm signal from the large hadronic background

In order to study the tracking and PID reconstruction capabilities of the \bar{P} ANDA detector, two benchmark channels have been chosen with decays containing only charged particles

$$\bar{p}p \rightarrow D^+D^-$$
$$\hookrightarrow K^-\pi^+\pi^-$$

$$\bar{p}p \rightarrow D^{*+}D^{*-}$$
$$\hookrightarrow D^0\pi^+$$
$$\hookrightarrow K^-\pi^+$$

Both channels were simulated at a beam energy corresponding to $\sqrt{s} = m$, the $\Psi(3770)$ for the D^+D^- channel, and the $\Psi(4040)$ for the $D^{*+}D^{*-}$ channel, respectively.

Resonance cross sections have been estimated from Breit-Wigner formula: scaling $\bar{p}p$ coupling from $J/\psi \rightarrow p\bar{p}$

$$\sigma_R(s) = \frac{4\pi\hbar^2 c^2}{s-2m_p^2 c^4} \frac{B_{in} B_{out}}{1 + (2(\sqrt{s} - M_R c^2)/\Gamma_R)^2}$$

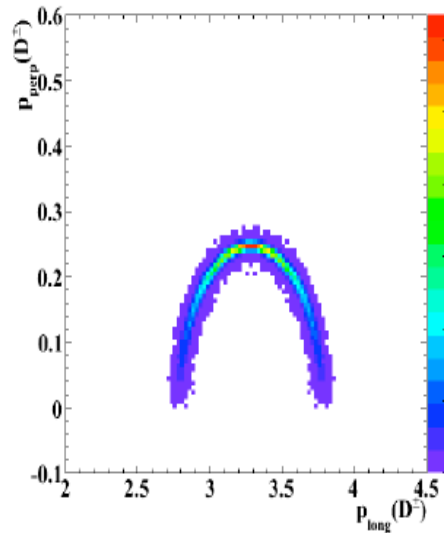
$$\sigma(\bar{p}p \rightarrow \Psi(3770) \rightarrow D^+D^-) = 3.9 \text{ nb}$$

$$\sigma(\bar{p}p \rightarrow \Psi(4040) \rightarrow D^{*+}D^{*-}) = 0.9 \text{ nb}$$

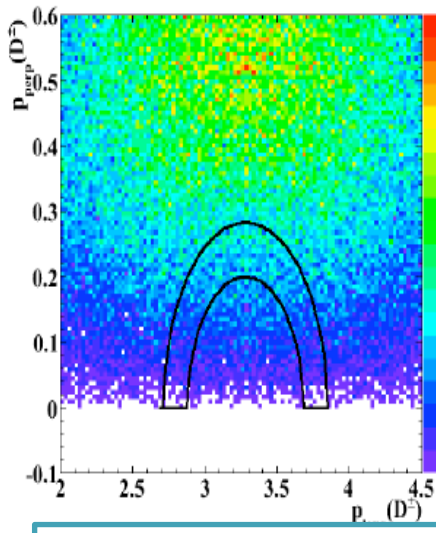
Results

2K $2(\pi^+\pi^-)$ background 10^6 larger than signal. Only cutting on vertex the bck can be reduced

p_T vs p_L signal



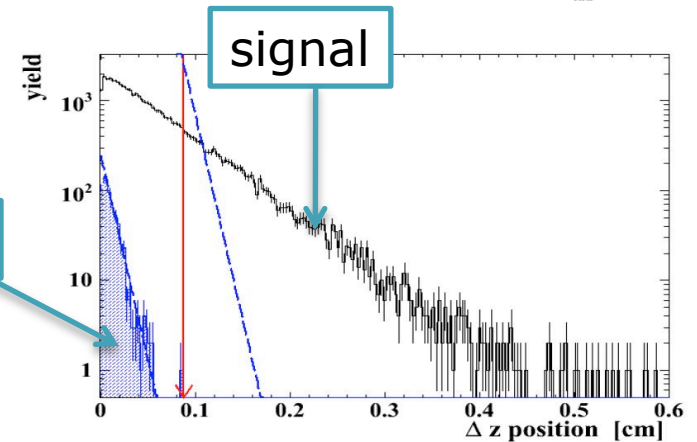
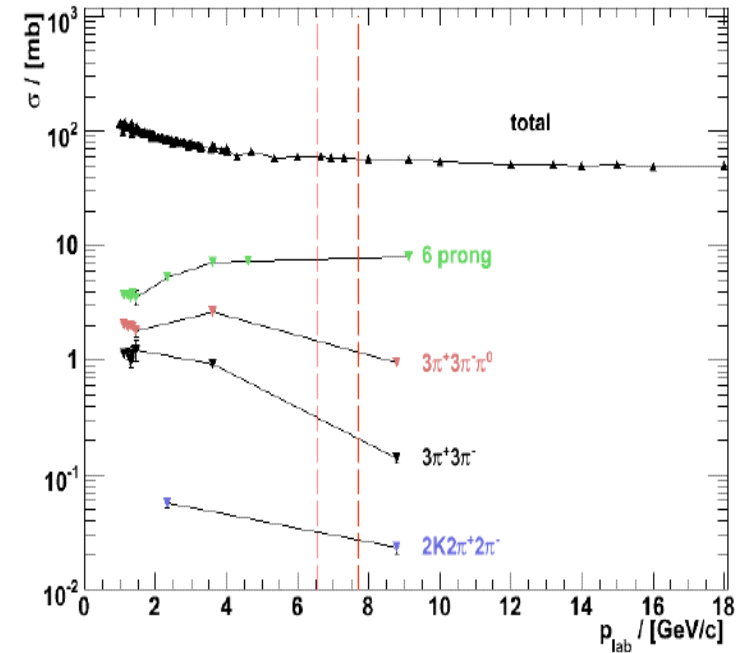
p_T vs p_L 2K4 π bck



bck 2k 4 π (scaled)

$\Delta z > 0.088$ cm
 $S/B = 1$ $\epsilon(\text{signal}) = 7.8\%$

$\bar{p}p \rightarrow X$ cross sections



Analysis done by
R. Jäkel

Baryonic Resonances

The agreement between QCD prediction and experimental results is even more poor in the Barionic sector.

Status of Ξ -resonances in PDG2008

Particle	$L_{2I,2J}$	Overall status	Status as seen in —				
			$\Xi\pi$	ΛK	ΣK	$\Xi(1530)\pi$	Other channels
$\Xi(1318)$	P_{11}	****					Decays weakly
$\Xi(1530)$	P_{13}	****	****				
$\Xi(1620)$		*	*				
$\Xi(1690)$		***		***	**		
$\Xi(1820)$	D_{13}	***	**	***	**	**	
$\Xi(1950)$		***	**	**		*	
$\Xi(2030)$	1	***		**	***		
$\Xi(2120)$		*		*			
$\Xi(2250)$		**					3-body decays
$\Xi(2370)$	1	**					3-body decays
$\Xi(2500)$		*		*	*		3-body decays

**** Existence is certain, and properties are at least fairly well explored.

*** Existence ranges from very likely to certain, but further confirmation is desirable and/or quantum numbers, branching fractions, *etc.* are not well determined.

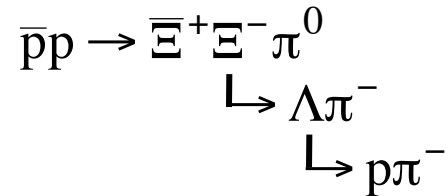
** Evidence of existence is only fair.

* Evidence of existence is poor.

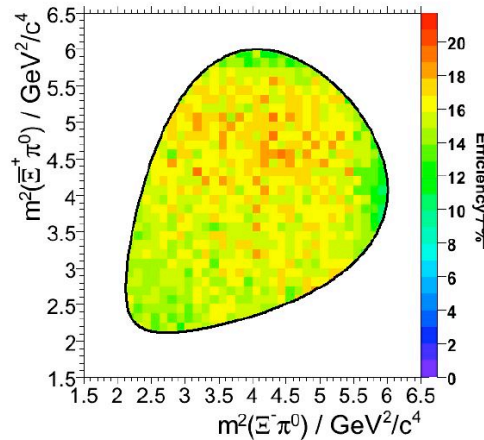
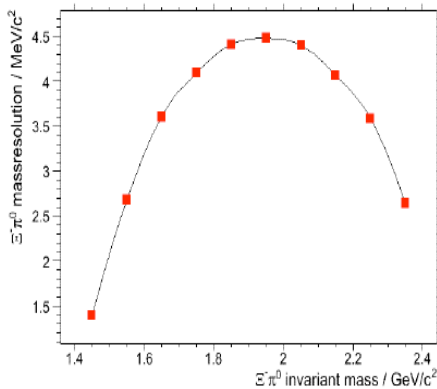
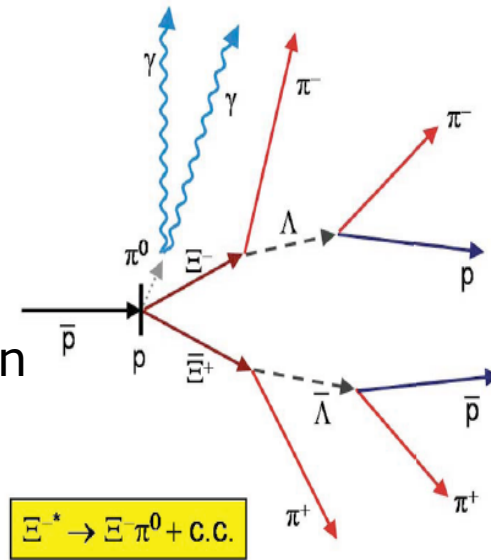
$\bar{p}p$ inelastic cross-section at 3 GeV/c is 53 mb with a ratio 1/1 between mesonic and barionic channels. At 12 GeV/c the ratio become ≈ 2.2

Baryon Spectroscopy

To test the ability of the PANDA spectrometer to deal with barionic states we studied:



at a beam momentum of 6.57 GeV/c where the cross-section $\bar{p}p \rightarrow \bar{\Xi}\Xi$ has been evaluated to be $0.3 \mu\text{b}$



Results of background studies:

- $S/B = 135$ for $\bar{p}p \rightarrow \bar{\Lambda} \Lambda \pi^+ \pi^- \pi^0$
- $S/B > 1896$ for $\bar{p}p \rightarrow \bar{\Sigma}(1385)^- \Sigma(1385)^+ \pi^0$
- $S/B > 47$ for $\bar{p}p \rightarrow \bar{p} p \pi^+ \pi^- \pi^+ \pi^- \pi^0$
- $S/B > 19$ for DPM generic

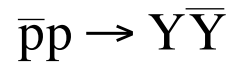
Analysis done by
J.Zohn

QCD dynamics

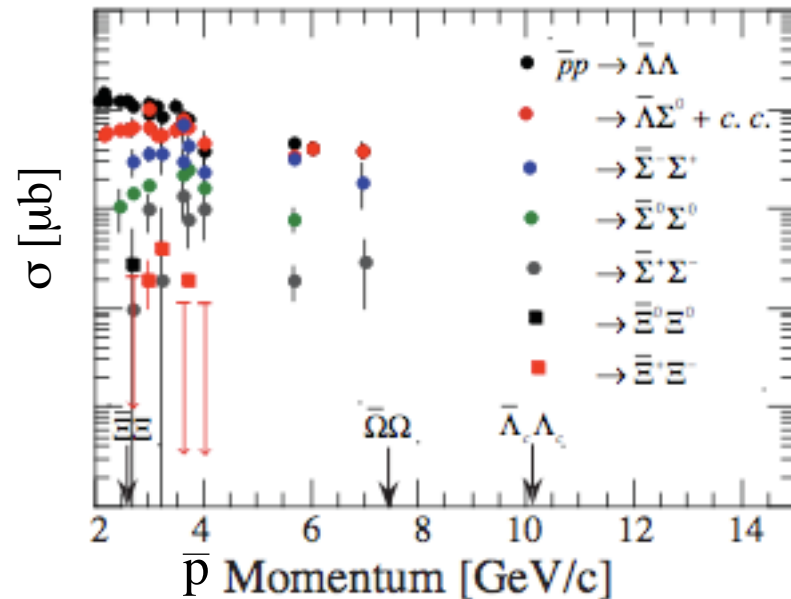
At high energy quarks and gluons degrees of freedom seem the right parameters to describe phenomena.

At the energy of $\bar{p}p$ collisions at HESR hadronic degrees seem more suited.

To understand the relative role of the 2 mechanisms we concentrated on the following channels:



Here to produce strangeness one has to produce an $s\bar{s}$ pair. This can be even extended to charmed hyperon.

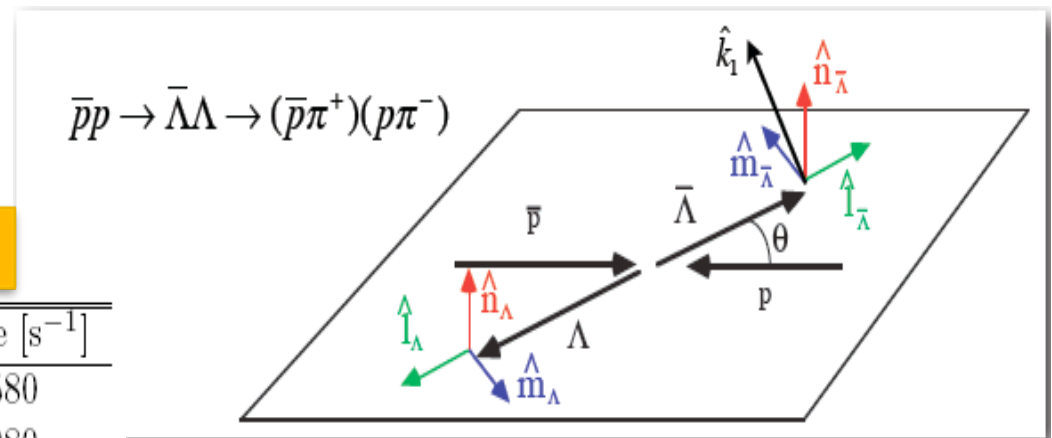


Finally, the parity violating weak decay of hyperons introduce an asymmetry in the distribution of the decay particles, allowing to access spin parameters.

$\bar{p}p \rightarrow \Lambda\bar{\Lambda}$

Estimated production rates

Momentum [GeV/c]	Reaction	Rate [s ⁻¹]
1.64	$\bar{p}p \rightarrow \Lambda\bar{\Lambda}$	580
4	$\bar{p}p \rightarrow \Lambda\bar{\Lambda}$	980
	$\bar{p}p \rightarrow \Xi^+\Xi^-$	30
15	$\bar{p}p \rightarrow \Lambda\bar{\Lambda}$	120



$$I_{\bar{\Lambda}\Lambda}(\theta, \hat{k}_1, \hat{k}_2) = \frac{I_0^{\bar{\Lambda}\Lambda}}{64\pi^3} \begin{bmatrix} 1 \\ +P_n(\bar{\alpha}k_{1n} + \alpha k_{2n}) \\ +C_{nn}(\bar{\alpha}\alpha k_{1n}k_{2n}) \\ +C_{nm}(\bar{\alpha}\alpha k_{1m}k_{2m}) \\ +C_{nl}(\bar{\alpha}\alpha k_{1l}k_{2l}) \\ +C_{ml}(\bar{\alpha}\alpha(k_{1m}k_{2l} + k_{1l}k_{2m})) \end{bmatrix}$$

- $I_0 = \sigma_{\text{tot}}$
- $I(\theta) = d\sigma/d\Omega$
- $P_n = \text{Polarisation}$
- $C_{ij} = \text{Spin correlations}$

Polarization can be determine from baryon emission angle of the weak Λ decay

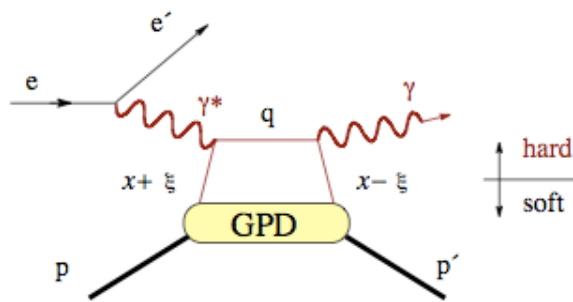
θ = C.M. scattering angle

\hat{k}_1, \hat{k}_2 = directional vectors of decay baryons

Nucleon Structure

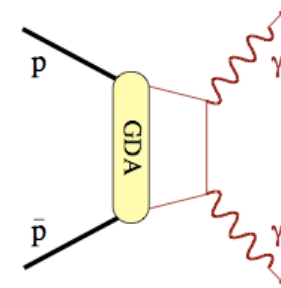
In the last year, it has been developed a solid QCD theoretical frame based on **Generalized Parton Distribution (GPD)** functions which describes different parton configurations in the nucleons.

Hand-bag diagram of DVCS



GPD formalism was successfully applied to describe DVCS phenomena, where it is possible to separate perturbative QCD hard process from the soft part of the diagram described by **GPD**

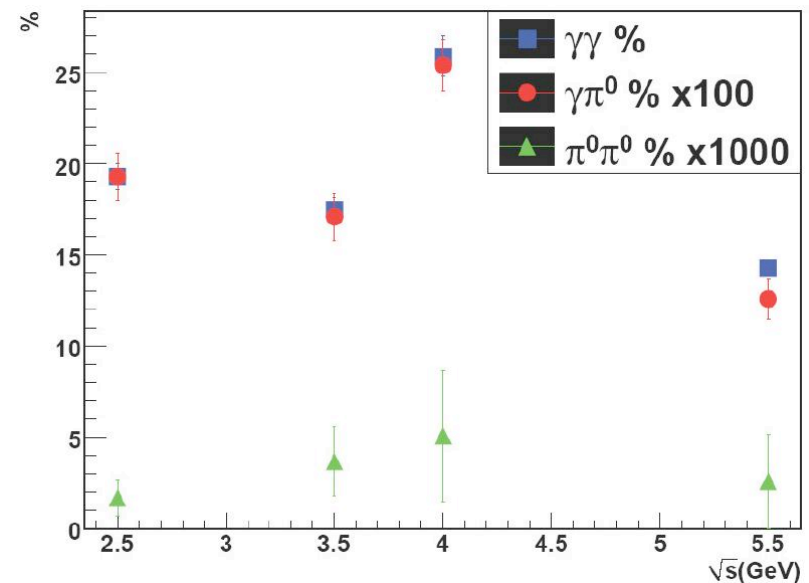
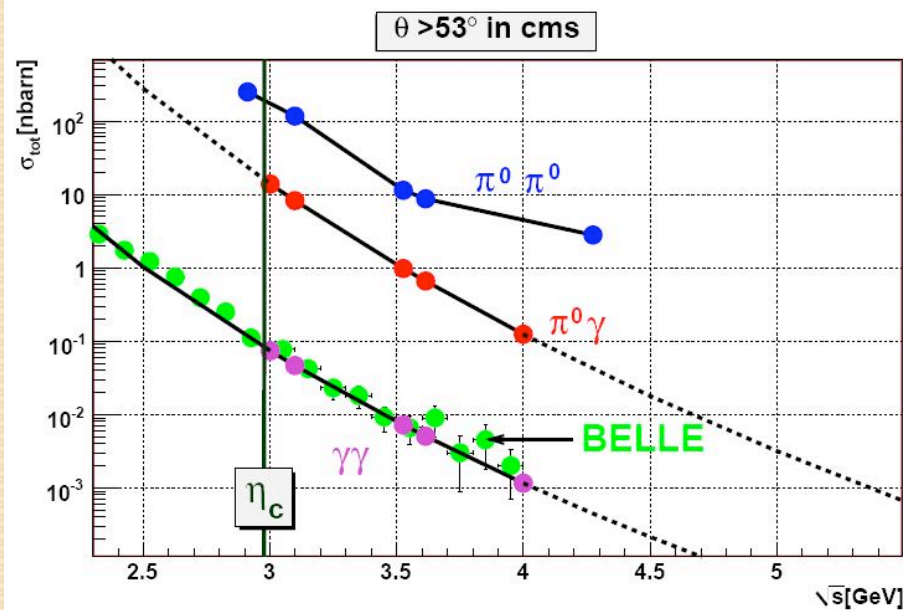
These concepts, applied to lepton scattering experiments, seem not to be universal, and can't be applied to WACS neither at very small nor at very large energies.



However, recent theoretical works have pointed out that the factorization technique in WACS could hold in the PANDA energy range.[EPJ A26 89 (2005), PLB B621 41(2005)]

$\bar{p}p \rightarrow \gamma\gamma$

Experimental challenge:
Detection of low energy photons in order
to suppress background from $\gamma\pi^0$, $\pi^0\pi^0$



The results of the simulations are encouraging, but better analyses should be developed.

Analysis done by
I. Brodski

Nucleon Structure: Form Factors

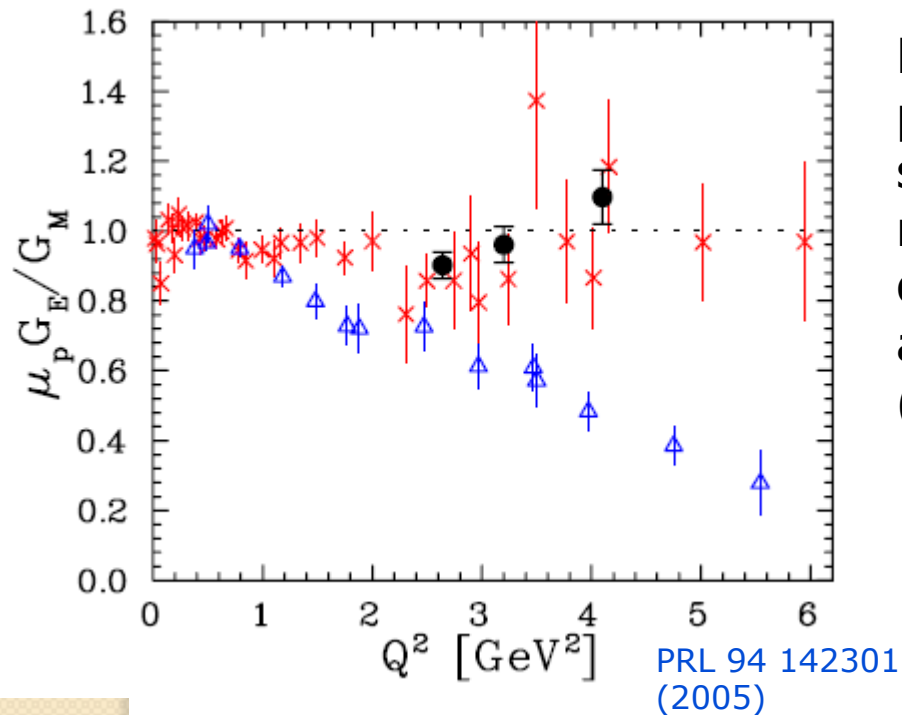
The idea is that of studying the process:

$$\bar{p}p \rightarrow e^+e^-$$

$$\frac{d\sigma}{d(\cos\theta^*)} = \frac{\pi\alpha^2\hbar^2c^2}{2xs} \left[|G_M|^2 (1 + \cos^2\theta^*) + \frac{4m_p^2}{s} |G_E|^2 (1 - \cos^2\theta^*) \right]$$

- FF are fundamental quantities of the nucleon (m , μ , ...)
- Understanding the Nucleon structure
- Comparison with Space-Like data that seems to show the non validity of the Born approximation
- Testing the hypothesis $G_E/G_M = 1$
- Intense theoretical activity

Space Like FF: present situation



Data on the ratio G_E/G_M for the proton including the older Rosenbluth separation data (**crosses**), most recent JLab Rosenbluth separation data (filled circles), and polarization transfer data (**triangles**)

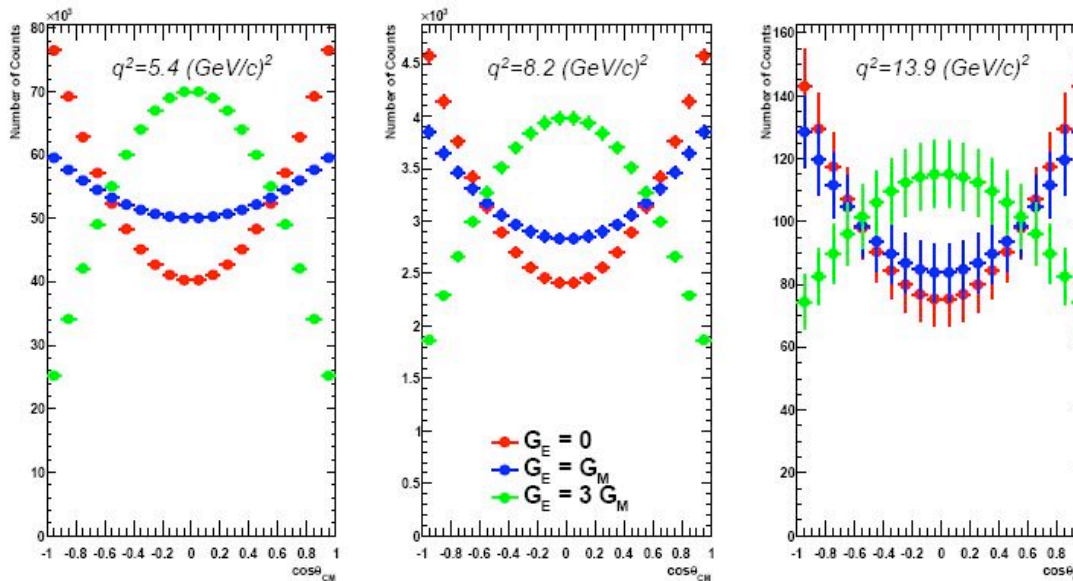
New Jlab data have been obtained with the recoil polarization method stating that:

$$\frac{G_E}{G_M} = -\frac{P_t}{P_l} \frac{(E_e + E_{e'})}{2m} \tan \frac{\theta_e}{2}$$

The old assumption $G(q^2) = \left(1 + \frac{q^2}{\lambda_D^2}\right)^{-2}$ seems no more valid

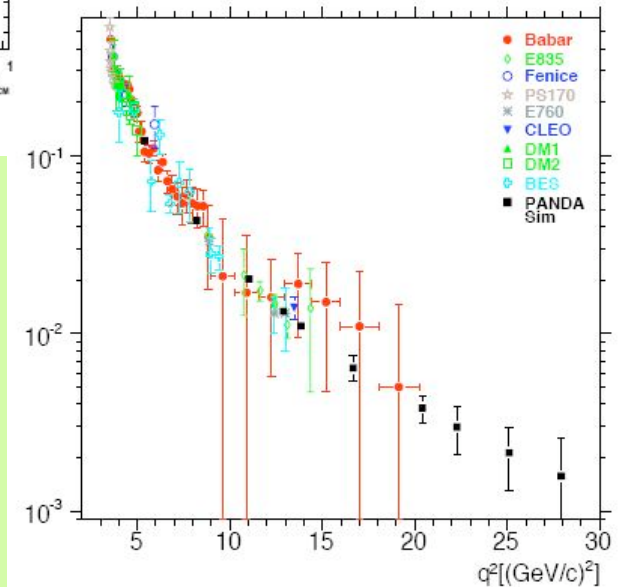
$$\lambda_D^2 = 0.71 \text{GeV}^2$$

Time Like FF



**2 fb $^{-1}$ for each q^2
with PANDA**

- With \bar{P} ANDA we will have access to almost total angular range
- Direct access to $|G_M(q^2)|$ and $|G_E(q^2)|$
- The sensitivity to $|G_E(q^2)|$ decreases while energy increase
- **2 γ** : odd $\cos \theta$ contributions in the CM

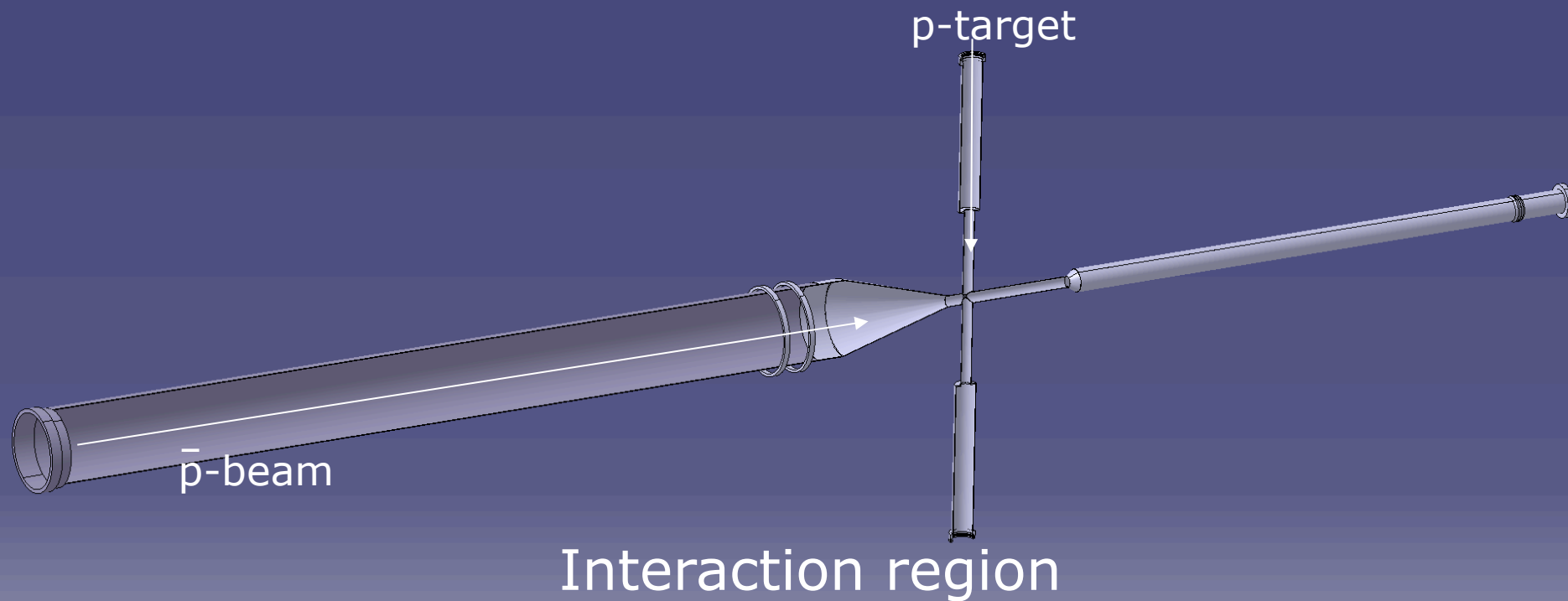


Plans for the TL FF

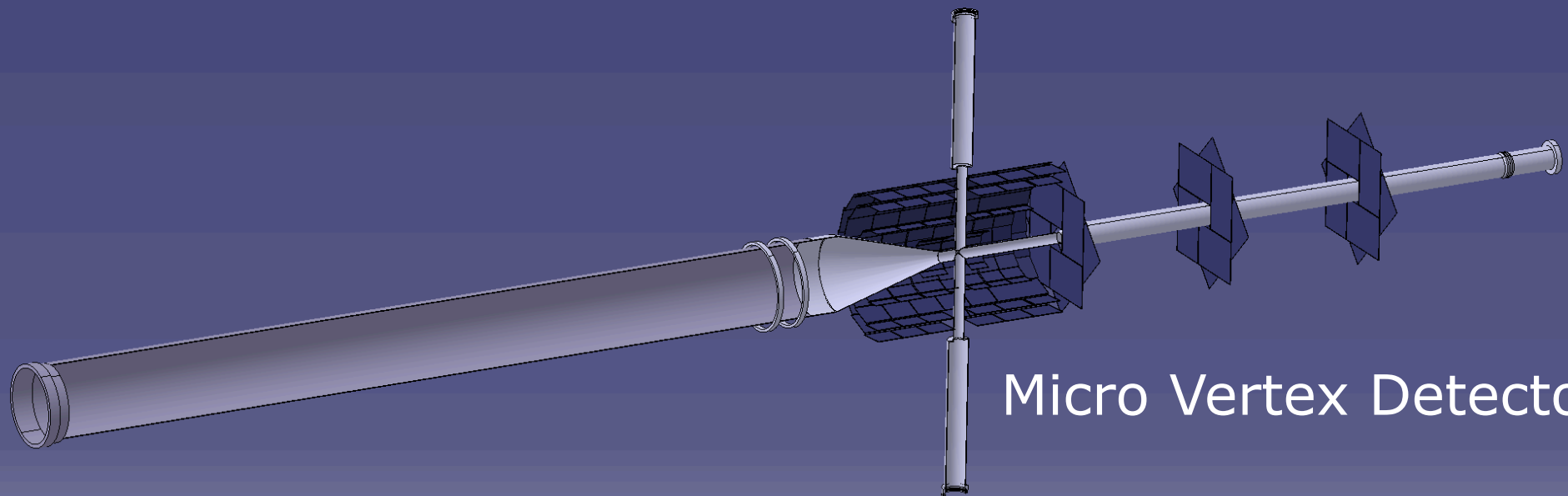
- Separate measurement of $|G_E|$ et $|G_M|$
- Precisions on the ratio $R=|G_E|/|G_M|$ and σ_R
 - $\Delta R/R < 1\%$ at low Q^2
 - $\Delta R/R = 10\%$ at $Q^2=10$ (GeV/c)²
 - Separation possible up to $Q^2=15$ (GeV/c)²
- Test of the 1γ hypothesis (symmetry of the angular distribution)
- Measure $|G_M|$ up to $Q^2=25$ (GeV/c)²
- Possibility to measure the phase difference $\varphi(G_E) - \varphi(G_M)$ in case of transverse polarization
- Double spin asymmetry will allow the independent measurements of G_E and G_M

PAX program

The \bar{P} ANDA Spectrometer



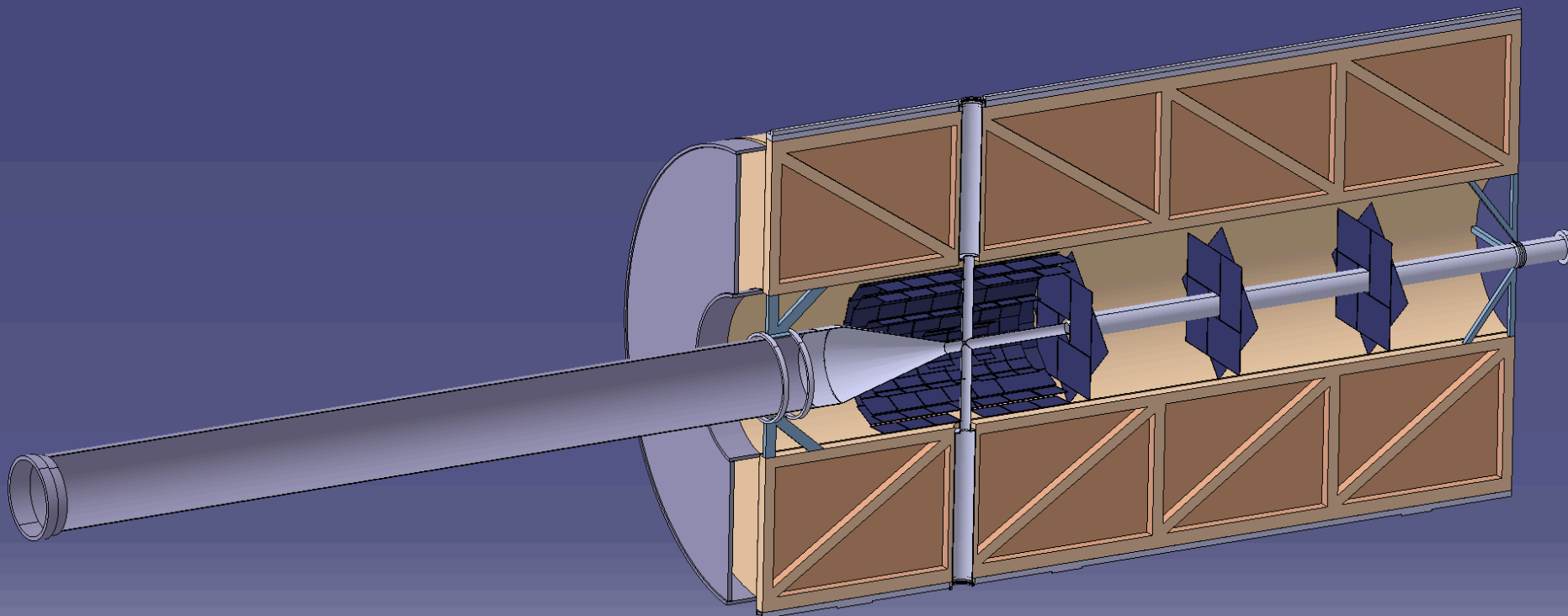
The \bar{P} ANDA Spectrometer



Micro Vertex Detector

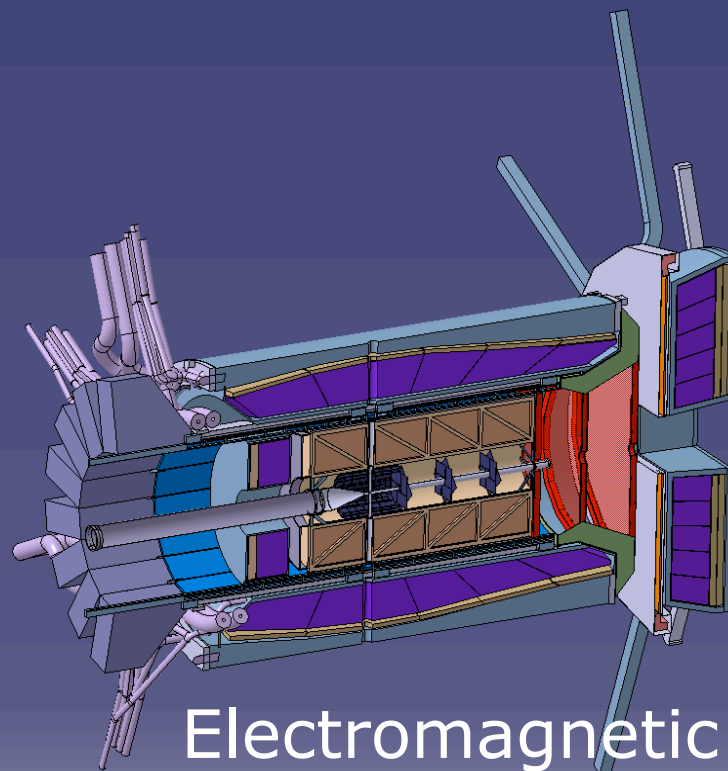


The PANDA Spectrometer



Central Tracker

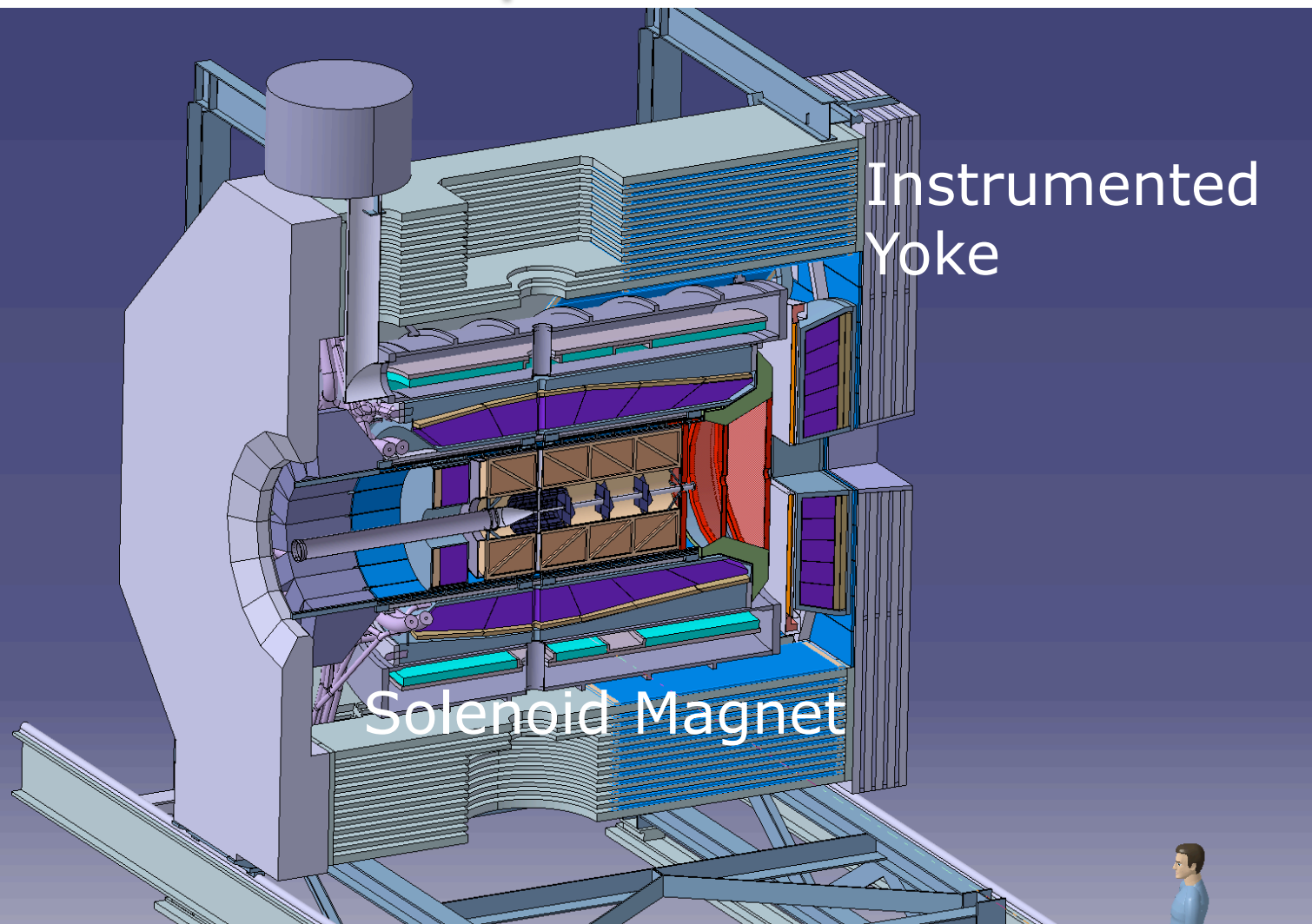
The PANDA Spectrometer



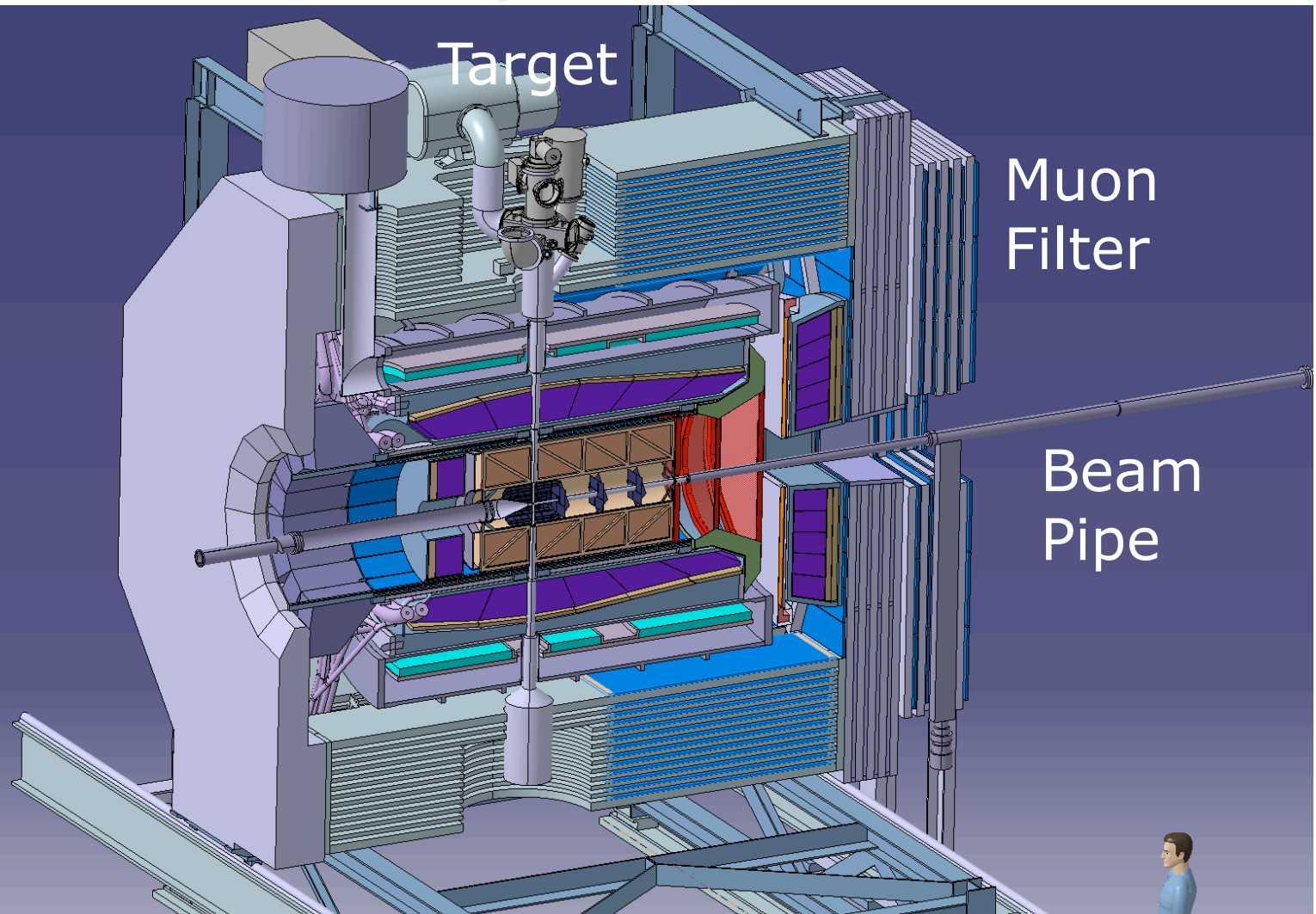
Electromagnetic
Crystal Calorimeters



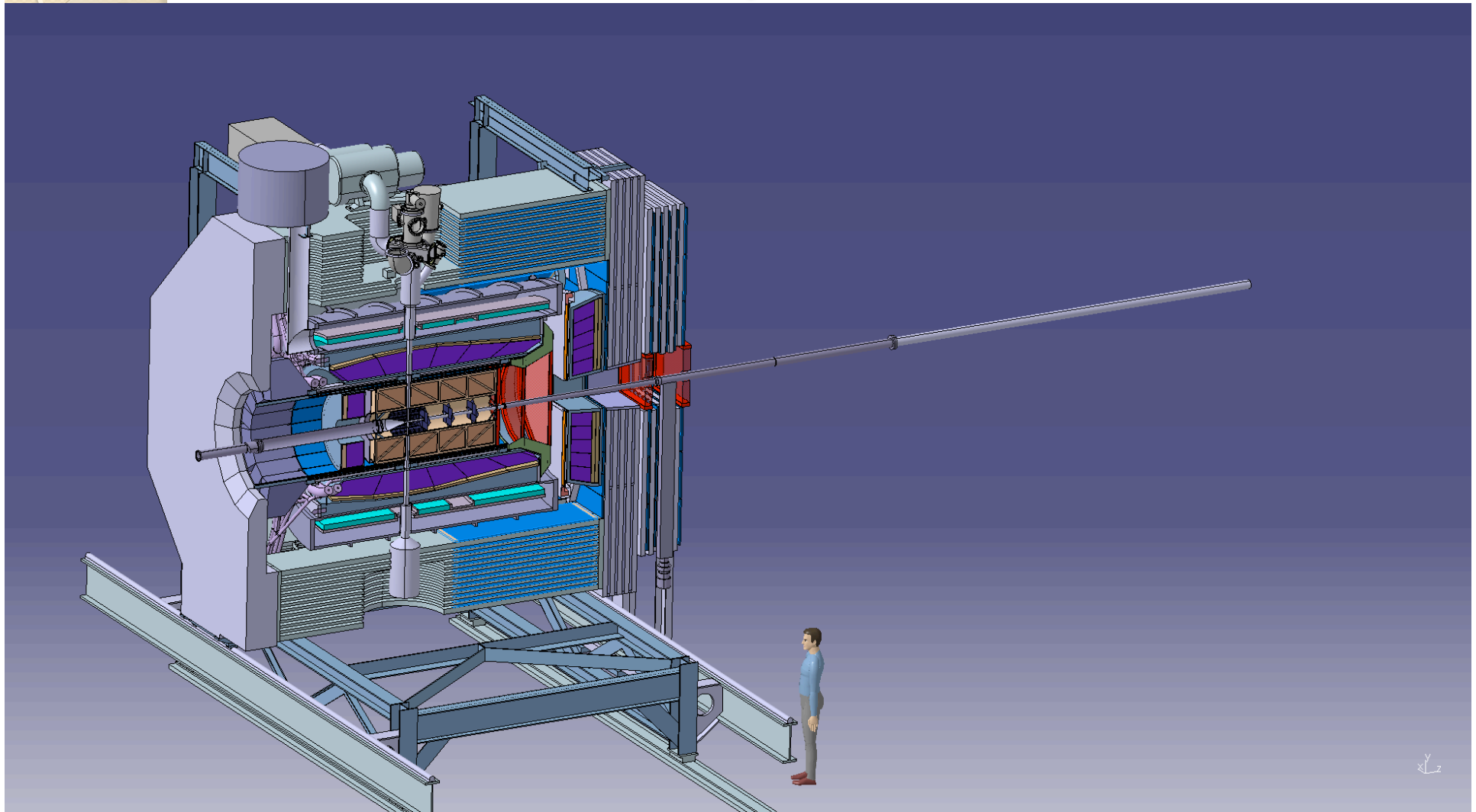
The PANDA Spectrometer



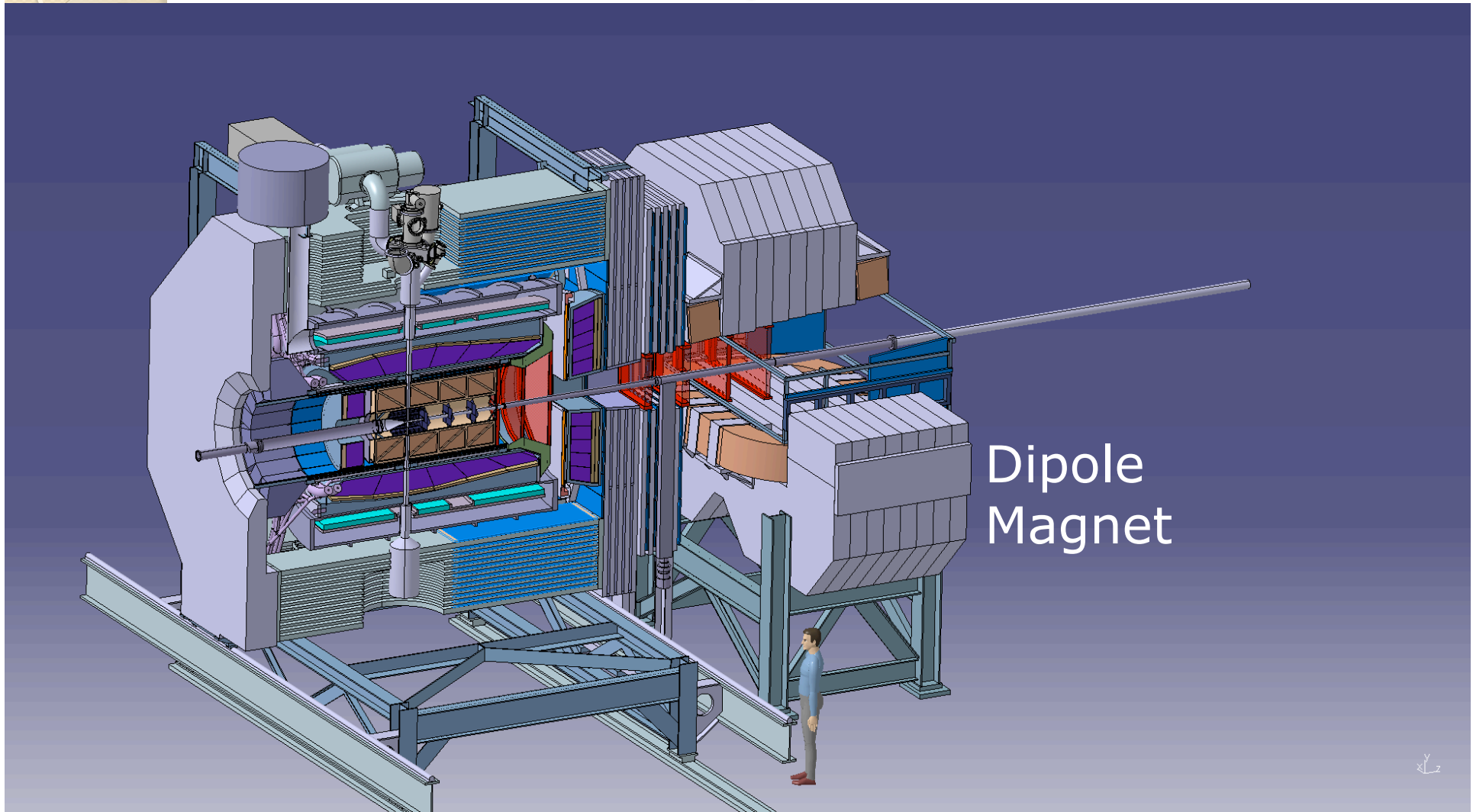
The \bar{P} ANDA Spectrometer



The \bar{P} ANDA Spectrometer

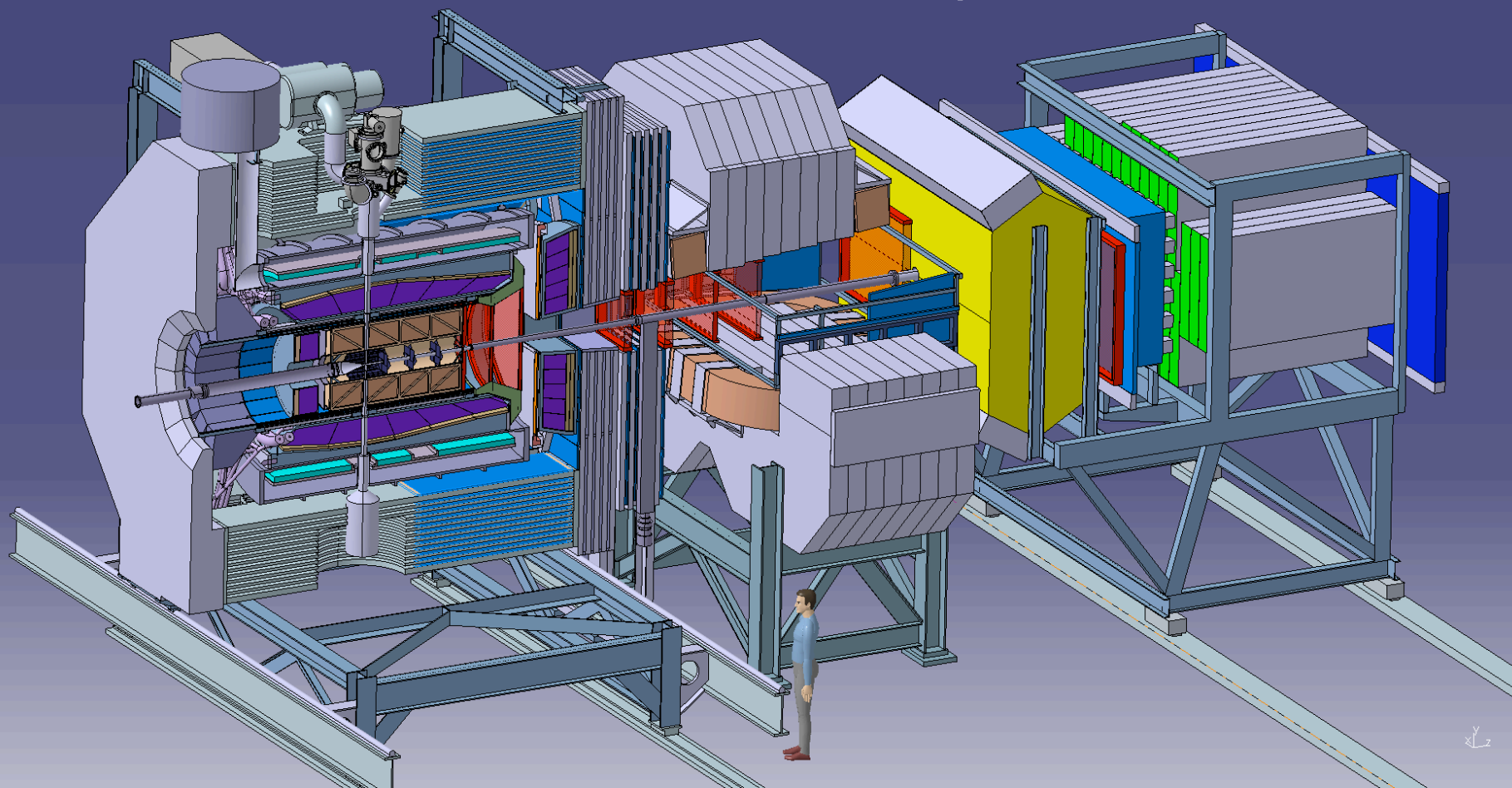


The \bar{P} ANDA Spectrometer



The \bar{P} ANDA Spectrometer

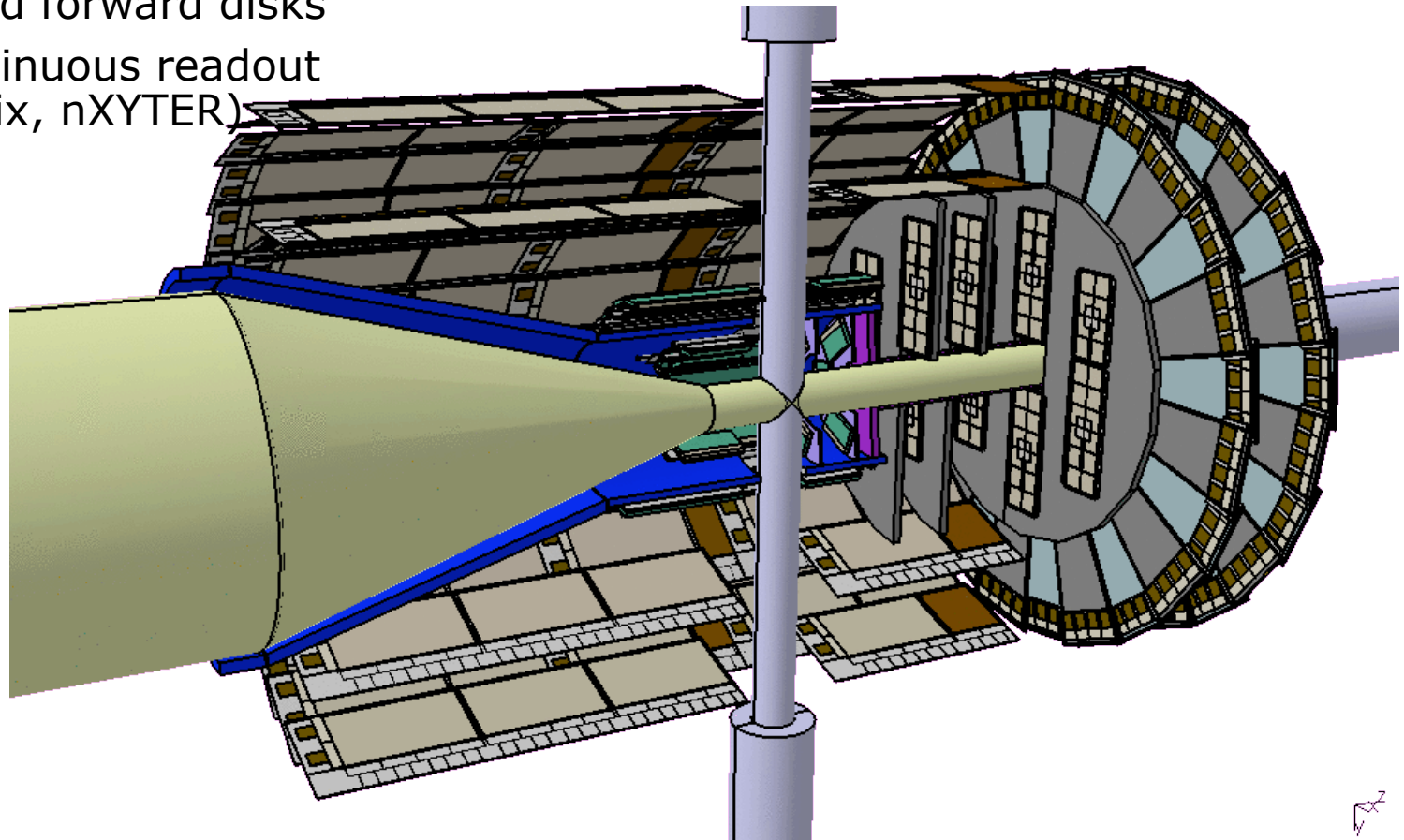
Forward Spectrometer



Vertex Detectors

Micro Vertex Detector

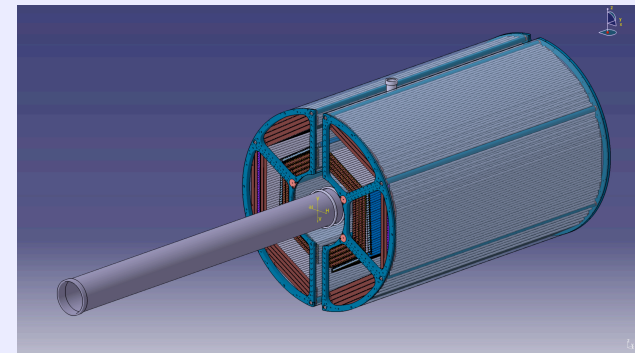
- 4 barrels and 6 disks
- *Inner layers*: hybrid pixels ($100 \times 100 \mu\text{m}^2$)
- *Outer layers*: double sided strips
- Mixed forward disks
- Continuous readout (ToPix, nXYTER)



Tracking Detectors

Central Tracker: 2 Alternatives

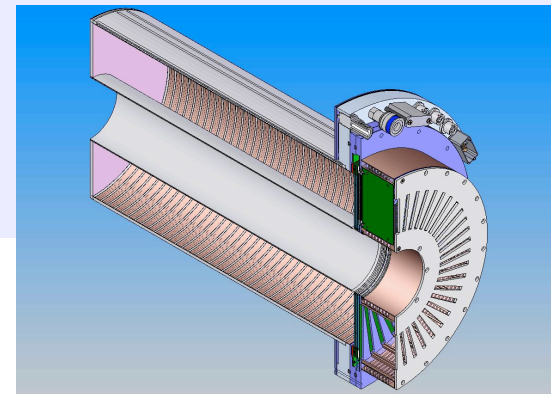
- Design figures:
 - $\sigma_{r\phi} \sim 150\mu\text{m}$, $\sigma_z \sim 1\text{mm}$
 - $\delta p/p \sim 1\%$ (with MVD)
 - Material budget $\sim 1\% X_0$
- **Final decision end of 2009**



- Straw Tube Tracker
 - 29 μm thin mylar tubes, 1 cm \emptyset
 - Stability by 1 bar overp.
- GEM Time Projection Chamber
 - Continuous sampling
 - GEMs to reduce ion feedback
 - Online tracklet finding

Forward GEM Tracker

- Large area GEM foils
- Ultra thin coating

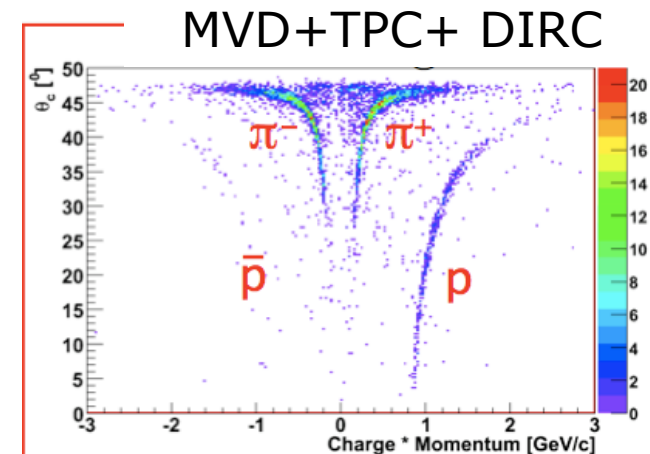
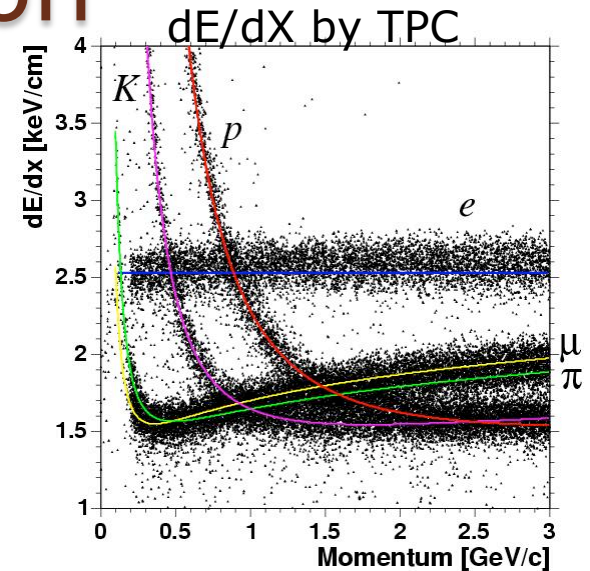


Particle Identification

- **PANDA PID Requirements:**
- Particle identification essential for PANDA
- Momentum range 200 MeV/c – 10 GeV/c
- Different processes for PID needed

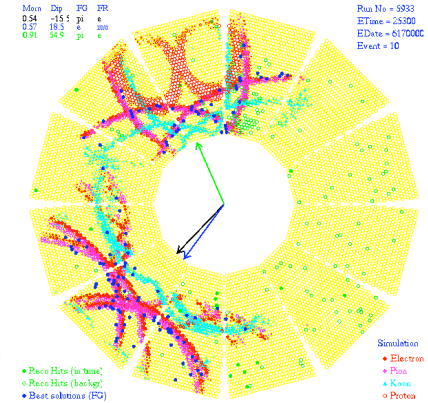
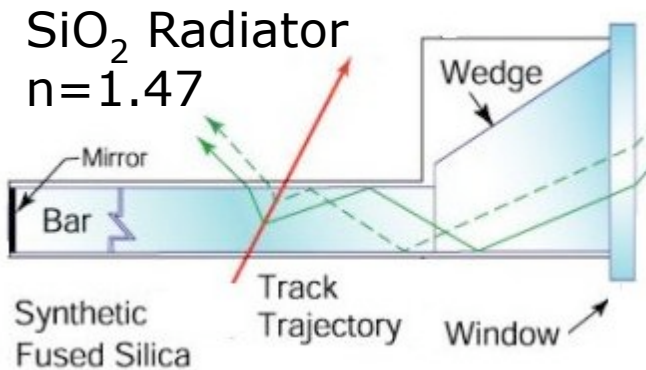
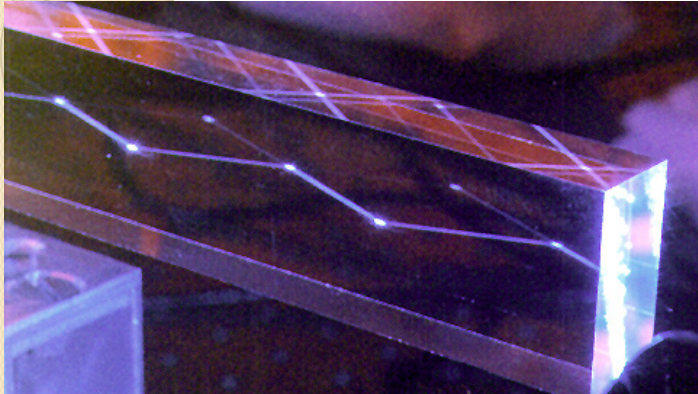
PID Processes:

- Cherenkov radiation: above 1 GeV
Radiators: quartz, aerogel, C4F10
- Energy loss: below 1 GeV
Best accuracy with TPC than with STT
- Time of flight
Problem: no start detector
- Electromagnetic showers: EMC for e and γ

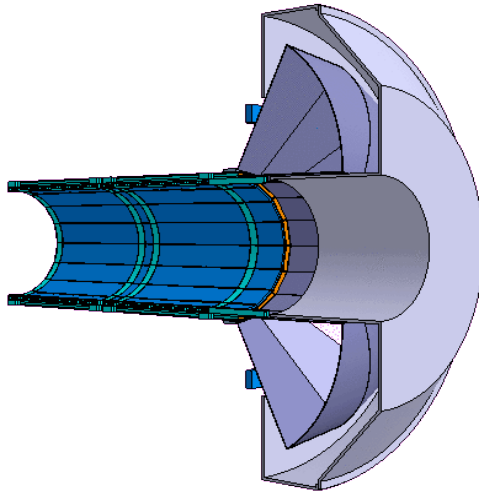


PANDA DIRC Detectors

Detection of Internally Reflected Cherenkov light



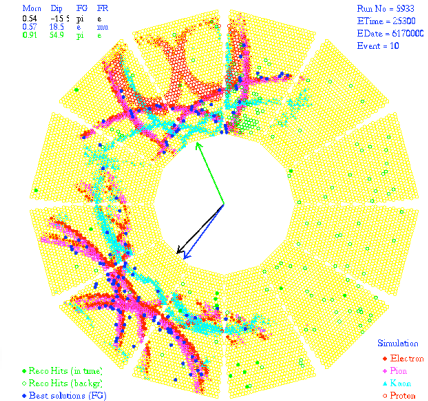
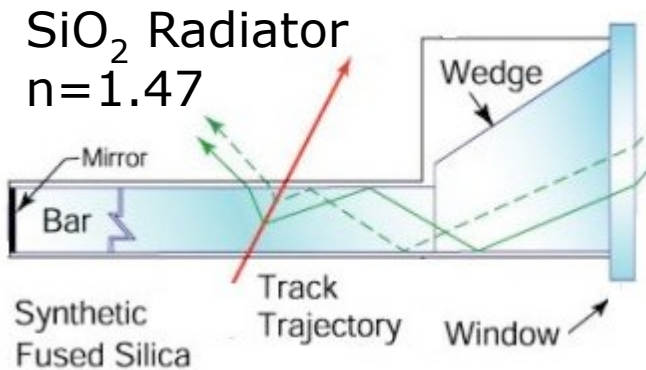
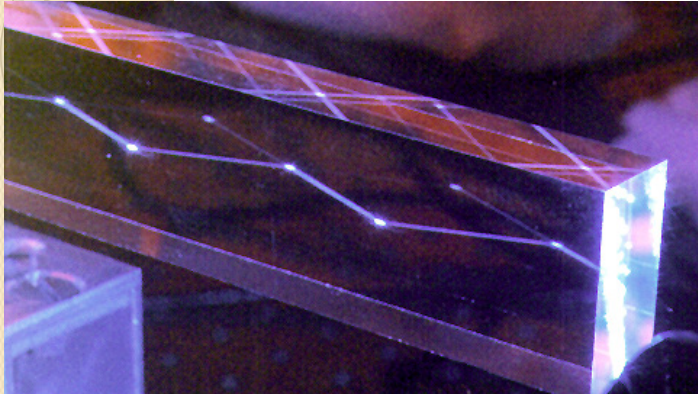
BaBar type Barrel DIRC



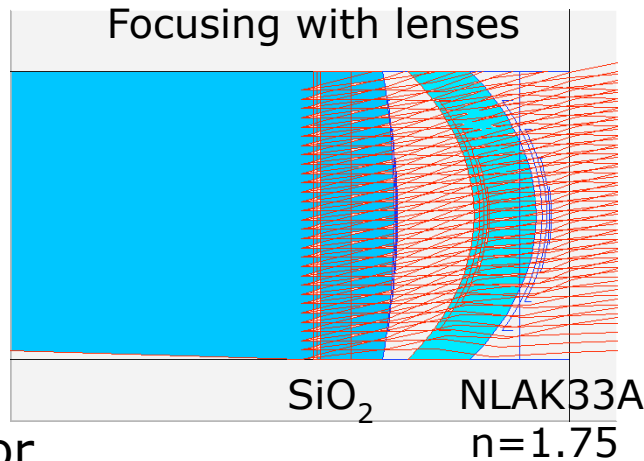
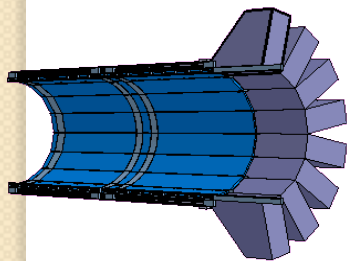
- Pin hole focusing
- Large water tank
- Readout with PMTs
(BaBar 11000, PANDA 7000)

PANDA DIRC Detectors

Detection of Internally Reflected Cherenkov light



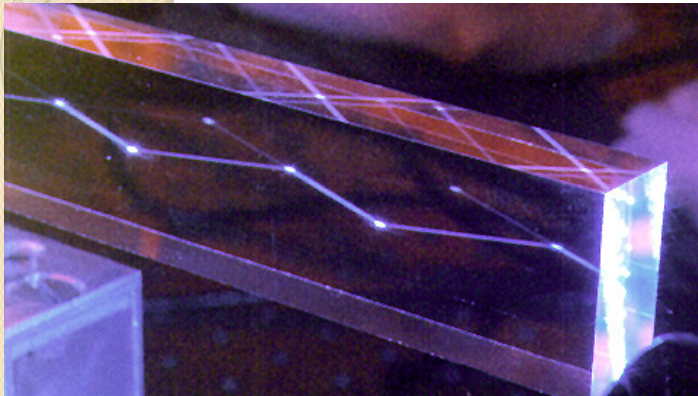
PANDA Barrel DIRC



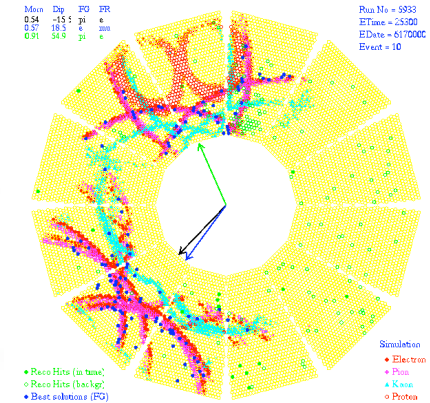
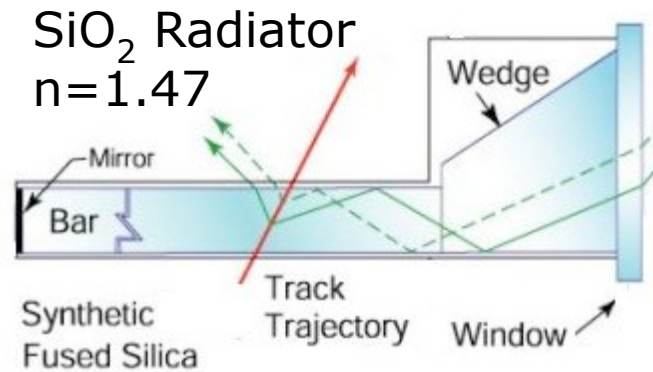
- Shorter radiator
- No large tank

PANDA DIRC Detectors

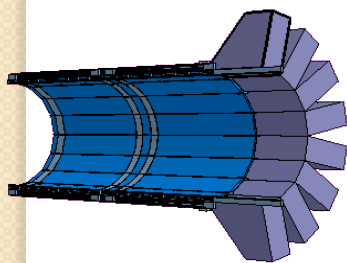
Detection of Internally Reflected Cherenkov light



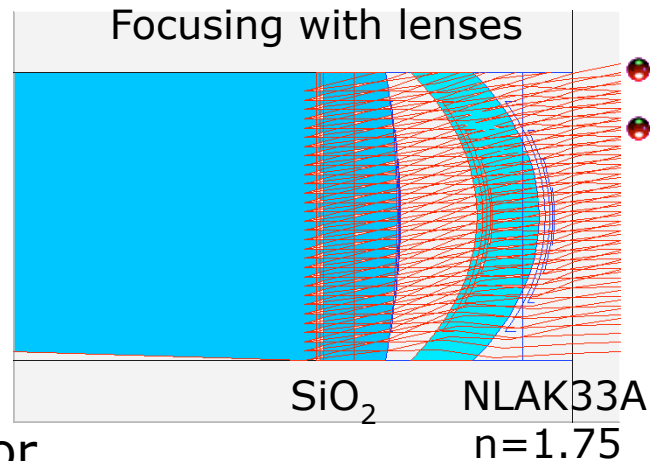
PANDA Barrel DIRC



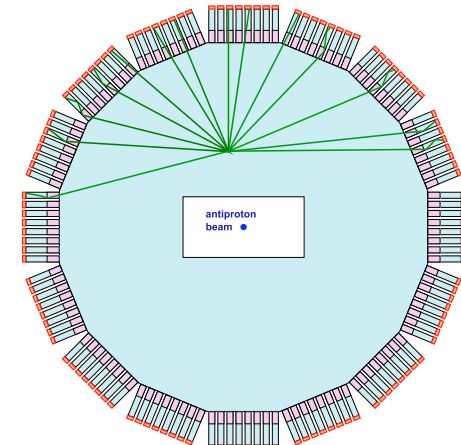
PANDA Disc DIRC



- Shorter radiator
- No large tank



- Disc shaped radiator
- Readout at rim



Electromagnetic Calorimeters

PANDA PWO Crystals

- PWO is dense and fast
- Low γ threshold is a challenge
- Increase light yield:
 - improved PWO II (2xCMS)
 - operation at -25°C (4xCMS)
- Challenges:
 - temperature stable to 0.1°C
 - control radiation damage
 - low noise electronics
- Delivery of crystals started

Electromagnetic Calorimeters

PANDA PWO Crystals

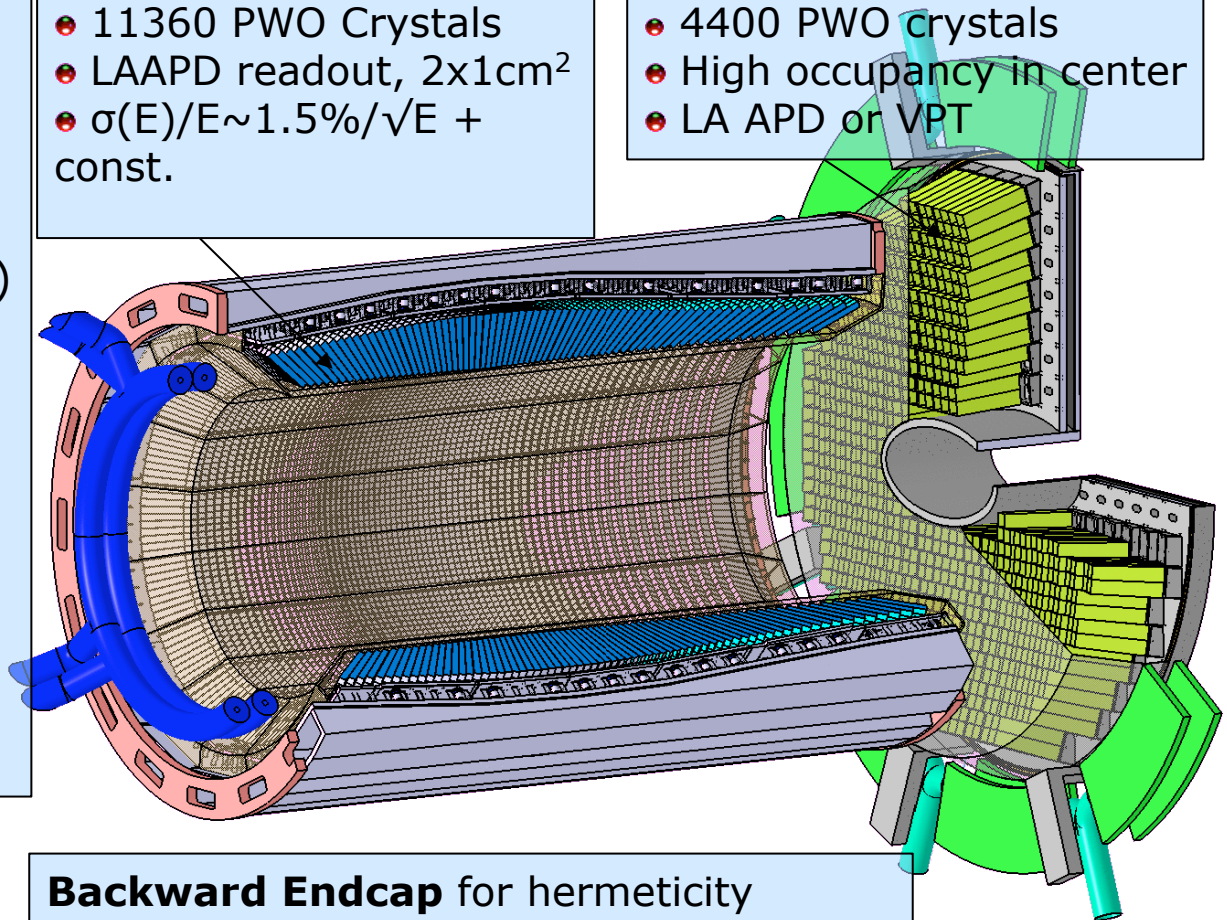
- PWO is dense and fast
- Low γ threshold is a challenge
- Increase light yield:
 - improved PWO II (2xCMS)
 - operation at -25°C (4xCMS)
- Challenges:
 - temperature stable to 0.1°C
 - control radiation damage
 - low noise electronics
- Delivery of crystals started

Barrel Calorimeter

- 11360 PWO Crystals
- LAAPD readout, $2 \times 1 \text{cm}^2$
- $\sigma(E)/E \sim 1.5\%/\sqrt{E} + \text{const.}$

Forward Endcap

- 4400 PWO crystals
- High occupancy in center
- LA APD or VPT



Backward Endcap for hermeticity
Forward EMC shashlyk behind dipole

The Scientific Program of $\bar{\text{P}}\text{ANDA}$ and PAX experiments

- The history of antiprotons;
- Overview of the FAIR facility and of the HESR;
- The $\bar{\text{P}}\text{ANDA}$ experimental program;
- The $\bar{\text{P}}\text{ANDA}$ detector;
- The PAX scientific program;
- The PAX experimental setup;
- Antiproton polarization possibilities.

Study of the nucleon structure at FAIR

Drell-Yan dilepton production

- double spin DY is the dream option
- new physics from unpolarised DY since the very beginning
- extense SSA program in DY and in hadron production

Generalised Distribution Amplitudes

- investigation of the TP diagramm al large p_T
- large p_T lepton and meson production
- test on factorisation (GDA + HB diagram)

Time-Like Electromagnetic Form Factors

- TL-FF investigation
- test on Rosenbluth separation in the TL region
- separate evaluation of G_E and G_M
- accessing single and double spin asymmetries

Collaborations: PANDA & PAX

Physics with polarized antiprotons at FAIR

The possibility to polarize \bar{p} will give access to new fundamental observables.

The main goal of PAX will be the study of nucleon structure using $\bar{p}p$ collision both at fix target and in collider mode

- Measurement of the **moduli and the phases of the e.m. form factors of the proton in the time-like region**
- **Transversity distribution h_1** , the last leading twist missing piece of the QCD description of the partonic structure of the nucleon;
- Study of **transverse single spin asymmetries**;

The Physics program

Transversity via Drell-Yan processes

High Energy

A_{TT} \longrightarrow direct access to transversity

Transverse Single Spin Asymmetries

A_N \longrightarrow QCD "theorem": $(\text{Sivers})_{\text{D-Y}} = - (\text{Sivers})_{\text{DIS}}$

Elastic processes

$A_N, A_{NN}, A_{LL}, A_{SS}, A_{SL}$ \longrightarrow spin mysteries like in pp ?

Time-like e.l.m. form factors

Low Energy

$p\bar{p} \rightarrow l^+l^-$ \longrightarrow form factors

Parton distribution functions

QCD description of hadron's internal structure relies on a hierarchy of parton correlation function. 3 functions are needed at leading twist:

- **unpolarized quark distribution $f_1(x)$** ;
- **helicity distribution $g_1(x)$** , for a longitudinally polarized quark inside a longitudinally polarized nucleon;
- **transversity distribution $h_1(x)$** , for the quark transversely polarized inside a transversely polarized hadron.

$$f_1 = \text{yellow circle} \quad q(x) \text{ spin averaged}$$

$$g_{1L} = \text{yellow circle with up arrow} - \text{yellow circle with down arrow} \quad \Delta q(x) \text{ helicity difference}$$

$$h_{1T} = \text{yellow circle with right arrow} - \text{yellow circle with left arrow} \quad \delta q(x) \text{ helicity flip}$$

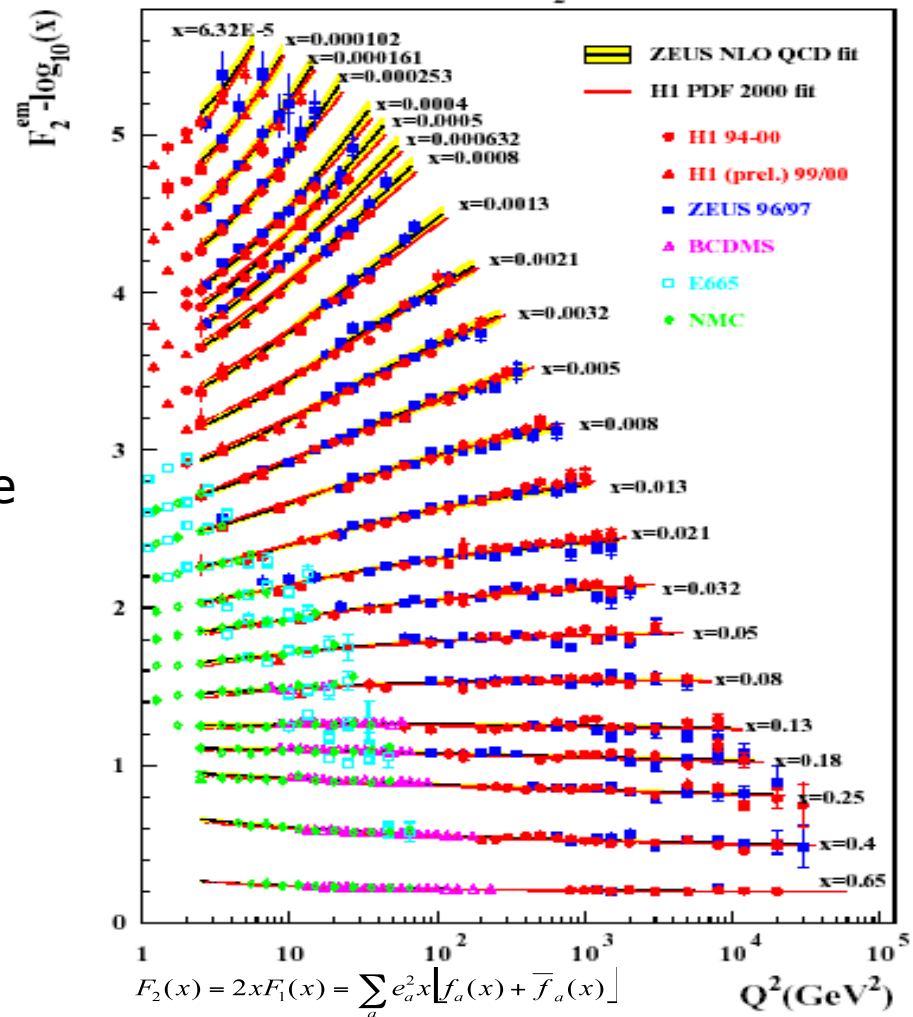
$f_1(x)$ and $g_1(x)$ are well known from DIS data.

$h_1(x)$, being chiral-odd, cannot be measured in DIS.

Unpolarized quarks

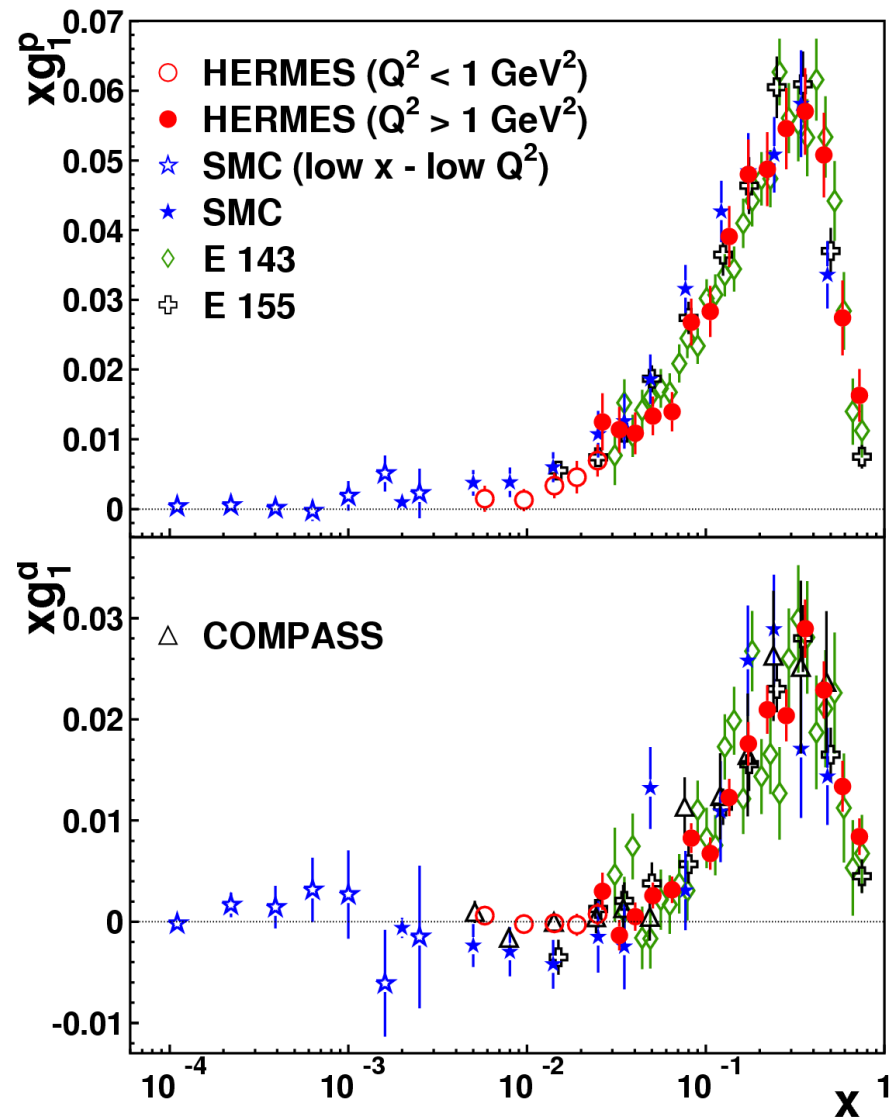
The knowledge of $f_1(x)$ is pretty good

World compilation of experimental data of unpolarized quark distribution functions $f_1(x)$ in a wide Q^2 range



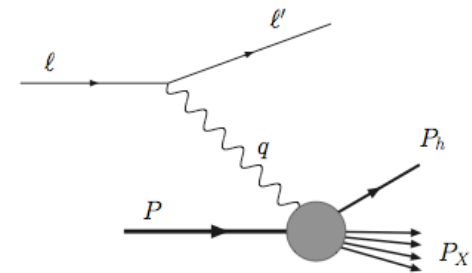
Helicity functions

World data set of helicity function $g_1(x)$



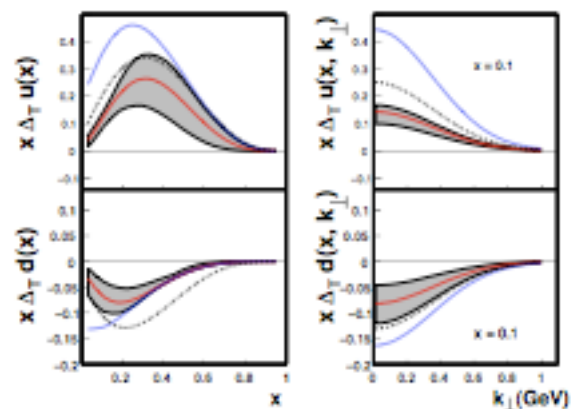
Transversity measurement 1

- Semi-Inclusive Deep Inelastic Scattering (SIDIS), here h_1 couples with a new unknown fragmentation function (Collins);



Recently HERMES and COMPASS published some data on spin asymmetry in SIDIS.

Belle from $e^+e^- \rightarrow h_1 h_2 X$ processes provides the first measurement of the Collins Fragmentation Function.



Therefore, a first evaluation of transversity has been done the obtained value is very low.

[M.Anselmino et al. Phys.Rev D75, 054032(2007)]

M.Anselmino et al.,
hep-ph 0812.4366v1

Transversity measurement 2

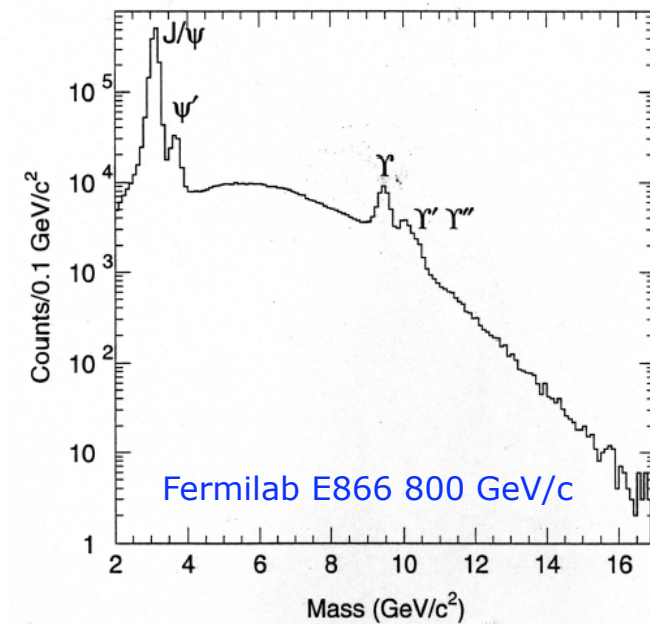
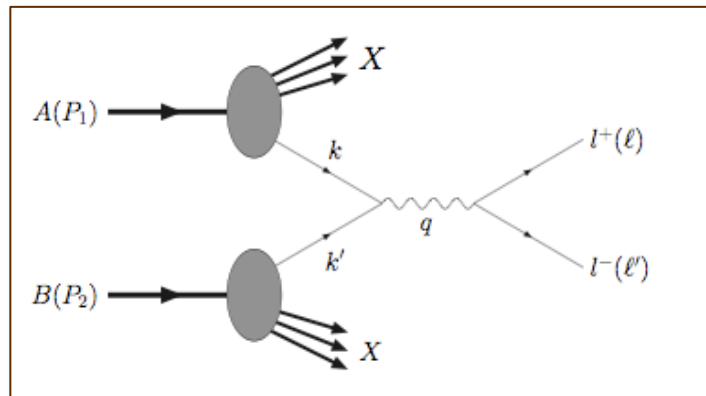
The most straightforward way to determine transversity is

● **Polarized Drell-Yan processes (DY),**

The advantage to study quark transverse polarization via DY are:

– Transversity distributions appear at leading-twist level

– The cross-section contains no other unknown quantities besides the transversity distributions



Transversity measurement 3

There are different experiments planning to measure transversity

At RICH by studying $p^\uparrow p^\uparrow \rightarrow X\mu^+\mu^-$
here is the disadvantage that a product of 2 transversity distribution is measured
Furthermore, mainly the sea quark content of the proton will be probed.

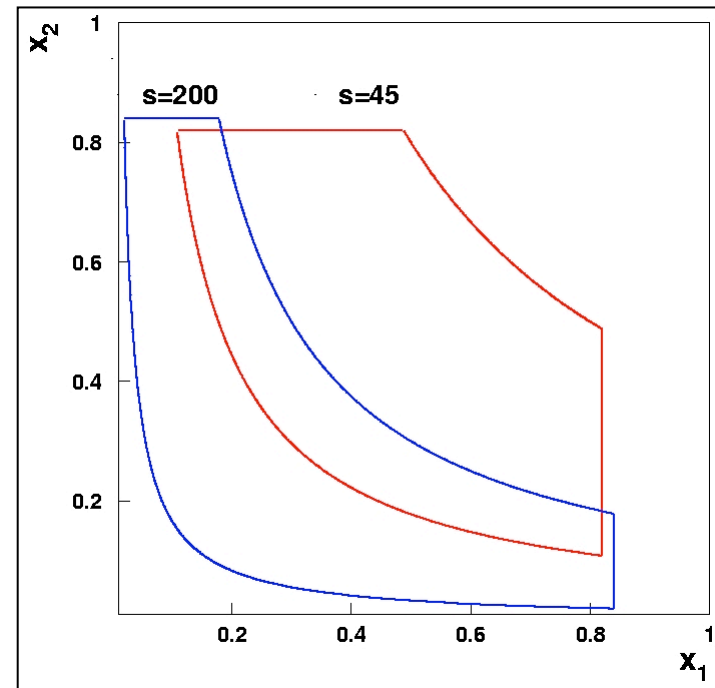
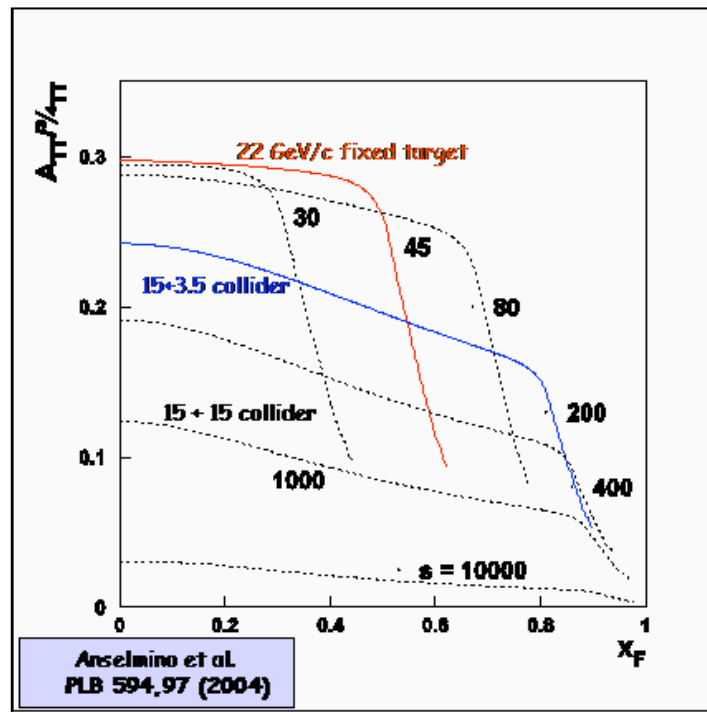
$$A_{TT} = \frac{\sin^2\theta \cos 2\varphi}{1 + \cos^2\theta} \frac{\sum_a e_a^2 h_1^a(x_1) h_1^{\bar{a}}(x_2)}{\sum_a e_a^2 f_1^a(x_1) f_1^{\bar{a}}(x_2)}$$

RHIC: $\tau = x_1 x_2 \sim 10^{-3} \rightarrow$ sea quarks $(A_{TT} \sim 0.01)$

Transversity measurement 4

By studying Drell-Yan processes in $\bar{p}p$ there are many advantages

$$A_{TT} = \frac{d\sigma^{\uparrow\uparrow} - d\sigma^{\uparrow\downarrow}}{d\sigma^{\uparrow\uparrow} + d\sigma^{\uparrow\downarrow}} = a_{TT} \frac{\sum_q e_q^2 h_1^q(x_1, M^2) h_1^{\bar{q}}(x_2, M^2)}{\sum_q e_q^2 f_1^q(x_1, M^2) f_1^{\bar{q}}(x_1, M^2)}$$

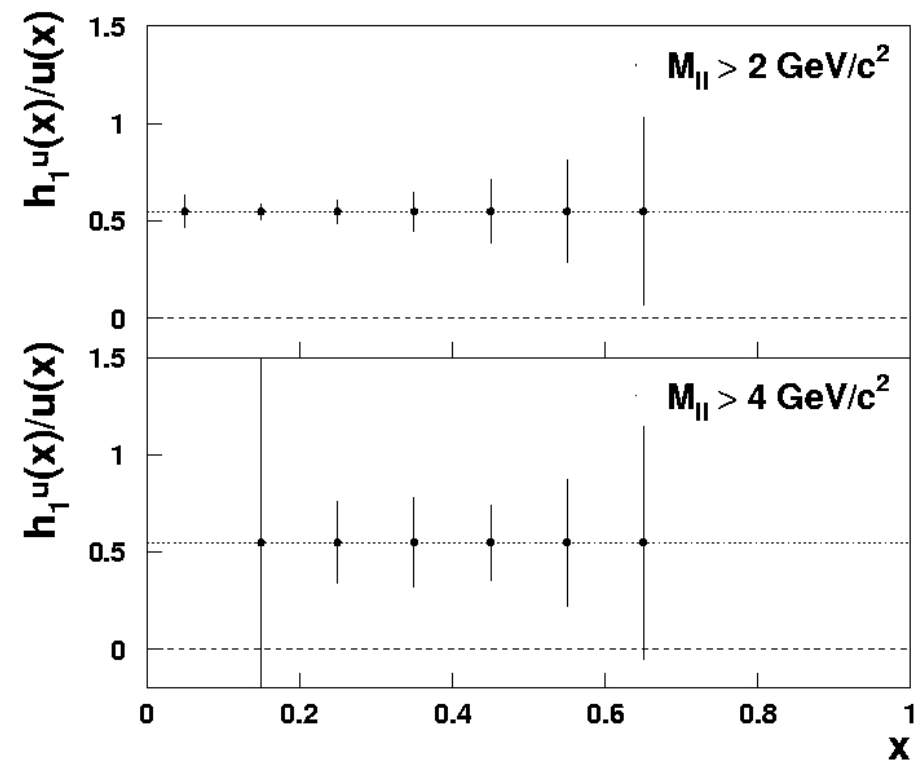
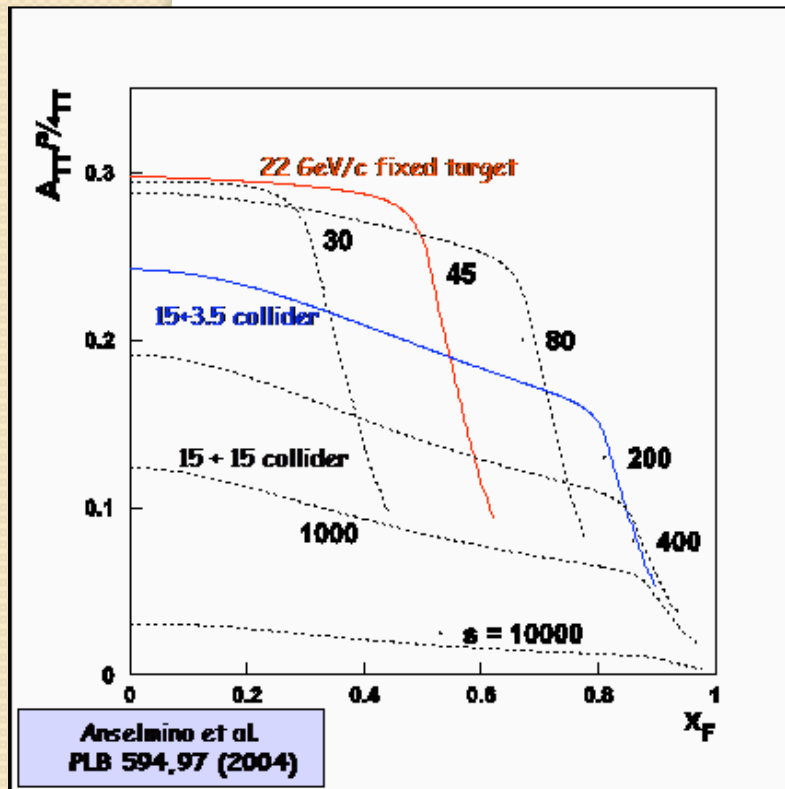


PAX: $\tau = x_1 x_2 \sim 10^{-1} \rightarrow$ valence and sea ($A_{TT} \sim 0.1$)

PAX measurement of h_1

1 year of data taking at 15+3.5 GeV/c collider $L = 2 \cdot 10^{30} \text{ cm}^{-2}\text{s}^{-1}$

($L \sim 10^{31}$ reachable)



10 % precision on the $h_1^u(x)$ in the valence region

Single Spin Asymmetries

Not only transversity, there are several other spin observables which can be measured

$$A_N = \frac{d\sigma^\uparrow - d\sigma^\downarrow}{d\sigma^\uparrow + d\sigma^\downarrow}$$

Large, up to 40%, unexpected Single Spin Asymmetries have been observed by many experiments $p^\uparrow p \rightarrow \pi X$, $\bar{p}^\uparrow p \rightarrow \pi X$ with c.m energies from 6.6 GeV to 200 GeV.

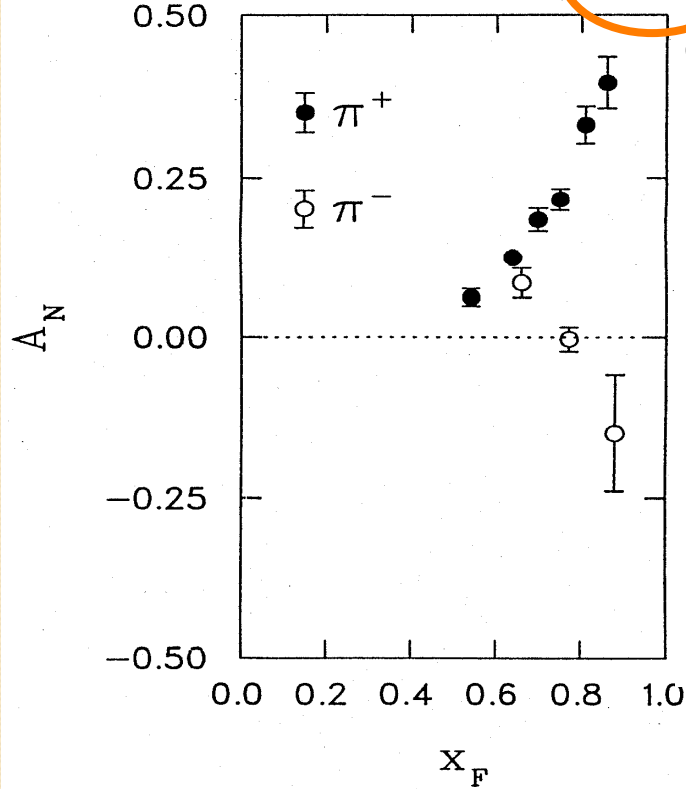
Transverse SSA from low to high energies

$$p p^\uparrow \rightarrow \pi X$$

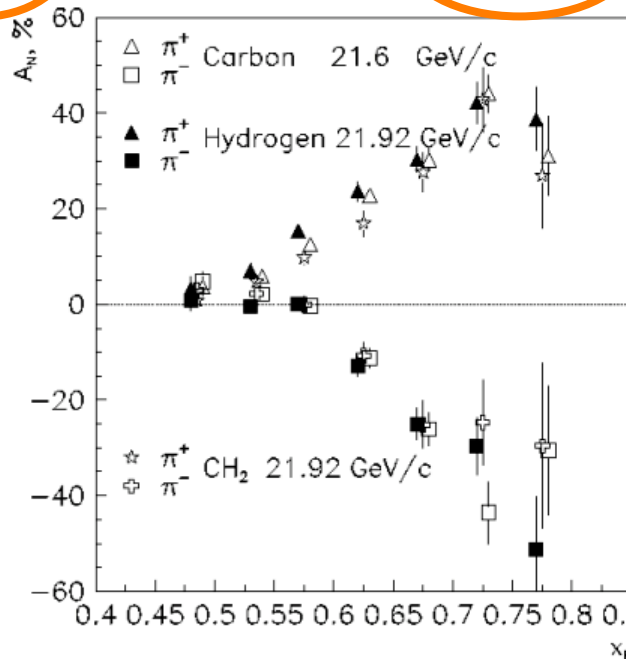
Argonne ZGS, $p_{\text{beam}} = 12 \text{ GeV}$

AGS, $p_{\text{beam}} = 22 \text{ GeV}$

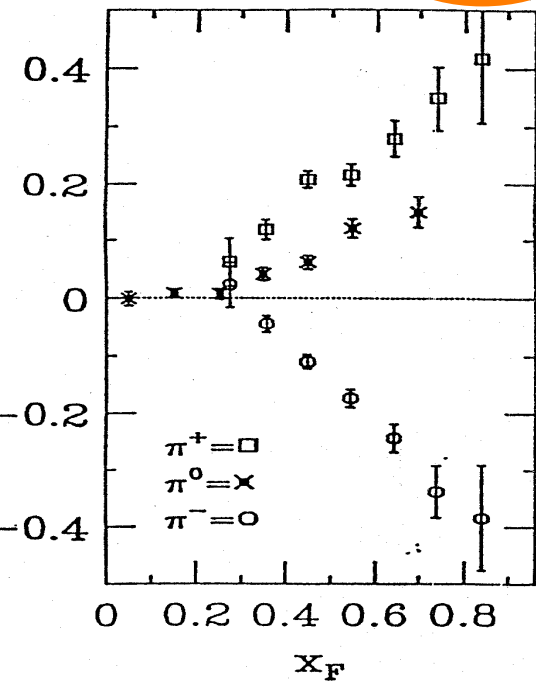
FNAL, $p_{\text{beam}} = 200 \text{ GeV}$



[PRL36(1976)]



[PRD65(2002)]

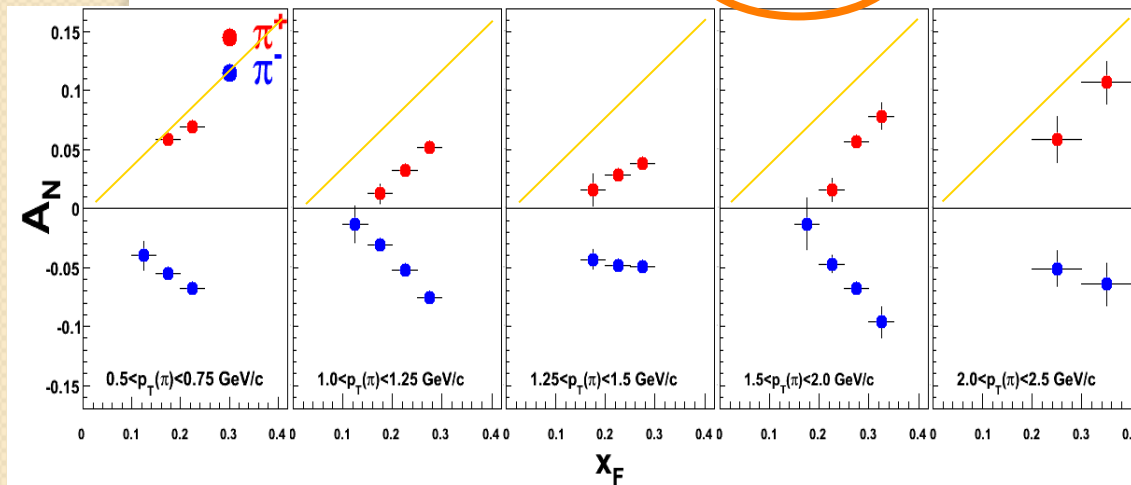


[PLB261(1991)]

Transverse SSA from low to high energies

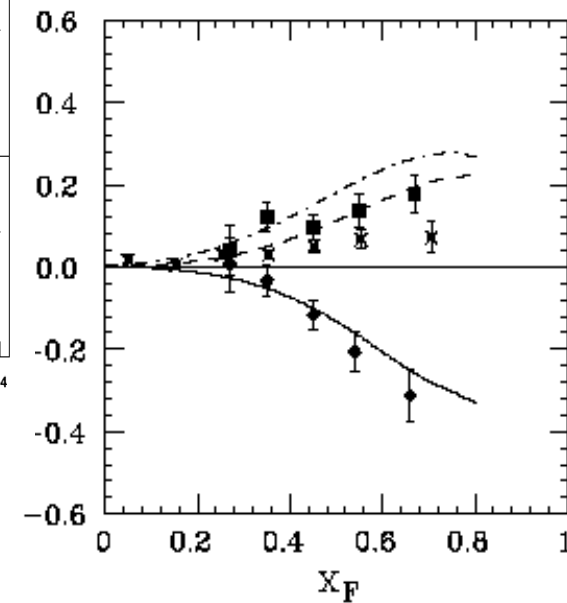
$$p p^\uparrow \rightarrow \pi X$$

RICH, $p_{\text{beam}} = 200 \text{ GeV}$



$$p \bar{p}^\uparrow \rightarrow \pi X$$

FNAL, $p_{\text{beam}} = 200 \text{ GeV}$



[PRL77(1996)]

Single Spin Asymmetries

Not only transversity, there are several other spin observables which can be measured

$$A_N = \frac{d\sigma^\uparrow - d\sigma^\downarrow}{d\sigma^\uparrow + d\sigma^\downarrow}$$

Large, up to 40%, unexpected Single Spin Asymmetries have been observed by many experiments with c.m energies from 6.6 GeV to 200 GeV.

The PAX experiment can provide new insight studying SSA in D meson production: $\bar{p}^\uparrow p \rightarrow DX$

$$\bar{p}p^\uparrow \rightarrow DX$$

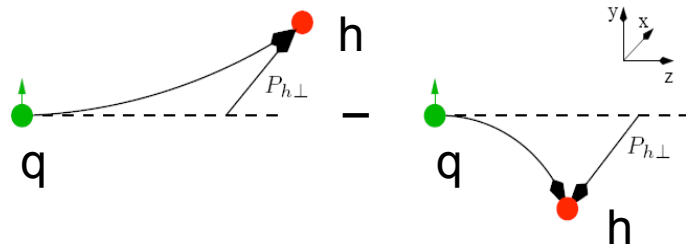
The study of this reaction can help disentangling between Sivers and Collins mechanisms.

How to explain SSA

"Collins- effect"

Collins fragmentation function

- correlates *transverse spin* of fragmenting *quark* and *transverse momentum* $P_{h\perp}$ of produced *hadron* h

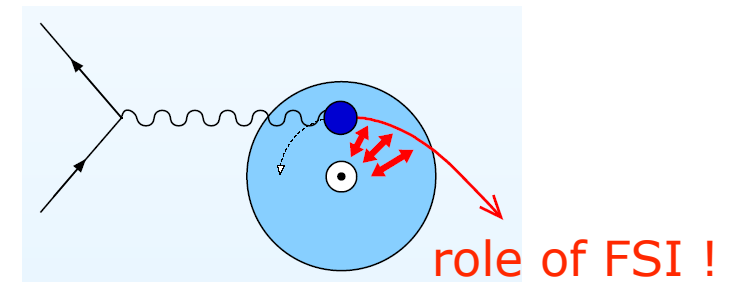


→ left-right (azimuthal) asymmetry in the direction of the outgoing hadron

"Sivers- effect"

Sivers distribution function

- distribution of unpolarised quarks in a transversely polarised nucleon → describes *spin-orbit correlations*

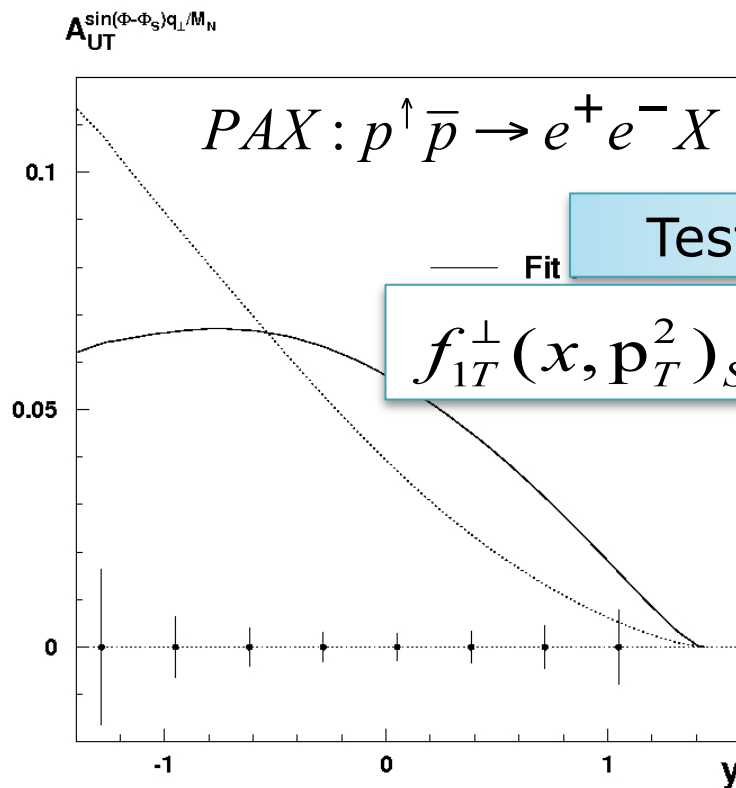


requires non-zero orbital angular momentum!

Collins effect cannot occur in $\bar{p}^\uparrow p \rightarrow DX$ $\bar{p}p^\uparrow \rightarrow DX$
 PAX could measure the sign of Sivers function

The Sivers function

The PAX measurements on SSA with transversely polarized protons together with the results from HERMES can provide the first test of the sign of Sivers function from SIDIS to DY.

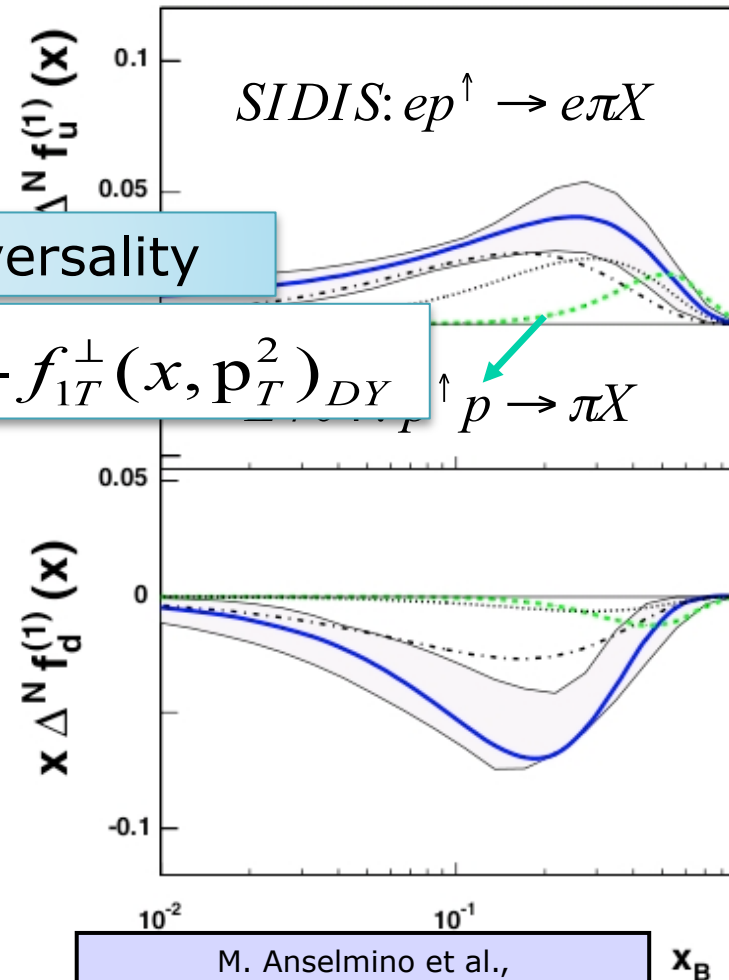


A.V. Efremov et al.,
Phys. Lett. B 612, 233 (2005)

$$x_{1/2} = \sqrt{M^2 / s} e^{\pm y}$$

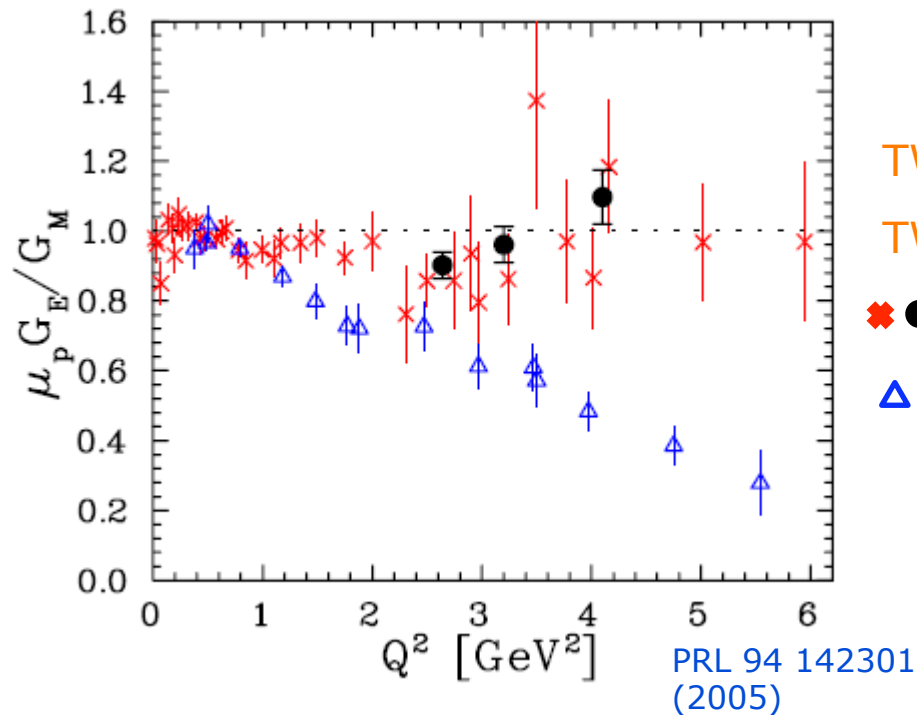
Test of Universality

$$f_{1T}^\perp(x, p_T^2)_{SIDIS} = -f_{1T}^\perp(x, p_T^2)_{DY} \uparrow p \rightarrow \pi X$$



M. Anselmino et al.,
Phys. Rev. D72, 094007 (2005)

Time Like proton Form Factors



TWO DIFFERENT METHODS

TWO DIFFERENT RESULTS!

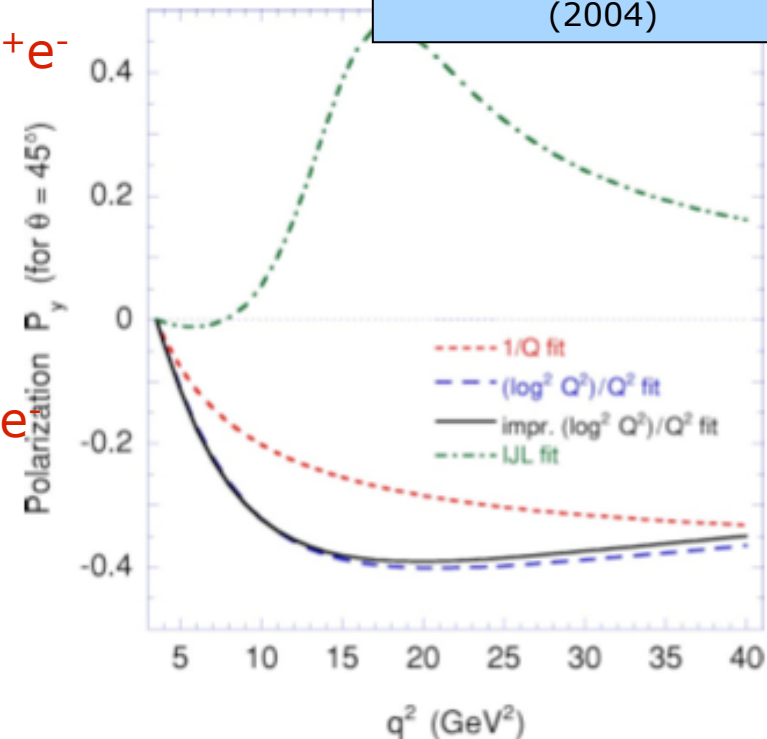
◆● Rosenbluth separation

△ Polarization Transfer

TL proton FF with polarization

S. Brodsky et al.,
Phys. Rev. D69 054022
(2004)

- Double-spin asymmetry in $\bar{p}p \uparrow \rightarrow e^+e^-$
 - independent G_E - G_M separation
 - test of Rosenbluth separation in the time-like region
- Single-spin asymmetry in $\bar{p}p \uparrow \rightarrow e^+e^-$
Measurement of relative phases of magnetic and electric FF in the time-like region



Predicted SSA $A_y = P_y$ in the timelike region for different models

$$A_y = \frac{\sin(2\theta) \cdot \text{Im}(G_E^* \cdot G_M)}{\left[\left(1 + \cos^2(\theta)\right) |G_M|^2 + \sin^2(\theta) |G_E|^2 / \tau \right] \sqrt{\tau}}$$

$$\tau = q^2 / 4m_p^2$$

The history of antiproton polarization

1985 Bodega Bay, CA: "International Workshop on Polarized Antiprotons Beam", AIP Conf. Proc. **145** (1986) 207

2007 Daresbury: "Polarized Antiprotons: How", AIP Conf. Proc. **1008** (2008)

2008 Bad Honnef: Heraeus Seminar: "Polarized Antiprotons"

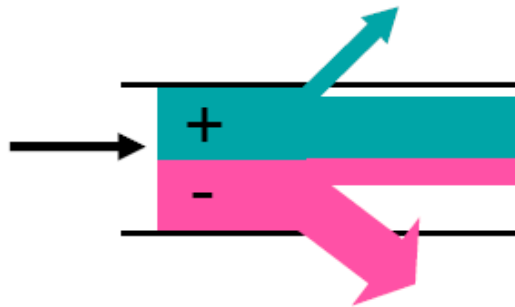
Intense beam of polarized antiprotons were never produced:

- Conventional methods (AtomicBeamSource) not applicable \bar{p} annihilate
- Polarized antiprotons from $\bar{\Lambda}$ decay [Fermilab]
-I < $1.5 \cdot 10^5 \text{s}^{-1}$ (P \approx 0.35)
- Antiproton scattering off liquid H2 target
-I < $2 \cdot 10^3 \text{s}^{-1}$ (P \approx 0.2)
- Little polarization from \bar{p} -C scattering experiments at LEAR

Methods not applicable at storage rings

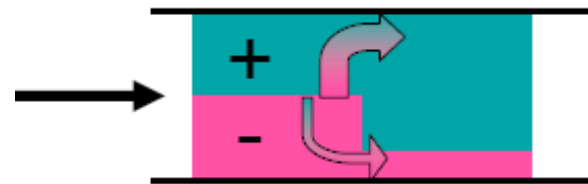
Polarized \bar{p} in a storage ring

- Spin filtering



selective loss

- Spin flip



selective flip

discard (one) substate
(more than the other)

Spin flip: a recent proposal

Antiproton beam polarization by interaction with a polarized positron beam

Eur. Phys. J. A 34, 447–461 (2007)
DOI 10.1140/epja/i2007-10462-x

THE EUROPEAN
PHYSICAL JOURNAL A

Special Article – Tools for Experiment and Theory

A surprising method for polarising antiprotons

Th. Walcher^{1,2,*}, H. Arenhövel¹, K. Aulenbacher¹, R. Barday¹, and A. Jankowiak¹

¹ Institut für Kernphysik, Johannes Gutenberg-Universität Mainz, D-55099 Mainz, Germany
² Laboratori Nazionali di Frascati, Istituto Nazionale di Fisica Nucleare, I-00044 Frascati (Rome), Italy

Received: 26 June 2007 / Revised: 11 January 2008
Published online: 6 February 2008 – © Società Italiana di Fisica / Springer-Verlag 2008
Communicated by E. De Sanctis

Abstract. We propose a method for polarising antiprotons in a storage ring by means of a polarized beam moving parallel to the antiprotons. If the relative velocity is adjusted to $v/c \approx 0.002$ the cross section for spin-flip is as large as about $2 \cdot 10^{13}$ barn as shown by new QED calculations of the triple

Available online at www.sciencedirect.com

ScienceDirect

Nuclear Instruments and Methods in Physics Research B 266 (2008) 3453–3457

ELSEVIER

NIM B
Beam Interactions
with Materials & Atoms
www.elsevier.com/locate/nimb

Polarization effects in non-relativistic ep scattering

A.I. Milstein, S.G. Salnikov, V.M. Strakhovenko*

Budker Institute of Nuclear Physics, 630090 Novosibirsk, Russia

Received 27 February 2008; received in revised form 21 April 2008
Available online 30 April 2008

Abstract

The cross section which addresses the spin-flip transitions of a proton (antiproton) interacting with a polarized non-relativistic electron or positron is calculated analytically. In the case of attraction, this cross section is greatly enhanced for sufficiently small relative velocities as compared to the result obtained in the Born approximation. However, it is still very small, so that the beam polarization time turns out to be enormously large for the parameters of e^{\pm} beams available now. This practically rules out a use of such beams to polarize stored antiprotons or protons.
© 2008 Elsevier B.V. All rights reserved.

PACS: 13.88.+e; 29.20.Dg; 29.27.Hj

Keywords: Electron; Proton; Scattering; Spin-flip; Stored beams; Polarization

$\approx 1 \text{ mbarn}$

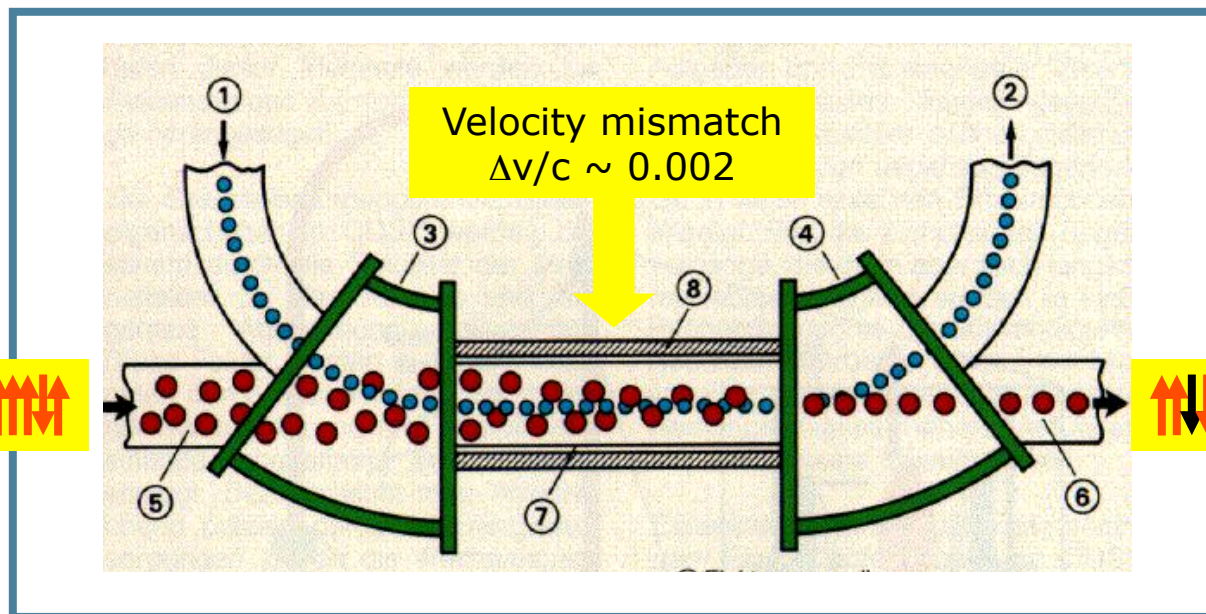
$2 \cdot 10^{13}$ barn

need of experimental test

Depolarization studies

- Use **proton** beam and co-moving **electrons**
- Turn experiment around: $p \vec{e} \rightarrow \vec{p}$ into $\vec{p} e \rightarrow p$
i.e. observe **depolarization** of a polarized proton beam

Polarized
proton beam

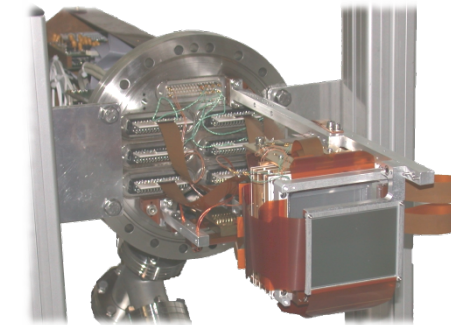
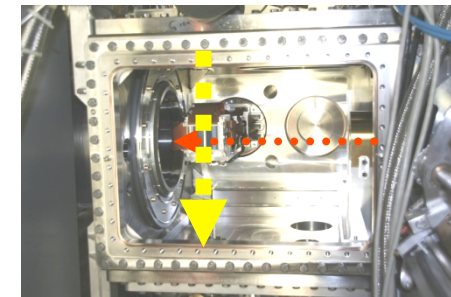
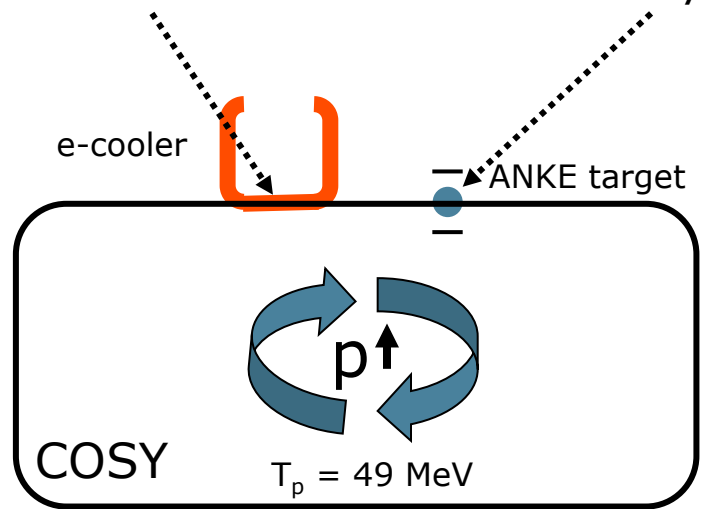


De-polarized
proton beam



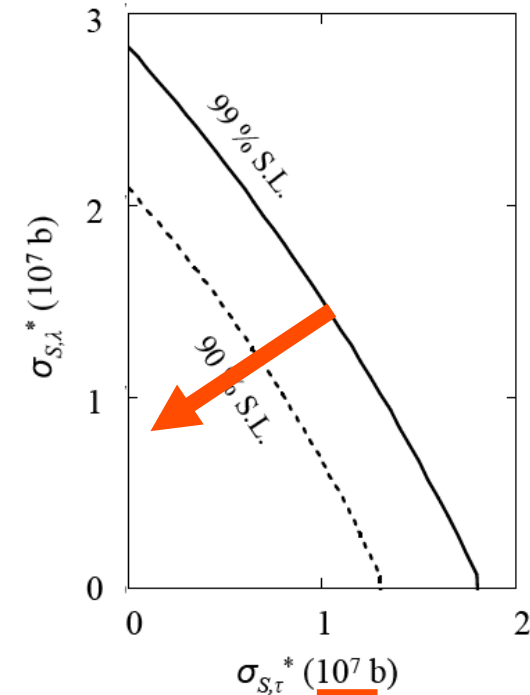
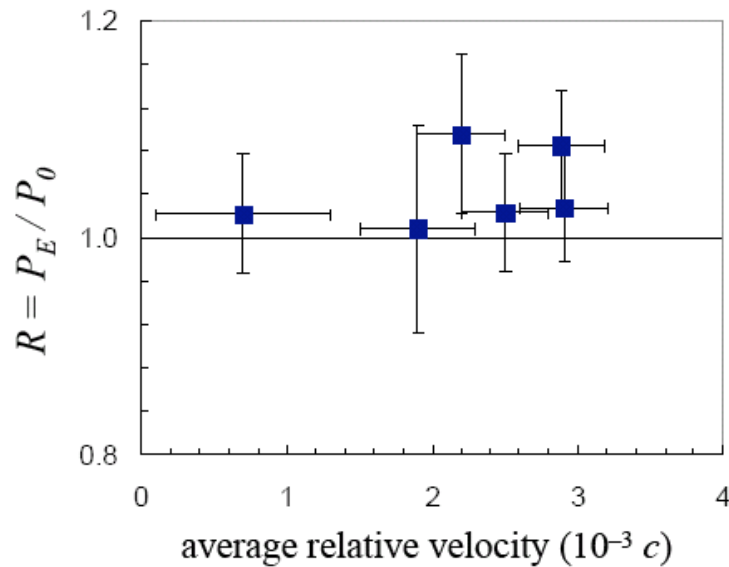
Depolarization test at COSY

pe interaction in **electron cooler** Polarization analysis by **pd elastic scattering**



Depolarization results

Results (submitted PL B, Febr. 09)



No effect observed

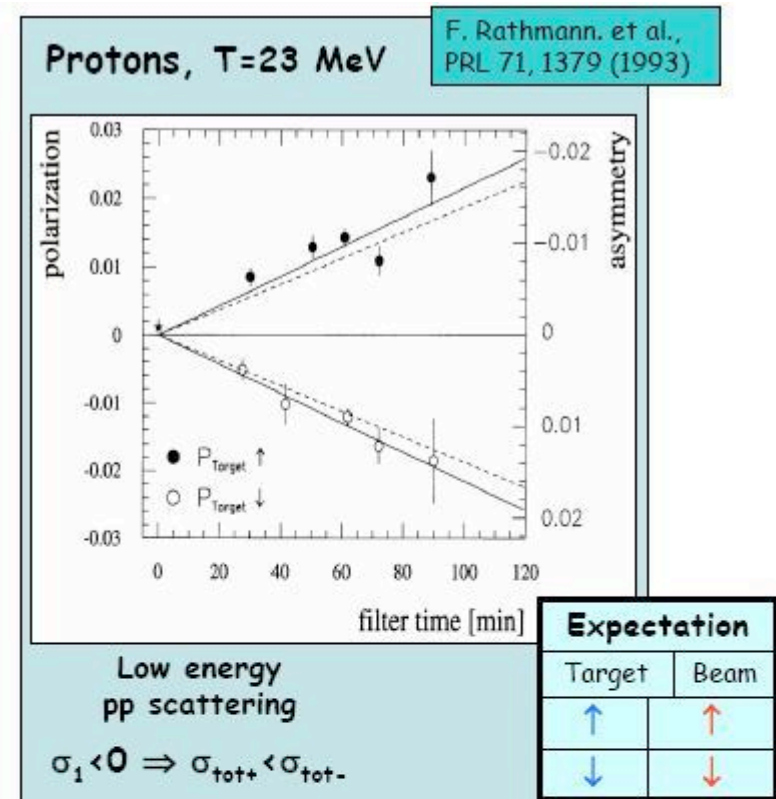
measured cross section at least 6 orders-of-magnitude smaller than predicted 10^{13} b

→ Cross section **too small**
to be a useful method !

FILTEX

In 1992 an experiment (FILTEX) at the Test Storage Ring (TSR) at MPI Heidelberg showed that an initially **unpolarized** stored 23 MeV **proton beam** could be polarized by spin-dependent interaction with a **polarized hydrogen gas target**

Interacting with polarized protons in the target, beam protons with $m = 1/2$ are scattered less often, than those with $m = -1/2$ → **the stored beam acquire a polarization parallel to the proton spin of the hydrogen atoms.**



The mechanism works, it is not clear why!!

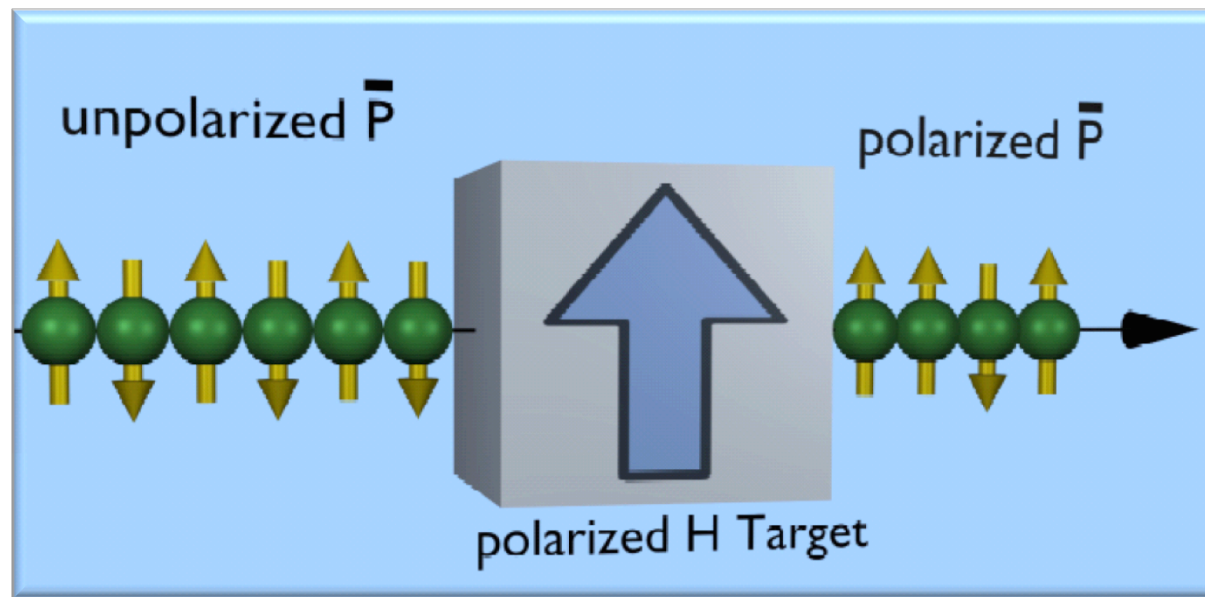
In 90', 5% proton loss
2.4% polarization

Understanding the physics

In order to be able to produce a beam of polarized \bar{p} it is important to understand the polarization mechanism measured by FILTEX: **hadronic effect**, **e.m. effect**

Spin Filtering

Polarization build-up via repeated interaction of the beam with a polarized target in a storage ring:



1. Spin-filtering experiment (with **protons**) at **COSY**
2. Spin-filtering experiment (with **antiprotons**) at **CERN/AD**

The PAX roadmap

PAX proposes to **produce** and **exploit polarized antiprotons** at FAIR

Commitment to find a method to effectively polarize antiprotons

Stepwise approach:

- 1) Electromagnetic (selective flip) - **NO !!**
- 2) Strong interaction (selective loss) - works !
 - COSY (in **2010**)
 - CERN AD (> **2011**)
- 3) APR (~ 2013) and asymmetric collider (?)

PAX Detector Concept

Physics: h_1 distribution $\sin^2\theta$
EMFF $\sin^2\theta$
 \bar{p} -p elastic high $|t|$



Azimuthally Symmetric:
BARREL GEOMETRY
LARGE ANGLES

Experiment: Flexible Facility



e^+e^-

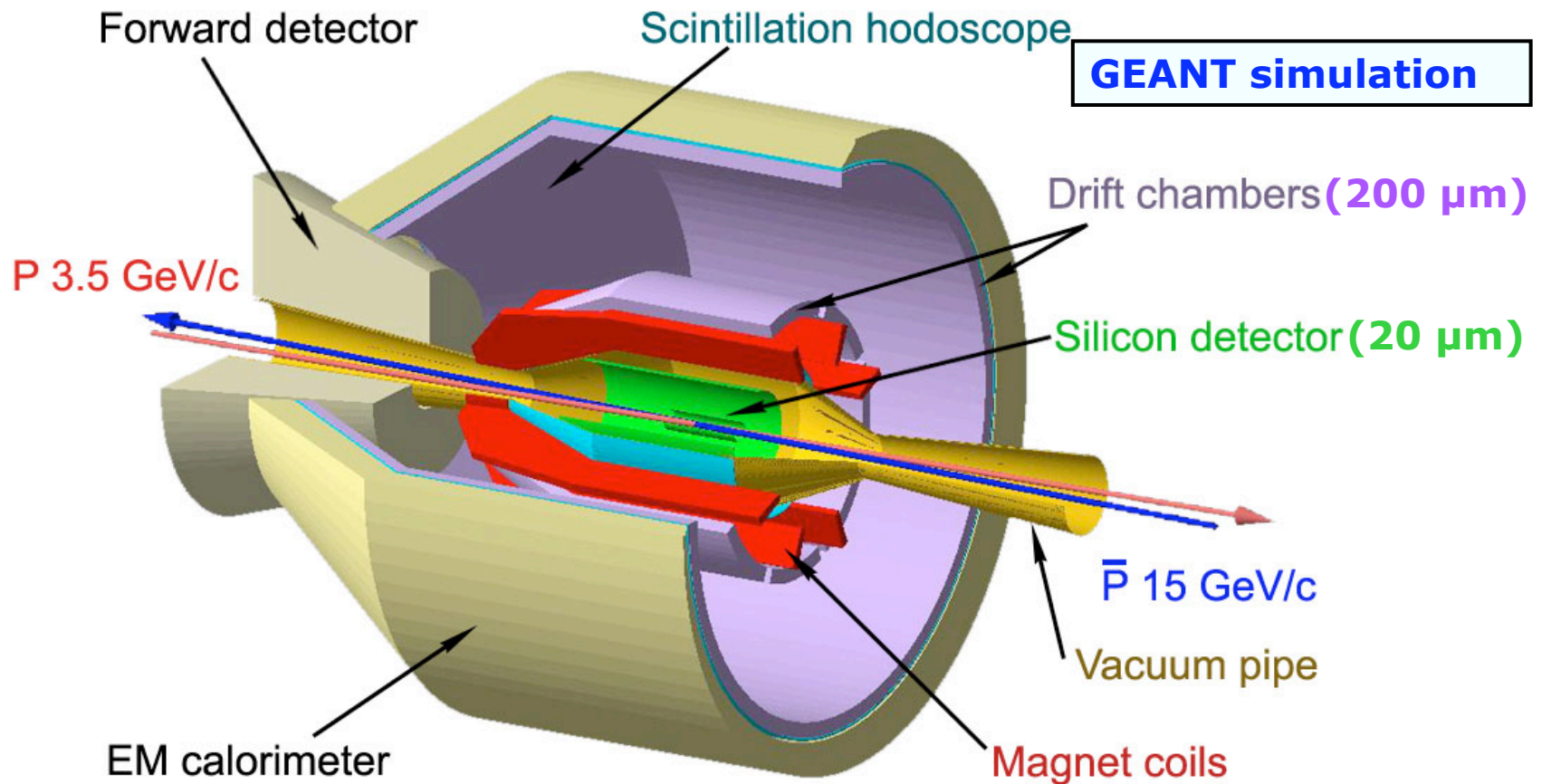
Detector: Extremely rare DY signal (10^{-7} p-pbar)
Maximum Bjorken-x coverage (M interval)
Excellent PID (hadron/e rejection $\sim 10^4$)
High mass resolution ($\leq 2\%$)
Moderate lepton energies (0.5-5 GeV)

Magnet: Keeps beam polarization vertical
Compatible with Cerenkov
Compatible with polarized target



TOROID
NO FRINGE FIELD

The PAX detector



GEANT simulation

1 m.

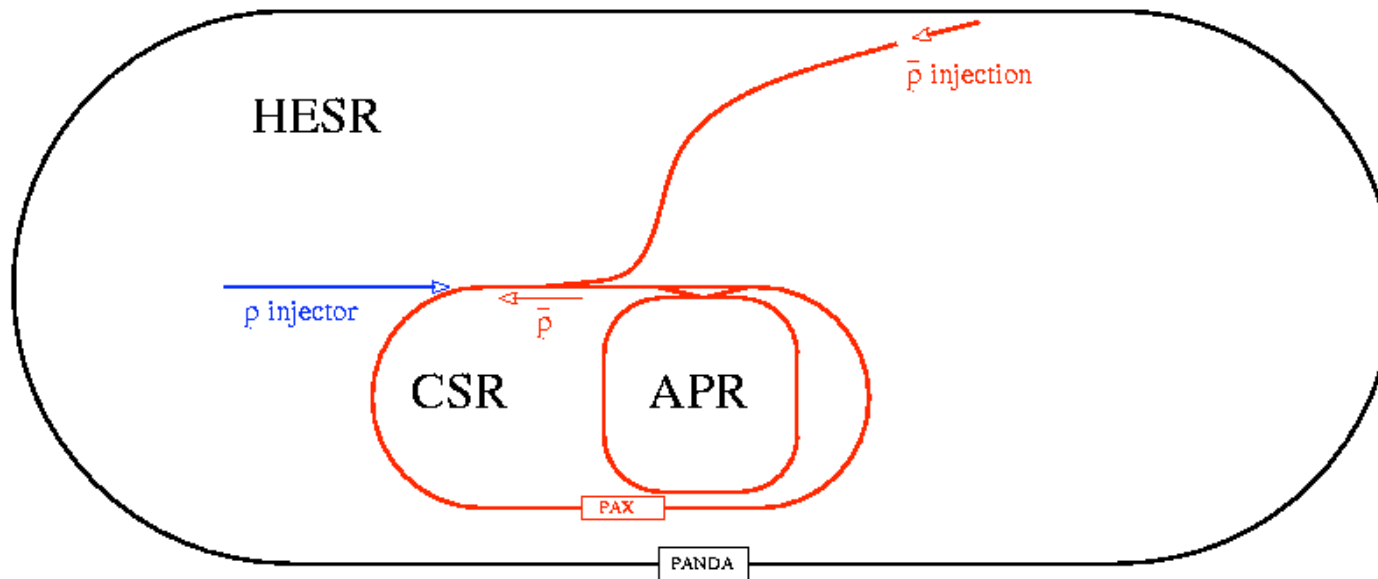
PAX Detector

Designed for Collider but compatible with fixed target

PAX phase 1: fix target

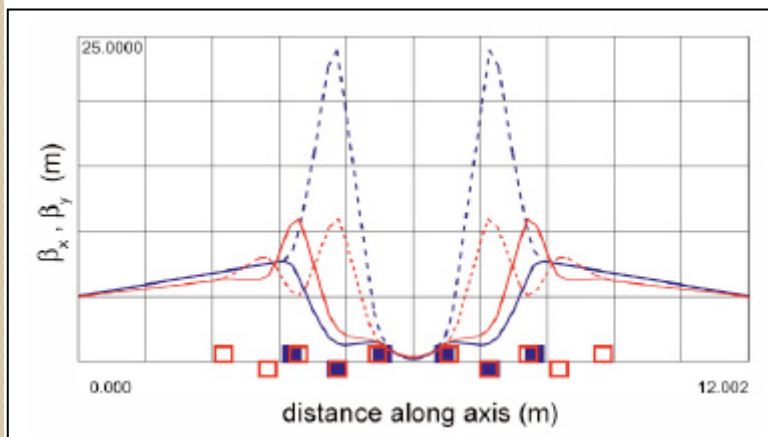
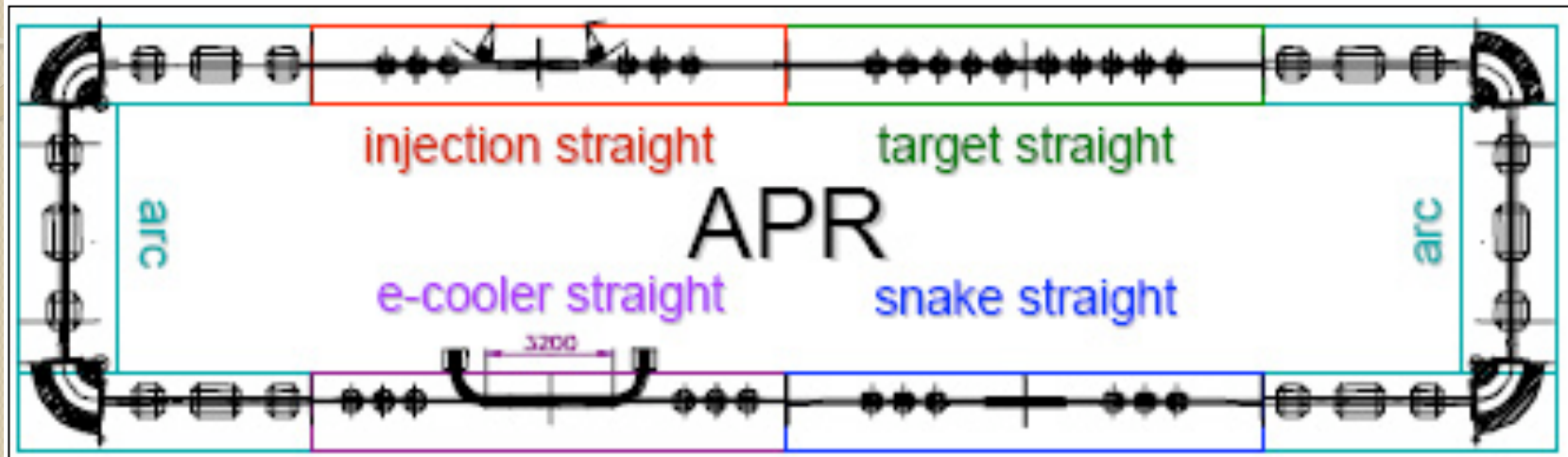
Program:

Fix target experiment: polarized antiprotons protons in CSR ($p > 200$ MeV/c) fixed polarized protons target



Phase I: Proton time-like FFs
Hard \bar{p} -p elastic scatt.

Antiproton Polarizer Ring



Energy	250 MeV
ϵ	250 mm mrad
Circumf.	86 m

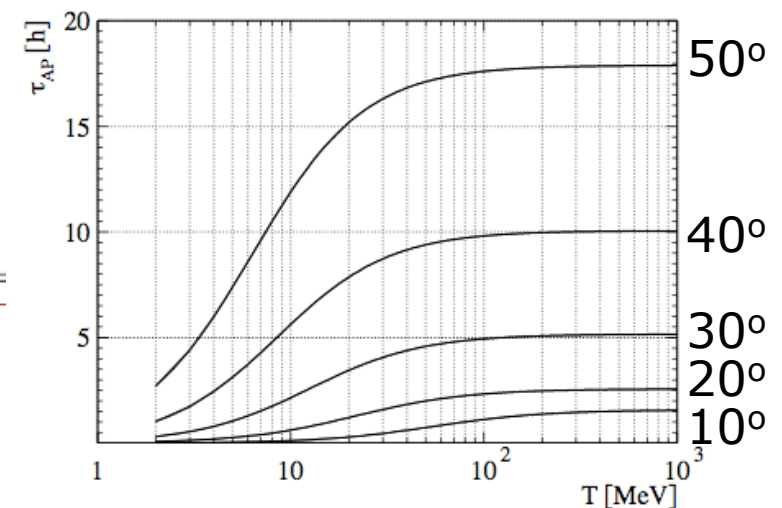
APR characteristics

Parameters of the APR and the polarizing target section

circumference of APR	L_{APR}	150 m
β -function at target	β	0.2 m
radius of vacuum chamber	r	5 cm
gap height of magnets	$2g$	14 cm
ABS flow into feeding tube	q	$1.5 \cdot 10^{17}$ atoms/s
storage cell length	L_{beam}	40 cm
feeding tube diameter	d_{feed}	1 cm
feeding tube length	L_{feed}	15 cm
longitudinal holding field	$B_{ }$	300 mT
electron polarization	Q_e	0.9
cell temperature	T	100 K

The buildup of polarization is due to the spin-dependent interaction in the target.

acceptance angles Ψ_{acc}

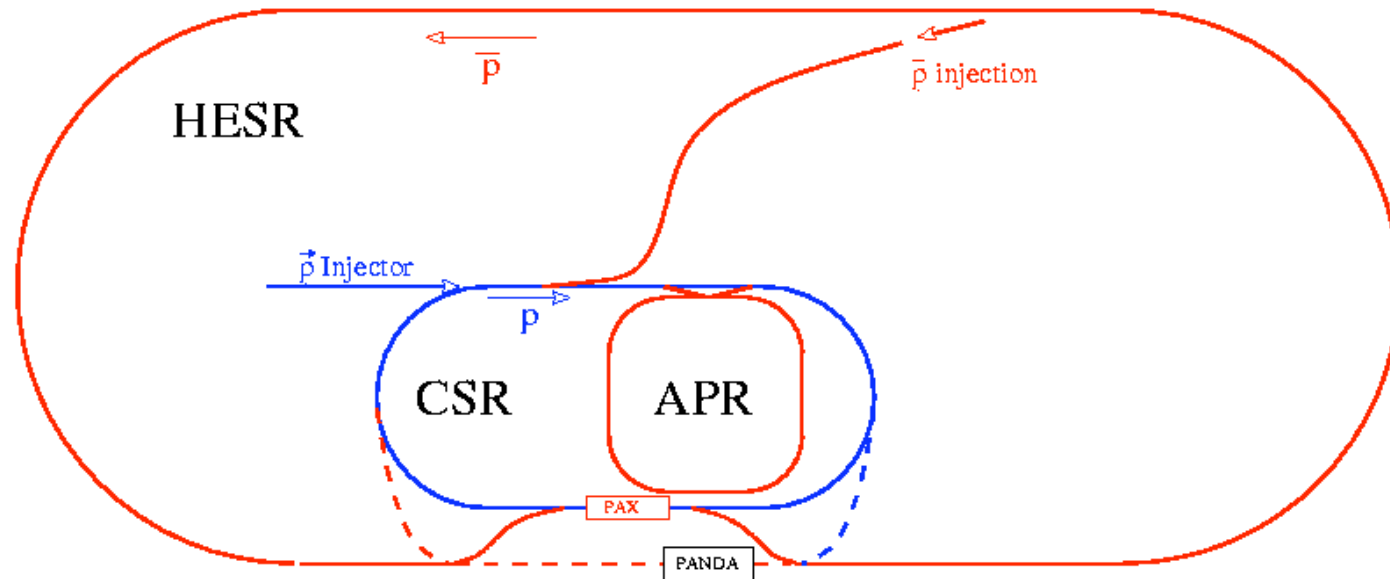


Beam lifetime in the APR as function of kinetic energy T

PAX phase 2: asymmetric collider

Program:

Asymmetric collider ($\sqrt{s}=15$ GeV):
polarized \bar{p} in HESR ($p=15$ GeV/c)
polarized p in CSR ($p=3.5$ GeV/c)



**Phase II: Transversity Distribution
DY Double Spin Assymetries**

Parameters

Parameter	Bunched		Coasting	
	CSR	HESR	CSR	HESR
Particles	pbar	p	pbar	p
Circum. [m]	183	574	183	574
P_{\max} [GeV/c]	3.65	15	3.65	15
s_{\max} [GeV ²]	~ 200		~ 200	
No. bunches	10	30	-	-
No. particles	5×10^{11}	2.4×10^{12}	5×10^{11}	1×10^{13}
Lifetime [hs]	~1500	~300	~1500	~300
Lum. [cm ⁻² s ⁻¹]	5×10^{30}		1.2×10^{31}	
Polar.	↑ ↑ , → → , ↑ →		↑ ↑ , → → , ↑ →	
p-p	yes		yes	

Summary and Outlook:



- Study of QCD bound states
 - Complete survey of charmonium energy region
 - Exclusive final states
- QCD dynamics
 - Missing resonances
 - Strange and Charm baryon
- Proton Timelike Form Factors
 - Very high-statistics measurement near threshold
 - Measure angular distribution $\Rightarrow |G_E|/|G_M|$
 - Extend q^2 range to 20-25 GeV²

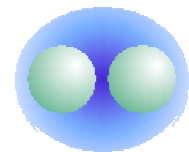


- Transversity in polarized $\bar{p}p$ DY
- Single Spin Asymmetries and Sivers Function
- Proton Timelike Form Factors
 - Measurement with polarized beams
 - Single- and double-spin observables
 - Moduli and phases of TL form factors

Backup Slides

Exotic hadrons

Regardless from the approach, the QCD spectrum is more rich than what is predicted by the naive quark model. Gluons carry color charge, therefore they can be explicit hadron components

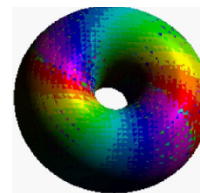

$$= \sum_i (q\bar{q})_i \sum_j g_j$$

The “exotic hadrons” fall in 3 general categories:

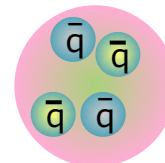
Hybrids $(q\bar{q}) g$



Glueballs gg

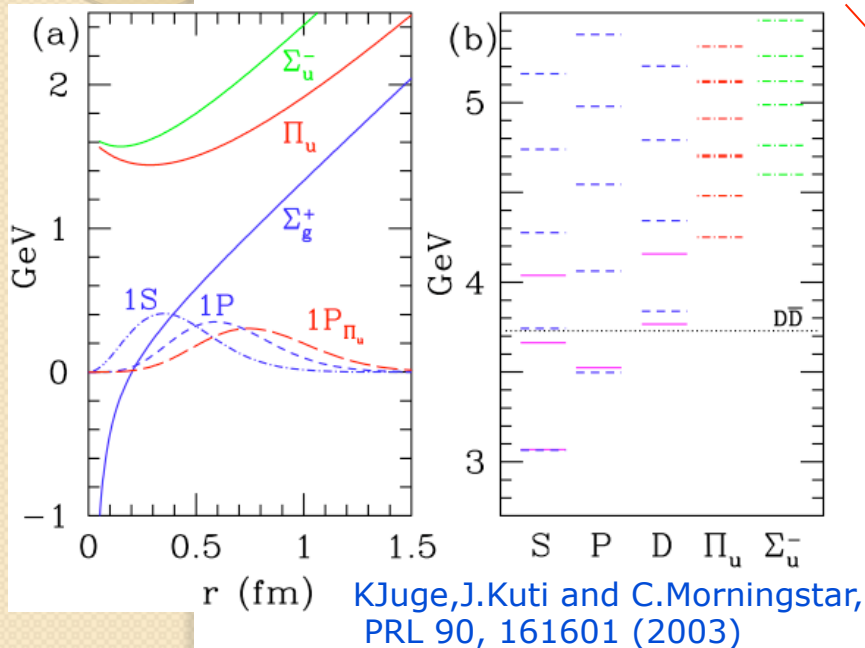


Multi-quarks $(q\bar{q})(\bar{q}q)$



Hybrids

In the simplest scenario, an hybrid is a meson with an explicit glue content. Adding a gluon ($J^P=1^+;1^-$) to a $q\bar{q}$ pair corresponds to create two possible hybrid states. Some of these combinations can even have exotic quantum numbers.

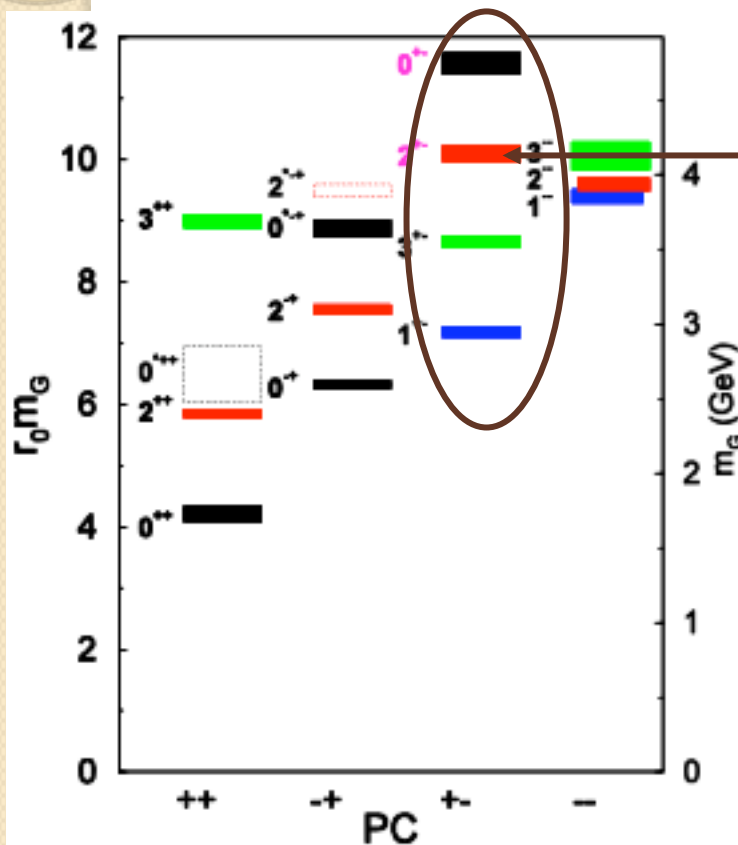


$q\bar{q}$	Gluon	
	$1^-(TM)$	$1^+(TE)$
$1S_0, 0^{++}$	$1^{++} \tilde{\chi}_{c1}$	$1^{--} \tilde{\psi}$
$3S_1, 1^{--}$	$0^{+-} \tilde{h}_{c0}$	$0^{-+} \tilde{\eta}_{c0}$
	$1^{+-} \tilde{h}_{c1}$	$1^{-+} \tilde{\eta}_{c1}$
	$2^{+-} \tilde{h}_{c2}$	$2^{-+} \tilde{\eta}_{c2}$

Theoretical models agree to expect 8 exotic charmonia in the 3-5 GeV/c^2 mass region. The lighter should be a 1^{-+} state with a mass of about $4.3 \text{ GeV}/c^2$. Quantum numbers and mass splitting are also predicted \rightarrow the observation of the whole pattern would be an unambiguous signature

Glueballs

LQCD makes rather accurate predictions for glueballs.
 As for hybrids they can have exotic quantum numbers → oddballs

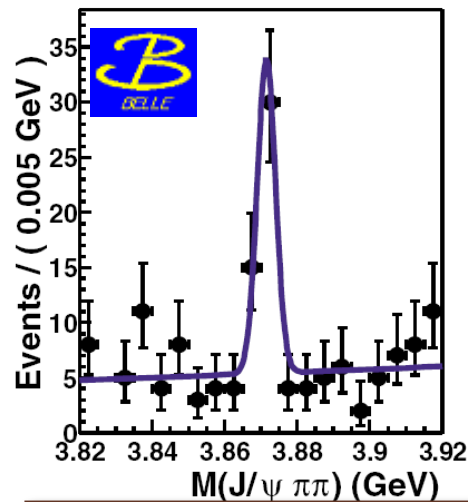


The lightest oddball, with $J^{PC}=2^{+-}$, is expected with a mass of $4.3 \text{ GeV}/c^2$.

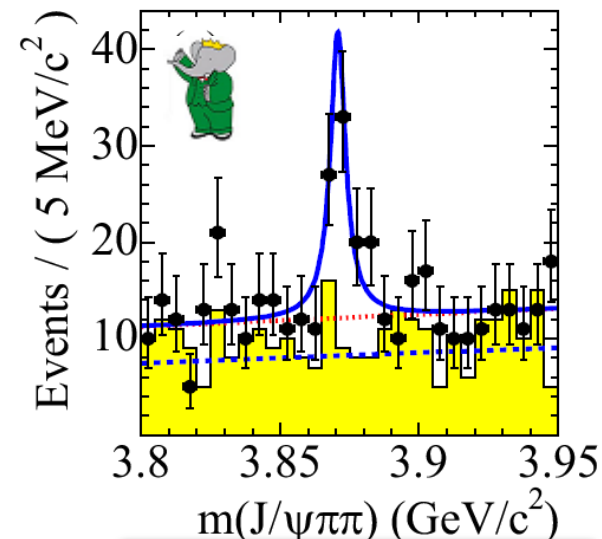
Glueballs don't have to obey to the OZI rule → they can decay in any channel.
 → their width is completely unknown

Multi-quarks

These states are expected to be loosely bound \rightarrow large widths. Nevertheless, the vicinity of a strong threshold can reduce the widths. This is the case of $a_0(980)$ and $f_0(975)$ that are close to the $K\bar{K}$ threshold, and can be an explanation for $X(3872)$.



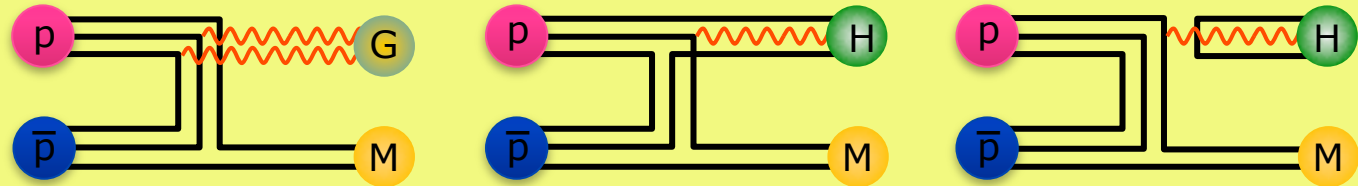
Phys.Rev. Lett.91,262001 (2003)



Phys.Rev. D71,071103 (2005)
Phys.Rev. D73,011101 (2006)

Spectroscopy with antiprotons

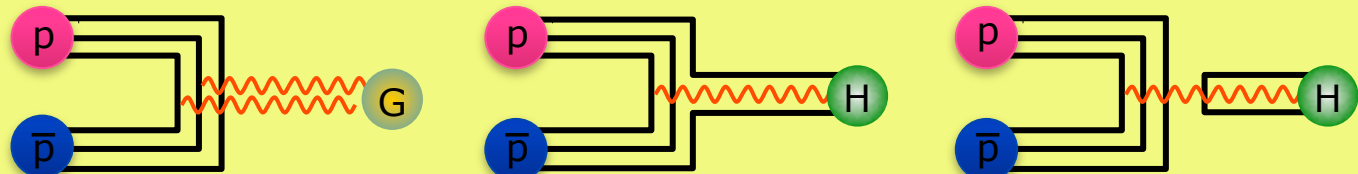
Two are the mechanisms to access particular final states:



Even **exotic** quantum numbers can be reached $\sigma \sim 100$ pb

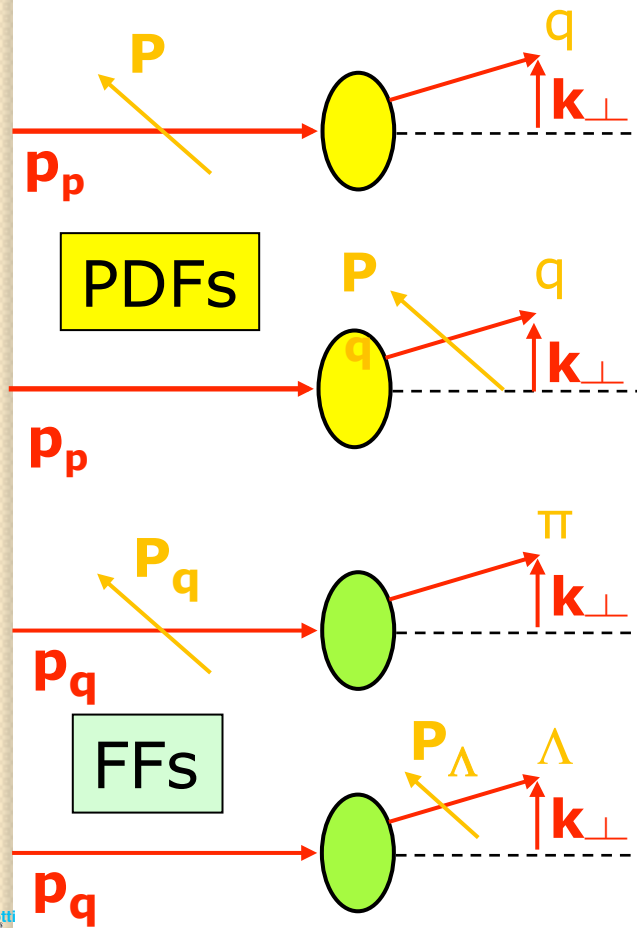
Exotic states are produced with rates similar to $q\bar{q}$ conventional systems

All **ordinary** quantum numbers can be reached $\sigma \sim 1$ μ b



Single Spin Asymmetries

Effects generating SSA



Sivers effect = number of partons in polarized proton depends on $\mathbf{P} \cdot (\mathbf{p} \times \mathbf{k}_\perp)$

Chiral-Even

Boer-Mulders effect = polarization of partons in unpolarized proton depends on $\mathbf{P}_q \cdot (\mathbf{p} \times \mathbf{k}_\perp)$

Chiral-Odd

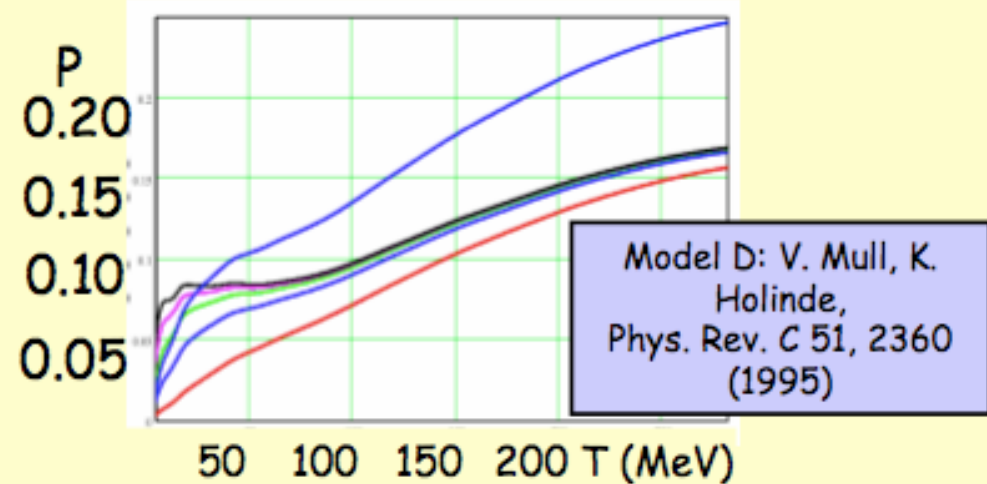
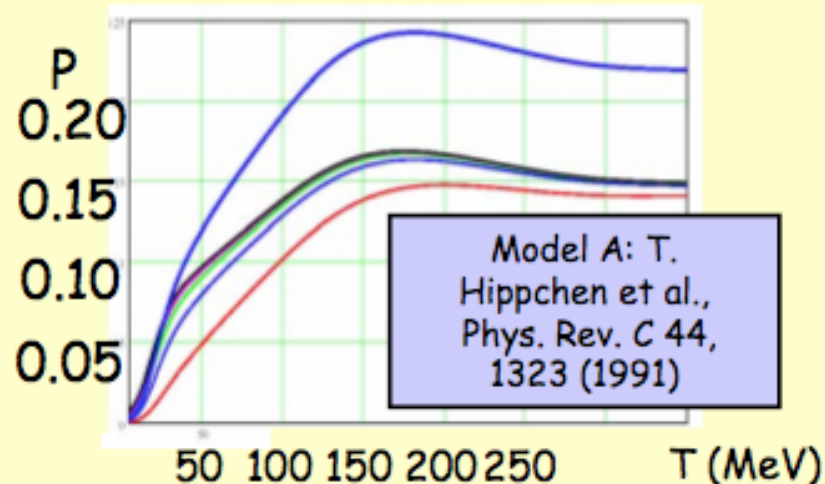
Collins effect = fragmentation of polarized quark depends on $\mathbf{P}_q \cdot (\mathbf{p}_q \times \mathbf{k}_\perp)$

Chiral-Odd

Polarizing FF = polarization of hadrons from unpolarized partons depends on $\mathbf{P}_\Lambda \cdot (\mathbf{p}_q \times \mathbf{k}_\perp)$

Polarization estimation

Since the mechanism of polarization via spin-filtering is not yet understood, the predictions must be tested experimentally.



Theoretical estimate of Antiproton Beam Polarization
(Hadronic Interaction: Longitudinal Spin Filtering)